Direct extraction of ring-down modes of binary black-hole mergers using auto-regression method

Hisaaki Shinkai (OIT)
真貝寿明(大阪工業大)
https://www.oit.ac.jp/is/shinkai/

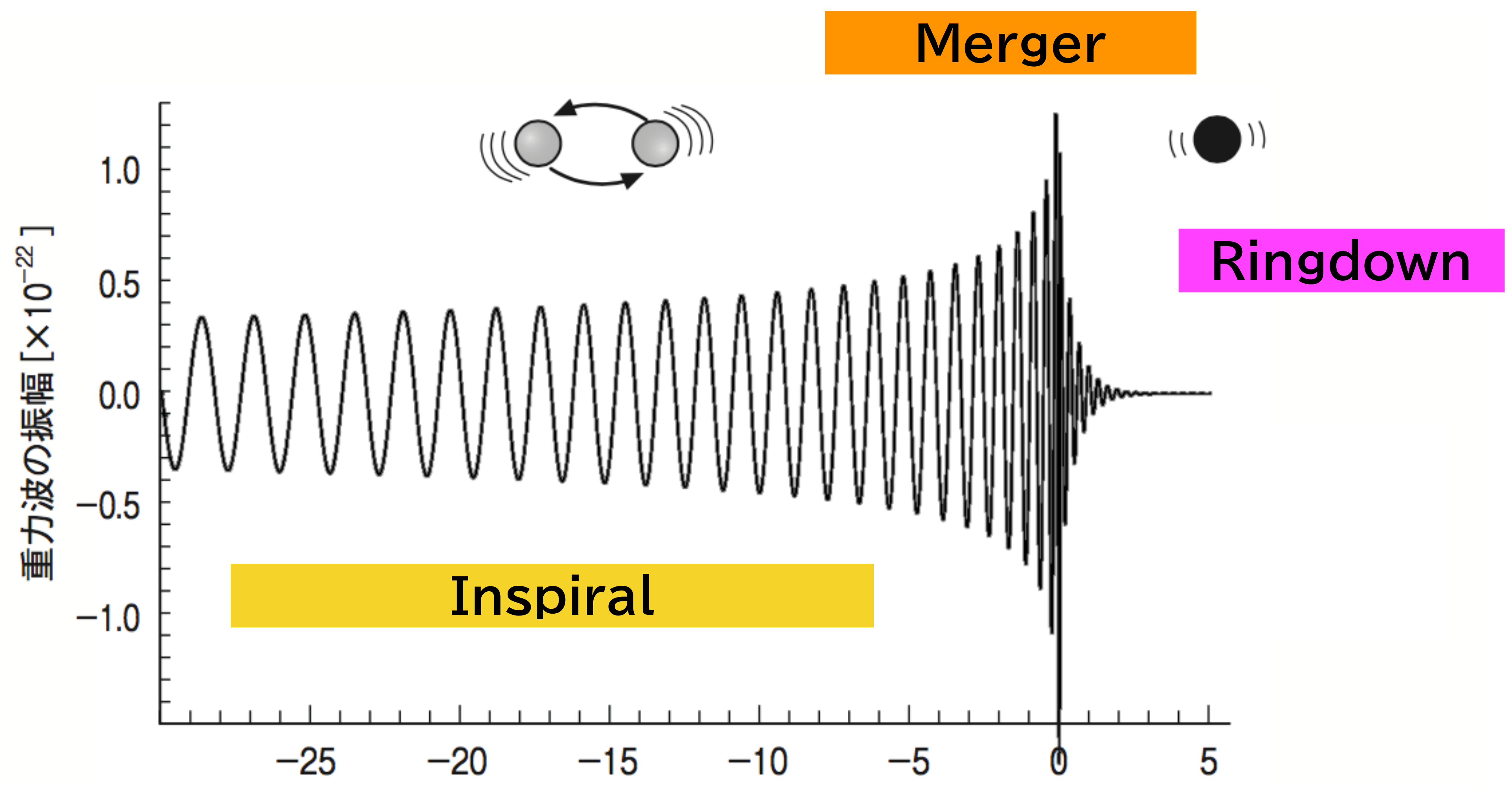

BH quasi-normal modes
⬅ BH perturbation in GR
➡ (M, a)

Strongest Field ever
➡ suitable for testing GR

Can we see freq. & damping rate?
Can we see overtones?
Can we see higher modes?
… as is predicted by GR

Ringdown part decays quickly. (damping rate = 3.7 ms for 60 Msun, a=0.75)
We need to develop a technique.
➡ Auto-Regressive model
➡ Apply O3 data.

➡➡ When the ringdown starts?
➡➡ Overtones? Higher modes?
➡➡ Consistent with GR?

Two acknowledges to the collaborators

Hisaaki Shinkai (OIT)
真貝寿明(大阪工業大)
https://www.oit.ac.jp/is/shinkai/

Rapid Response Team participation

Human vetting of the event validation by non-experts.

Three Timezones: L+V+K   8 hrs/day

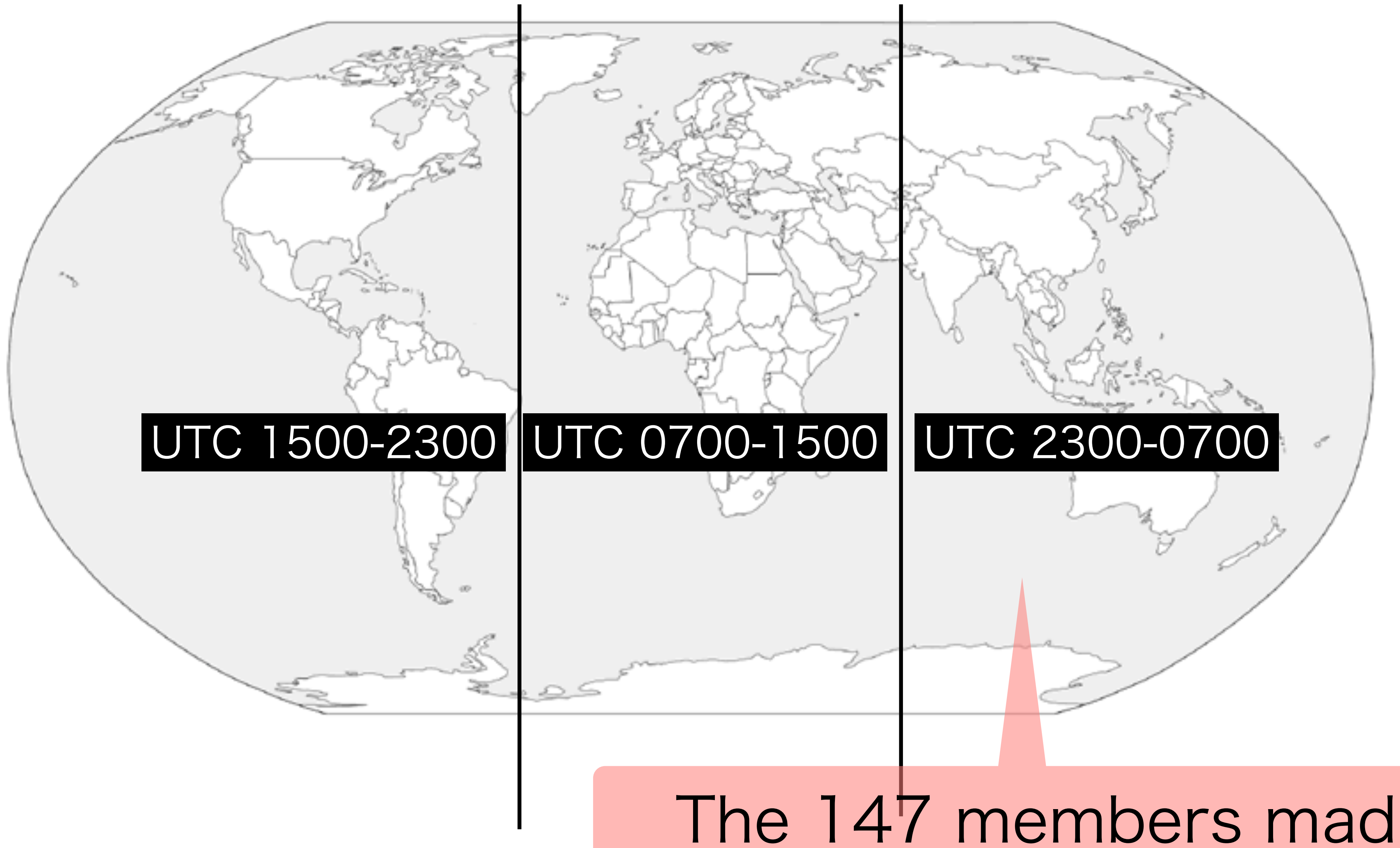

The 147 members made registrations for the shift until October 1, 2023.

EPO activities in Taiwan

https://techart.nthu.edu.tw/THE2022/

關於展覽

印象清華2022-
“宇宙的漣漪”
天文科普藝術節

愛因斯坦於1915年發表的廣義相對論，徹底改變了我們對重力和宇
宙的認識。「印象清華2022-“宇宙的漣漪”天文科普藝術節」活動包
含有靜態與動態的展覽，以及一系列的專家演講與座談會，除了介紹
重力波科學外，更希
科技藝術以另一角度
術跨域合作的科普
般民眾與學生都能

活動地點/時間：
國立清華大學圖書館
開幕茶會：2022/4/

Transient Catalog O1/O2/O3a,b has 90 events

重　力　波

重力波の生成機構　一般相対性理論によれば，大質量でコンパクトな天体が加速度運動することにより，重力波が発生する．重力波源としては連星の合体や超新星爆発，非球対称な星の高速回転や，宇宙初期に起源をもつ重力波が宇宙空間を伝播していると考えられる．これらのうち，データとの相関解析を可能にする波形予測ができるのは，連星合体からの重力波である．十分に合体前はニュートン力学に相対論補正を加えたポスト・ニュートン展開により，合体前後は数値シミュレーションにより，合体後ブラックホールが生じる場合にはブラックホール時空の摂動によっても波形モデルが得られる。これらのモデルと重力波干渉計で得られる信号の相関をとることで，連星ブラックホール（以下 BBH）や連星中性子星（BNS），および中性子星・ブラックホール連星（NSBH）の合体現象による重力波の検出、および、パラメータ推定が 2015 年以来可能になった．

重力波の観測　これまでに，米欧のレーザー干渉計 LIGO, Virgo によって，O3b と呼ばれる観測期間終了までに，BBH 波源の重力波が 83 例，BNS 波源が 2 例，NSBH 波源が 3 例，片方が BH で相方が不明なもの 2 例の合計 90 例が報告されている．日本の KAGRA（かぐら）も O3b 観測期間の最後に共同観測に入った．次の観測期間 O4 は，2022 年 12 月開始が予定されている（2022 年 7 月現在）。

重力波イベントは，観測された年月日を用いて，GW150914 の形で命名される．O3a 期より，時分秒を加えた名称が正式となった．重力波イベントは速報体制が取られ，多波長電磁波追観測が可能になっているが，これまでに波源が特定されたのは GW170817 のみである．

重力波レーザー干渉計の位置と腕の向き
（例えば N 36° W は，北から西方に 36° の向きを指す.）

干渉計	所在地	腕長 (km)	緯度	経度	X-腕	Y-腕
LIGO Hanford	米国	4	46°27′19″ N	119°24′28″ W	N 36° W	W 36° S
LIGO Livingston	米国	4	30 33 46　N	90 46 27　W	W 18° S	S 18° E
Virgo	欧州	3	43 37 53　N	10 30 16　E	N 19° E	W 19° N
KAGRA	日本	3	36 24 36　N	137 18 36　E	E 28.3° N	N 28.3° W

過去の観測期間

観測期	Advanced LIGO	Advanced Virgo	KAGRA
	年 月 日　年 月 日	年 月 日　年 月 日	年 月 日　年 月 日
O1	2015 9 12 –2016 1 19	–	–
O2	2016 11 30 –2017 8 25	2017 8 1 –2017 8 25	–
O3a	2019 4 1 –2019 9 30	同左	–
O3b	2019 11 1 –2020 3 27	同左	
O3GK	–	–	2020 4 7 –2020 4 21

観測された中で特筆すべきイベント　突発的重力波カタログ 3（GWTC3）として 2021 年 11 月に発表されたものが最新の重力波イベントカタログである．

GW150914　最初に報告された重力波直接観測イベント． BBH の存在を明らかにし，太陽質量（$M_\odot$）の 30 倍以上の BH の存在を初めて確認した．報告された BBH のイベントの中でも最もシグナル・ノイズ比 (SNR) が高い．GW170817　最初に報告された BNS イベント．直後に多くの追観測がなされ，マルチ・メッセンジャー天文学の初めての成功例となった．重力波波形から得られた中性子星の状態方程式に対する制限は核密度 $\rho_{\rm nuc} = 2.8 \times 10^{14}{\rm g/cm^3}$ の 2 倍の密度における圧力として $(2\rho_{\rm nuc}) = 3.5^{+2.7}_{-1.7} \times 10^{34}{\rm dyn/cm^2}$(90% 信頼区間) である．$\gamma$ 線が重力波のピークと 1.7 秒差で到着したことから重力波伝播速度の光速からのずれの割合は 1×10^{-15} 以下と制限された．また，可視・赤外における追観測から鉄以上の重元

1

Grav Wave

by T.Tanaka ＋ HS

過去の観測期間

観測期	Advanced LIGO	Advanced Virgo	KAGRA
	年 月 日　年 月 日	年 月 日　年 月 日	年 月 日　年 月 日
O1	2015 9 12 –2016 1 19	–	–
O2	2016 11 30 –2017 8 25	2017 8 1 –2017 8 25	–
O3a	2019 4 1 –2019 9 30	同左	–
O3b	2019 11 1 –2020 3 27	同左	
O3GK	–	–	2020 4 7 –2020 4 21

Gravitational Wave Transient Catalog

		released	arXiv	ref.	BHBH	NSNS	NSBH	BH+?	total
GWTC-1	O1+O2	2018/12/3	1811.12907	PRX 9 (2019) 031040	10	1			11
GWTC-2	O3a	2020/10/28	2010.14527	PRX 11 (2011) 021053	36	1		2	39
GWTC-2.1	+	2021/8/2	2108.01045		+8-3				5
GWTC-3	O3b	2021/11/5	2111.03606		32		3		35
				total	83	2	3	2	90

https://www.gw-openscience.org

Transient Catalog O1/O2/O3a,b has 90 events

報告されたおもな重力波（2022 年 7 月現在）

連星の質量を M_1, M_2 としたときの，チャープ質量 $M_c = (M_1M_2)^{3/5}/(M_1+M_2)^{1/5}$，質量比（中央値の比）$M_2/M_1$，有効スピン $\chi_{\rm eff}$，最終的に形成された BH の質量 $M_{\rm final}$(NS を含む場合は全質量 $M_{全} = M_1 + M_2$)，距離，波源特定精度（平方度）$(\Delta\theta)^2$，シグナル・ノイズ比を示す．幅のある量は 90% の信頼区間．(種類ごとに日付順．BBH については，GW190521 と SNR が 17.3 より大きいもののみ．)

イベント (BBH)	$M_c(M_\odot)$	質量比	$\chi_{\rm eff}$	$M_{\rm final}(M_\odot)$	距離 (Mpc)	$(\Delta\theta)^2$	SNR	
GW150914	$28.6^{+1.7}_{-1.5}$	0.86	$-0.01^{+0.12}_{-0.13}$	$63.1^{+3.4}_{-3.0}$	440^{+150}_{-170}	182	24.4	good event for test
GW190412	$13.3^{+0.5}_{-0.5}$	0.32	$0.21^{+0.12}_{-0.13}$	$35.6^{+4.8}_{-4.5}$	720^{+240}_{-220}	240	19.8	
GW190521	$63.3^{+19.6}_{-14.6}$	0.58	$-0.14^{+0.5}_{-0.45}$	$147.4^{+40.0}_{-16.0}$	3310^{+2790}_{-1800}	1000	14.3	too heavy, low freq.
GW190521_074359	$32.8^{+3.2}_{-2.8}$	0.77	$0.1^{+0.13}_{-0.13}$	$72.6^{+6.5}_{-5.4}$	1080^{+580}_{-530}	470	25.9	
GW190814	$6.11^{+0.06}_{-0.05}$	0.11	$0^{+0.07}_{-0.07}$	$25.7^{+1.3}_{-1.3}$	230^{+40}_{-50}	22	25.3	too light, high freq.
GW191109_010717	$47.5^{+9.6}_{-7.5}$	0.72	$-0.29^{+0.42}_{-0.31}$	$107^{+18.0}_{-15.0}$	1290^{+1130}_{-650}	1600	17.3	too heavy, low freq.
GW191204_171526	$8.55^{+0.38}_{-0.27}$	0.69	$0.16^{+0.08}_{-0.05}$	$19.21^{+1.79}_{-0.95}$	650^{+190}_{-250}	350	17.5	too light, high freq.
GW191216_213338	$8.33^{+0.22}_{-0.19}$	0.64	$0.11^{+0.13}_{-0.06}$	$18.87^{+2.8}_{-0.94}$	340^{+120}_{-130}	490	18.6	too light, high freq.
GW200112_155838	$27.4^{+2.6}_{-2.1}$	0.79	$0.06^{+0.15}_{-0.15}$	$60.8^{+5.3}_{-4.3}$	1250^{+430}_{-460}	4300	19.8	
GW200129_065458	$27.2^{+2.1}_{-2.3}$	0.84	$0.11^{+0.11}_{-0.16}$	$60.3^{+4.0}_{-3.3}$	900^{+290}_{-380}	130	26.8	
GW200224_222234	$31.1^{+3.2}_{-2.6}$	0.81	$0.1^{+0.15}_{-0.15}$	$68.6^{+6.6}_{-4.7}$	1710^{+490}_{-640}	50.0	20	
GW200311_115853	$26.6^{+2.4}_{-2.0}$	0.81	$-0.02^{+0.16}_{-0.2}$	$59^{+4.8}_{-3.9}$	1170^{+280}_{-400}	35	17.8	
イベント (BNS)	$M_c(M_\odot)$	質量比	$\chi_{\rm eff}$	$M_{全}(M_\odot)$	距離 (Mpc)	$(\Delta\theta)^2$	SNR	
GW170817	$1.186^{+0.001}_{-0.001}$	0.87	$0^{+0.02}_{-0.01}$	–	$40^{+7.0}_{-15.0}$	16	33	
GW190425	$1.44^{+0.02}_{-0.02}$	0.62	$0.07^{+0.07}_{-0.05}$	$3.4^{+0.3}_{-0.1}$	150^{+80}_{-60}	8700	12.4	
イベント (NSBH)	$M_c(M_\odot)$	質量比	$\chi_{\rm eff}$	$M_{全}(M_\odot)$	距離 (Mpc)	$(\Delta\theta)^2$	SNR	
GW190917_114630	$3.7^{+0.2}_{-0.2}$	0.22	$-0.08^{+0.21}_{-0.43}$	$11.6^{+3.1}_{-2.9}$	720^{+300}_{-310}	2100	8.3	
GW200105_162426	$3.42^{+0.08}_{-0.08}$	0.21	$0.0^{+0.13}_{-0.18}$	$10.7^{+1.5}_{-1.4}$	270^{+120}_{-110}	7900	13.7	
GW200115_042309	$2.43^{+0.05}_{-0.07}$	0.24	$-0.15^{+0.24}_{-0.42}$	$7.2^{+1.8}_{-1.7}$	290^{+150}_{-100}	370	11.3	

Tests of General Relativity with GWTC-3（LVK paper）

LVK PRD accepted, arXiv:2112.06861

1. residuals test
2. inspiral–merger–ringdown consistency test
3. parametrized tests of GW generation
4. spin-induced moments
5. modified GW dispersion relation
6. polarization content
7. ringdown
8. echoes searches

Event	Inst.	D_L [Gpc]	$(1+z)M$ [$M_\odot$]	$(1+z)\mathcal{M}$ [$M_\odot$]	$(1+z)M_f$ [$M_\odot$]	χ_f	SNR	RT	IMR	PAR	SIM	MDR	POL	RD	ECH
		Properties						Tests performed							
GW191109_010717	HL	$1.29^{+1.13}_{-0.65}$	140^{+21}_{-17}	$60.1^{+9.8}_{-9.3}$	135^{+19}_{-15}	$0.61^{+0.18}_{-0.19}$	$17.3^{+0.5}_{-0.5}$	✓	–	–	–	–	✓	✓	✓
GW191129_134029	HL	$0.79^{+0.26}_{-0.33}$	$20.10^{+2.94}_{-0.64}$	$8.49^{+0.06}_{-0.05}$	$19.19^{+3.07}_{-0.67}$	$0.69^{+0.03}_{-0.05}$	$13.1^{+0.2}_{-0.3}$	✓	–	✓	✓	✓	–	–	✓
GW191204_171526	HL	$0.65^{+0.19}_{-0.25}$	$22.74^{+1.94}_{-0.48}$	$9.70^{+0.05}_{-0.05}$	$21.60^{+2.05}_{-0.50}$	$0.73^{+0.03}_{-0.03}$	$17.5^{+0.2}_{-0.2}$	✓	–	✓	✓	✓	✓	–	✓
GW191215_223052	HLV	$1.93^{+0.89}_{-0.86}$	$58.4^{+4.8}_{-3.7}$	$24.9^{+1.5}_{-1.4}$	$55.8^{+4.8}_{-3.3}$	$0.68^{+0.07}_{-0.07}$	$11.2^{+0.3}_{-0.4}$	✓	–	–	–	✓	✓	–	✓
GW191216_213338	HV	$0.34^{+0.12}_{-0.13}$	$21.17^{+2.93}_{-0.66}$	$8.94^{+0.05}_{-0.05}$	$20.18^{+3.06}_{-0.70}$	$0.70^{+0.03}_{-0.04}$	$18.6^{+0.2}_{-0.2}$	✓	–	✓	✓	✓	✓	–	✓
GW191222_033537	HL	$3.0^{+1.7}_{-1.7}$	119^{+16}_{-13}	$51.0^{+7.2}_{-6.5}$	114^{+14}_{-12}	$0.67^{+0.08}_{-0.11}$	$12.5^{+0.2}_{-0.3}$	✓	–	–	–	✓	✓	✓	✓
GW200115_042309	HLV	$0.29^{+0.15}_{-0.10}$	$7.8^{+1.9}_{-1.8}$	$2.58^{+0.01}_{-0.01}$	$7.7^{+1.9}_{-1.8}$	$0.42^{+0.09}_{-0.05}$	$11.3^{+0.3}_{-0.5}$	✓	–	✓	–	–	–	–	✓
GW200129_065458	HLV	$0.90^{+0.29}_{-0.38}$	$74.6^{+4.5}_{-3.8}$	$32.1^{+1.8}_{-2.6}$	$70.9^{+4.2}_{-3.4}$	$0.73^{+0.06}_{-0.05}$	$26.8^{+0.2}_{-0.2}$	✓	✓	✓	✓	✓	✓	✓	✓
GW200202_154313	HLV	$0.41^{+0.15}_{-0.16}$	$19.01^{+1.99}_{-0.34}$	$8.15^{+0.05}_{-0.05}$	$18.12^{+2.09}_{-0.35}$	$0.69^{+0.03}_{-0.04}$	$10.8^{+0.2}_{-0.4}$	✓	–	✓	–	✓	–	–	✓
GW200208_130117	HLV	$2.23^{+1.00}_{-0.85}$	91^{+11}_{-10}	$38.8^{+5.2}_{-4.8}$	$87.5^{+10.3}_{-9.1}$	$0.66^{+0.09}_{-0.13}$	$10.8^{+0.3}_{-0.4}$	✓	✓	–	–	✓	✓	–	✓
GW200219_094415	HLV	$3.4^{+1.7}_{-1.5}$	103^{+14}_{-12}	$43.7^{+6.3}_{-6.2}$	98^{+13}_{-11}	$0.66^{+0.10}_{-0.13}$	$10.7^{+0.3}_{-0.5}$	✓	–	–	–	✓	✓	–	✓
GW200224_222234	HLV	$1.71^{+0.49}_{-0.64}$	$94.9^{+8.3}_{-7.2}$	$40.9^{+3.5}_{-3.8}$	$90.2^{+7.5}_{-6.4}$	$0.73^{+0.07}_{-0.07}$	$20.0^{+0.2}_{-0.2}$	✓	✓	–	–	✓	✓	✓	✓
GW200225_060421	HL	$1.15^{+0.51}_{-0.53}$	$41.2^{+3.0}_{-4.0}$	$17.65^{+0.98}_{-1.97}$	$39.4^{+2.9}_{-3.6}$	$0.66^{+0.07}_{-0.13}$	$12.5^{+0.3}_{-0.4}$	✓	✓	✓	✓	✓	✓	–	✓
GW200311_115853	HLV	$1.17^{+0.28}_{-0.40}$	$75.9^{+6.2}_{-5.7}$	$32.7^{+2.7}_{-2.8}$	$72.4^{+5.6}_{-5.1}$	$0.69^{+0.07}_{-0.08}$	$17.8^{+0.2}_{-0.2}$	✓	✓	✓	–	✓	✓	✓	✓
GW200316_215756	HLV	$1.12^{+0.47}_{-0.44}$	$25.5^{+8.7}_{-1.1}$	$10.68^{+0.12}_{-0.12}$	$24.3^{+9.0}_{-1.1}$	$0.70^{+0.04}_{-0.04}$	$10.3^{+0.4}_{-0.7}$	✓	–	✓	✓	–	–	–	✓

2. inspiral–merger–ringdown consistency test

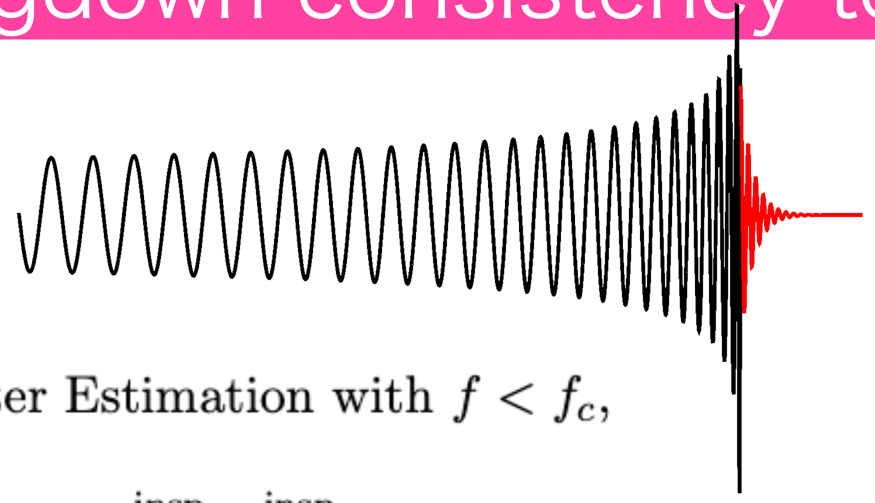

with $f > f_c$,

$M_f^{\rm postinsp}, \chi_f^{\rm postinsp}$

Parameter Estimation with $f < f_c$,

$M_f^{\rm insp}, \chi_f^{\rm insp}$

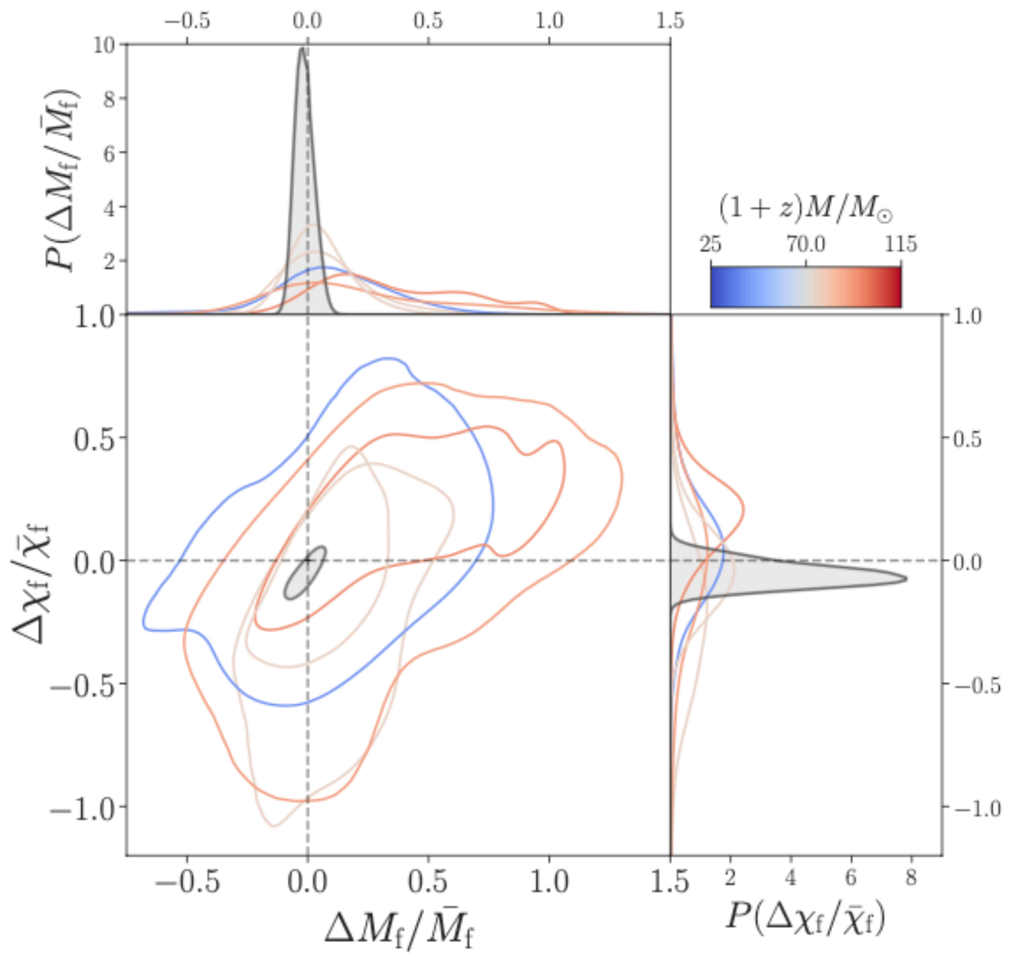

$$\frac{\Delta M_f}{\bar{M}_f} = 2\frac{M_f^{\rm insp} - M_f^{\rm postinsp}}{M_f^{\rm insp} + M_f^{\rm postinsp}}, \quad \frac{\Delta\chi_f}{\bar{\chi}_f} = 2\frac{\chi_f^{\rm insp} - \chi_f^{\rm postinsp}}{\chi_f^{\rm insp} + \chi_f^{\rm postinsp}},$$

Waveform models

IMRPhenomXPHM - phenomenological PN-based models, calibrated to NR

Event	$f_c^{\rm IMR}$ [Hz]	$\rho_{\rm IMR}$	$\rho_{\rm insp}$	$\rho_{\rm postinsp}$	$Q_{\rm GR}^{\rm 2D}$ [%]
GW200129_065458	136	25.7	20.1	16.0	1.5
GW200208_130117	98	9.9	7.2	6.8	10.5
GW200224_222234	107	19.4	14.3	13.1	20.7
GW200225_060421	213	12.9	11.1	6.6	1.3
GW200311_115853	122	17.5	13.5	11.0	15.2

the fraction of the posterior enclosed by the isoprobabilty contour that passes through (0, 0)
[smaller values indicate better consistency]

No statistically significant deviations from GR

7. ringdown test

$$h_+(t) - ih_\times(t) = \sum_{\ell=2}^{+\infty}\sum_{m=-\ell}^{\ell}\sum_{n=0}^{+\infty} \mathcal{A}_{\ell mn} \exp\left[-\frac{t-t_0}{(1+z)\tau_{\ell mn}}\right] \exp\left[\frac{2\pi i f_{\ell mn}(t-t_0)}{1+z}\right] {}_{-2}S_{\ell mn}(\theta,\phi,\chi_f)$$

time-domain ringdown analysis pyRing, based on damped sinusoids,

parametrized ringdown analysis pSEOB, based on the SEOBNRv4HM waveform model.

Event	Redshifted final mass $(1+z)M_f$ [$M_\odot$] IMR	Kerr$_{220}$	Kerr$_{221}$	Kerr$_{\rm HM}$	Final spin χ_f IMR	Kerr$_{220}$	Kerr$_{221}$	Kerr$_{\rm HM}$	Higher modes $\log_{10}\mathcal{B}^{\rm HM}_{220}$	Overtones $\log_{10}\mathcal{B}^{221}_{220}$	$\log_{10}\mathcal{O}^{\rm modGR}_{\rm GR}$
GW191109_010717	$132.7^{+21.9}_{-13.8}$	$181.7^{+28.5}_{-30.6}$	$179.0^{+23.7}_{-21.7}$	$174.5^{+38.1}_{-30.1}$	$0.60^{+0.22}_{-0.19}$	$0.81^{+0.10}_{-0.24}$	$0.81^{+0.08}_{-0.14}$	$0.77^{+0.11}_{-0.21}$	−0.11	1.03	−0.27
GW191222_033537	$114.2^{+14.3}_{-11.7}$	$111.4^{+69.3}_{-29.7}$	$110.3^{+36.2}_{-23.8}$	$118.3^{+97.0}_{-46.2}$	$0.67^{+0.08}_{-0.10}$	$0.46^{+0.41}_{-0.41}$	$0.52^{+0.31}_{-0.43}$	$0.60^{+0.28}_{-0.66}$	0.08	−0.83	−0.20
GW200129_065458	$71.8^{+4.4}_{-3.9}$	$60.0^{+16.7}_{-8.9}$	$77.0^{+14.4}_{-14.2}$	$219.1^{+110.4}_{-140.0}$	$0.75^{+0.06}_{-0.06}$	$0.31^{+0.43}_{-0.28}$	$0.74^{+0.17}_{-0.59}$	$0.54^{+0.35}_{-0.59}$	−0.00	−0.47	−0.09
GW200224_222234	$90.3^{+6.4}_{-6.3}$	$84.4^{+23.2}_{-20.3}$	$88.6^{+15.5}_{-15.2}$	$119.4^{+142.6}_{-34.3}$	$0.73^{+0.06}_{-0.07}$	$0.61^{+0.27}_{-0.49}$	$0.60^{+0.23}_{-0.42}$	$0.64^{+0.27}_{-0.59}$	0.20	0.95	−0.11
GW200311_115853	$72.1^{+5.4}_{-4.7}$	$68.5^{+23.6}_{-13.5}$	$72.2^{+28.6}_{-16.3}$	$213.2^{+167.8}_{-141.5}$	$0.68^{+0.07}_{-0.08}$	$0.30^{+0.44}_{-0.28}$	$0.58^{+0.30}_{-0.47}$	$0.56^{+0.32}_{-0.54}$	0.02	−1.16	−0.15

>0 supports higher modes

>0 supports first overtone

>0 disagreement with GR

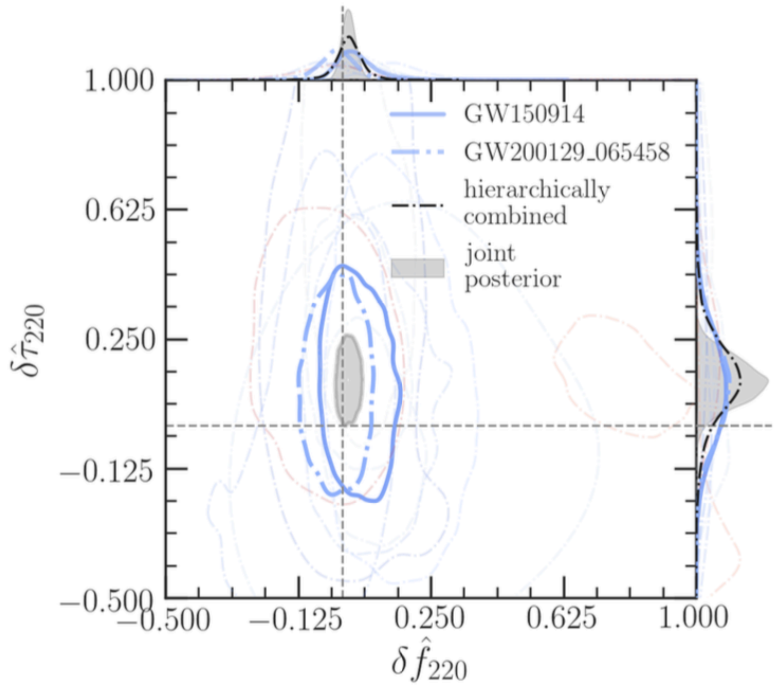

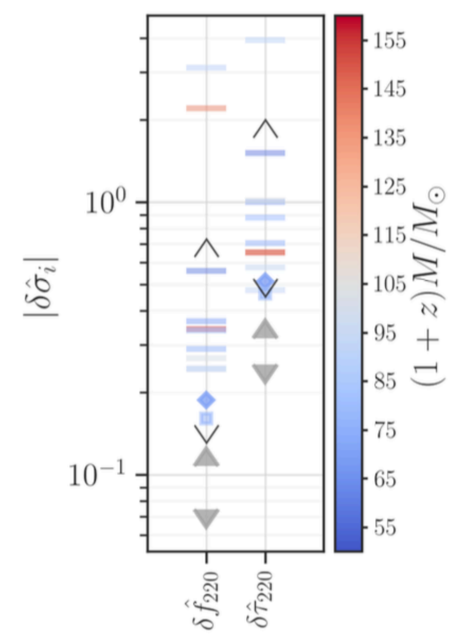

No statistically significant deviations from GR

Fitting data with linear func.

$$
\begin{aligned}
x_n &= a_1 x_{n-1} + a_2 x_{n-2} + \cdots + a_M x_{n-M} + \varepsilon \\
&= \sum_{j=1}^{M} a_j x_{n-j} + \varepsilon
\end{aligned}
$$

e.g. $x_n = A e^{-rn\Delta t} \cos(\omega n \Delta t)$

$$
\begin{aligned}
Z_1 &= e^{-(r-j\omega)\Delta t} \\
Z_2 &= e^{-(r+j\omega)\Delta t}
\end{aligned}
\quad \Rightarrow \quad x_n = \frac{A}{2}(Z_1^n + Z_2^n) = (Z_1 + Z_2)x_{n-1} - Z_1 Z_2 x_{n-2}
$$

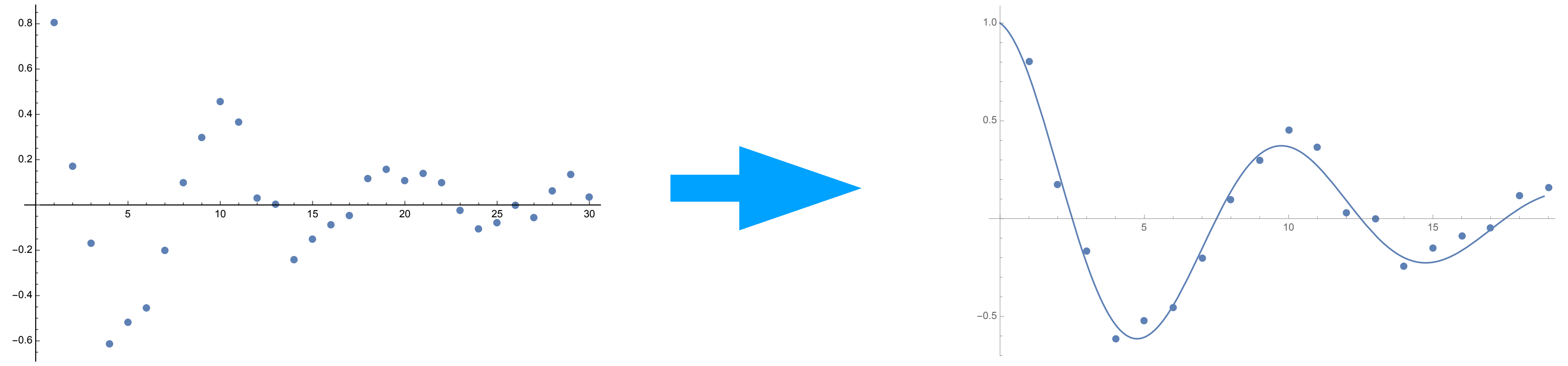

can be applied also to noisy data by adjusting M

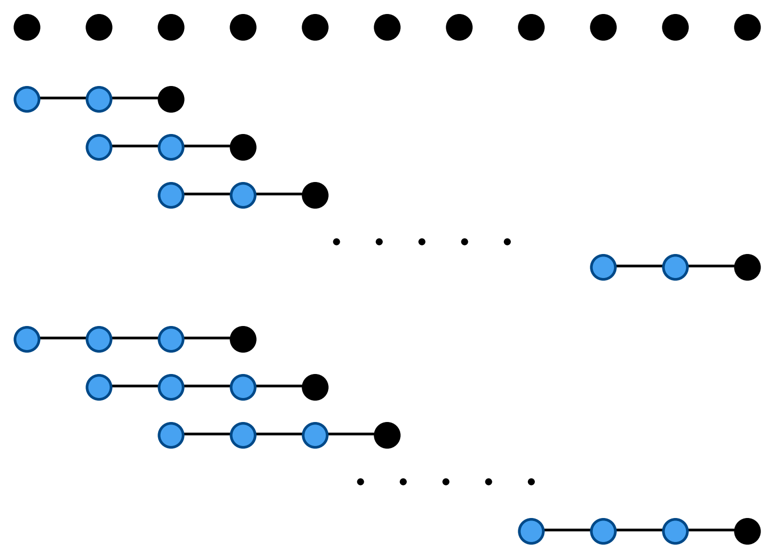

- find a_j (Burg method)
- find M (FPE final prediction error method)
- re-construct wave signal from fitted function
- apply FFT with arbitrary precision.

power spectrum

$$
p(f) = \frac{\sigma^2}{\left| 1 - \sum_{j=1}^{M} a_j e^{-I 2\pi j f \Delta t} \right|^2}
$$

characteristic eq.

$$
f(z) = 1 - \sum_{j=1}^{M} a_j z^j = 0
$$

$|z_k|$ says amplitude,
$\arg(z_k)$ says frequency.

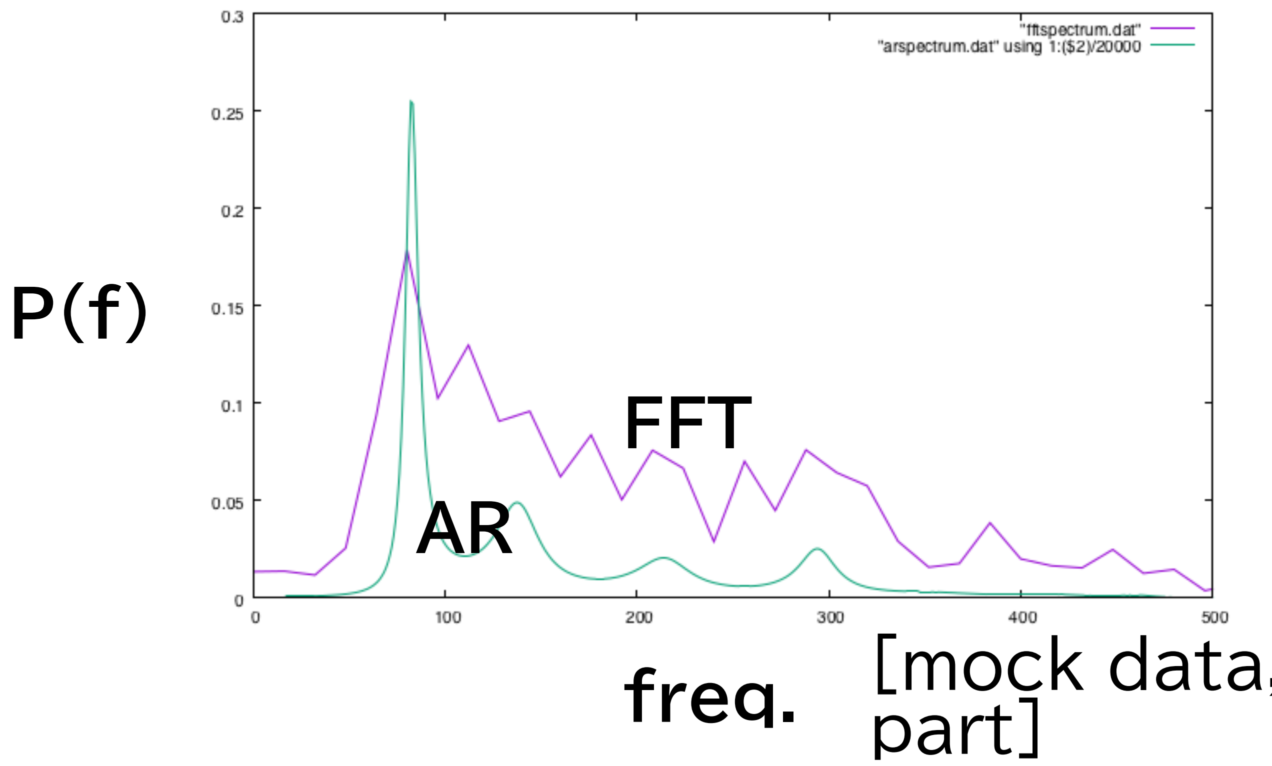

[mock data, SNR=40, inspiral part]

The order M can be fixed at 2~8.

Even for short segment, AR model shows precise power-spectrum.

Method of Auto-Regressive model for extracting GW signal

sampling rate=4096 segment = 1/16 sec = 256 points
or = 1/64 sec = 64 points

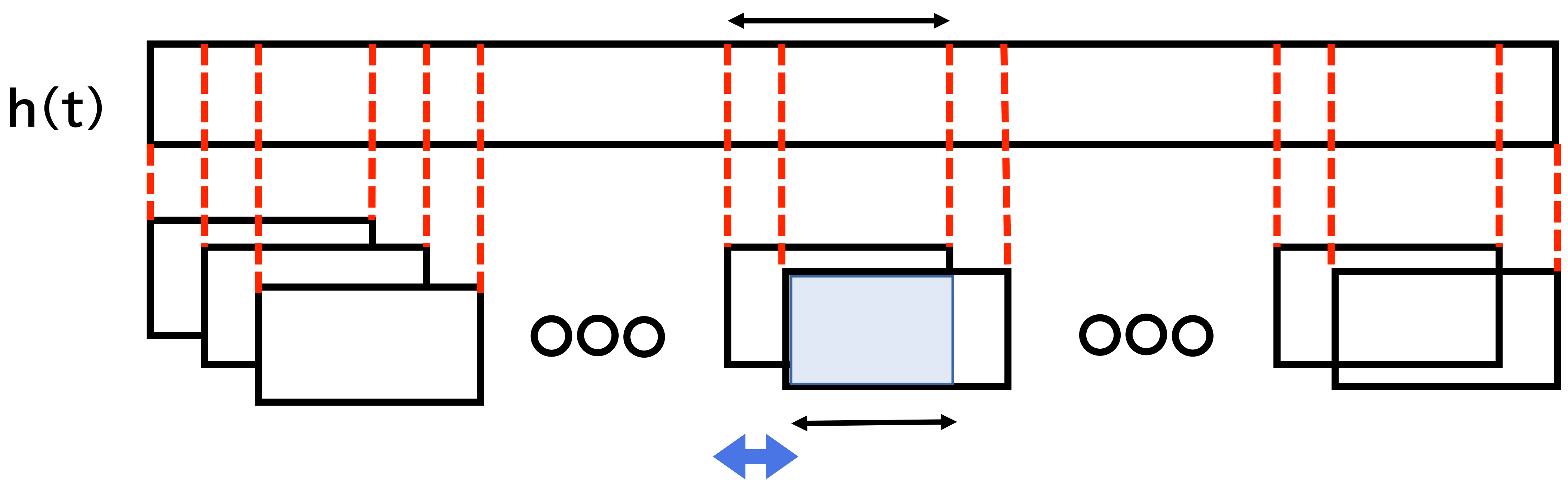

shift = 1/4096 sec = 1points

We analyse the (whitened) data around the event reported.

Using AR method, we extract frequencies $f_{\rm real}$, and damping rate τ (= f imag).

No Prior Models, Only from Data | Independent to each detector

We search constant-frequency signals (ring-down mode !?)

The variance of $f_{\rm real}$ < 1-sigma, $\tau(= f$ imag) < 1.25-sigma

We can extract the existing period for each mode

We can pick up several such (f, τ) in a single segment

Can extract multipul modes simalteneously

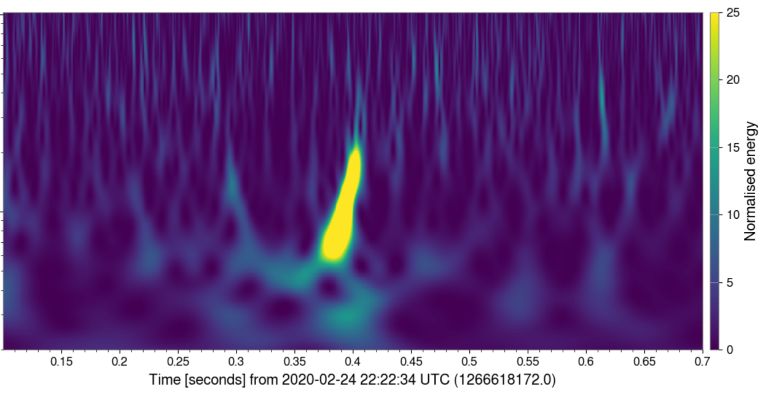

GW200224_222234 Hanford

freq

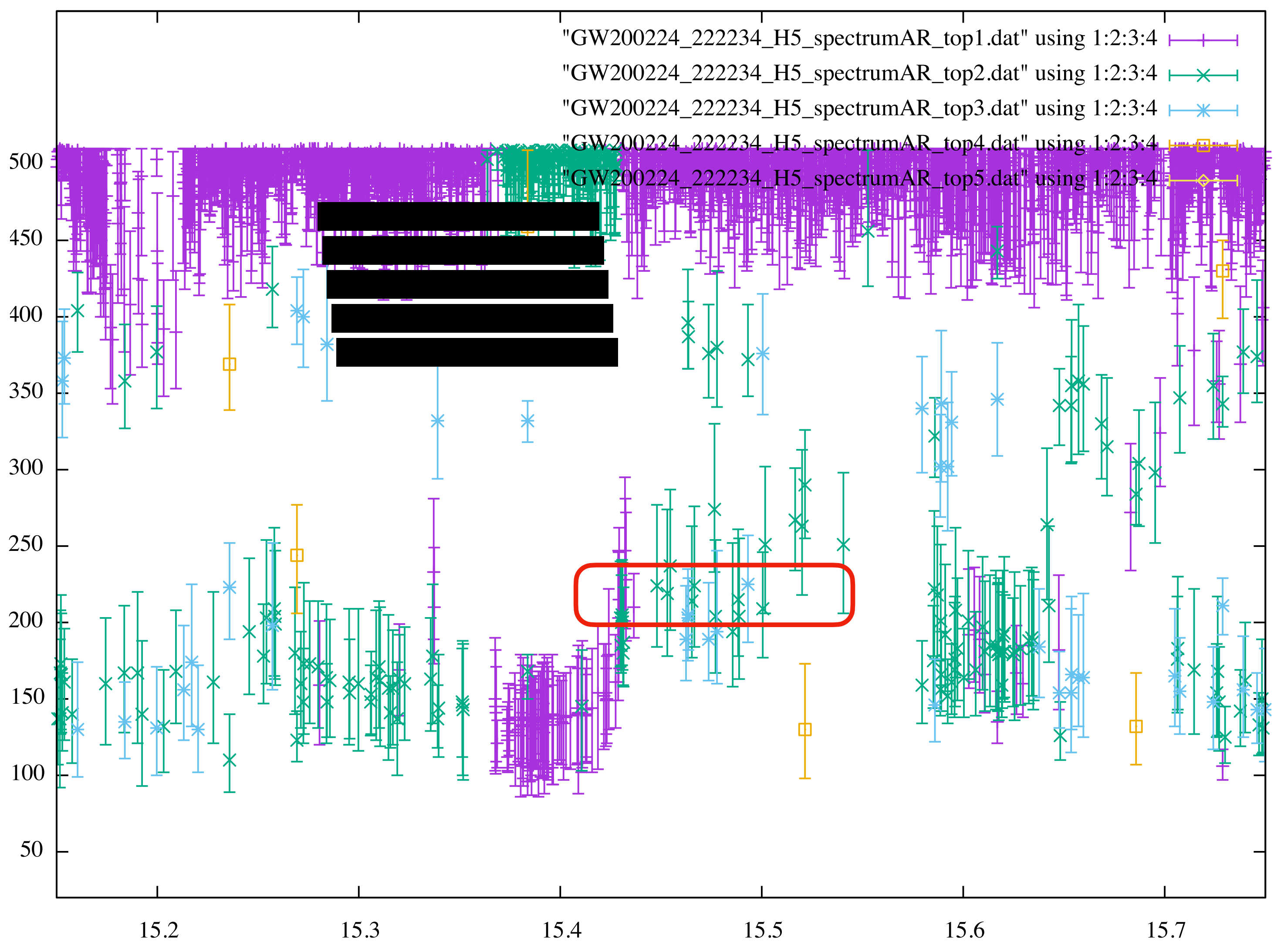

time

Refer the LVK catalog data (M_f, a_f) + redshift z

Derive (f, τ) and let them the GR predictions

$$f_R = f_1 + f_2(1-a)^{f_3}$$
$$Q \equiv \frac{f_R}{2f_I} = q_1 + q_2(1-a)^{q_3}$$

$$f_{\rm qnm}[{\rm Hz}] = \frac{c^3}{2\pi GM} f_R \sim 32314.1 \left(\frac{M_\odot}{M}\right) f_R.$$

$$a = 1 - \left(\frac{Q-q_1}{q_2}\right)^{1/q_3}$$
$$M[M_\odot] = 32314.1 \times \frac{f_1 + f_2(1-a)^{f_3}}{f_{\rm qnm}[{\rm Hz}]}$$

Berti, Cardoso & Will PRD 73, 064030 (2006).

Does AR extract ringdown mode properly?
Consistent values from 3 detectors (Hanford, Livingston, Virgo) ?
Consistent values with LVK catalog

When the ringdown starts?
Ovetones? Higher modes?
Consistent with GR?

Calibration of transient time of GW at each detector

GW150914

Hanford

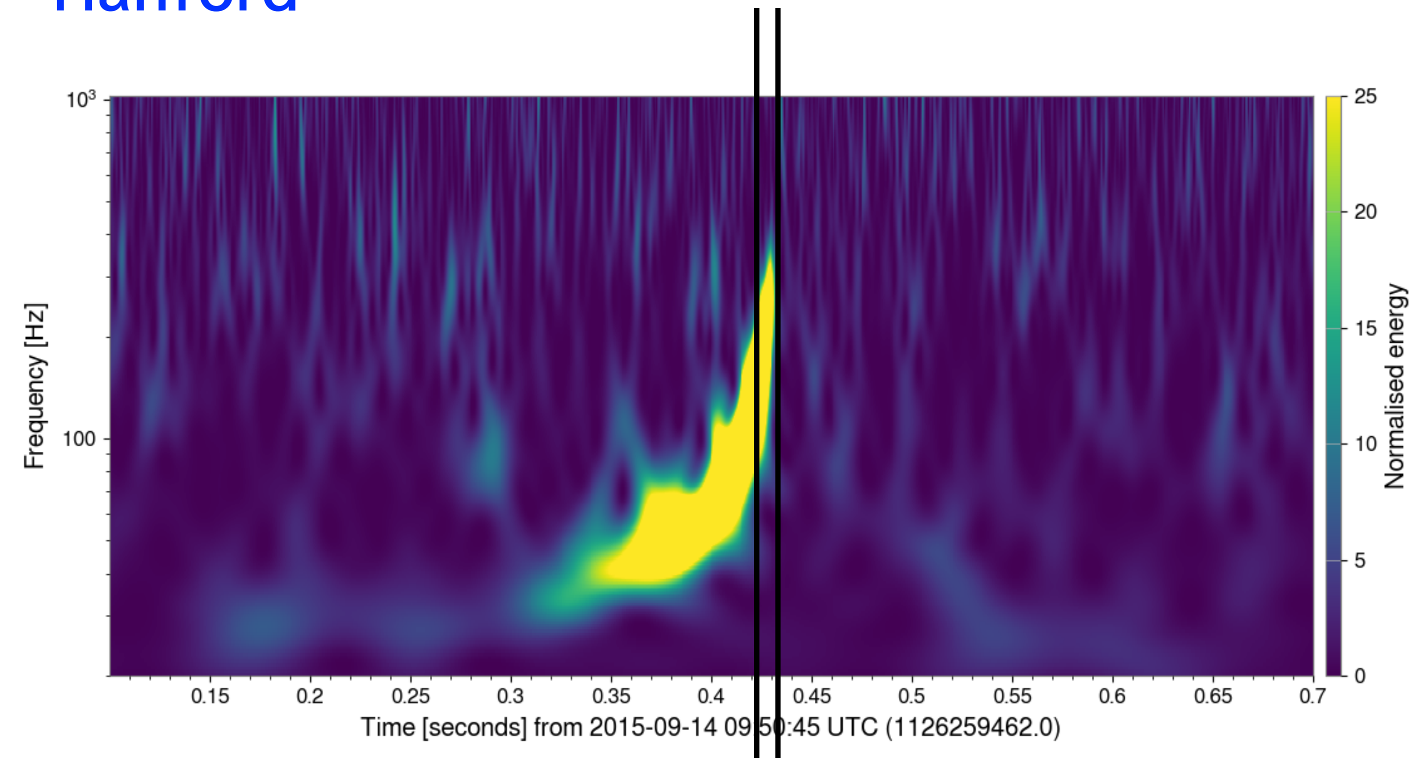

Livingston

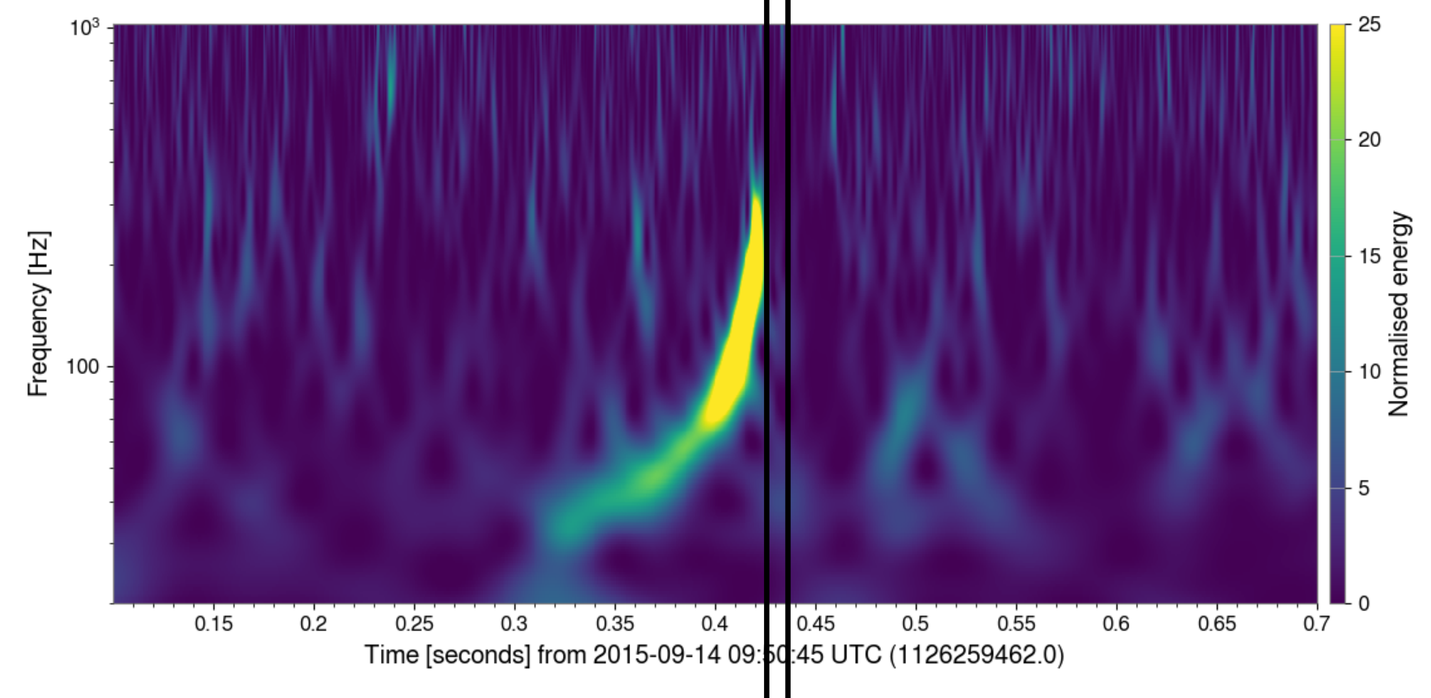

filters to remove the strong instrumental spectral lines seen in the Fig. 3 spectra. *Top row, left:* H1 strain. *Top row, right:* L1 strain. GW150914 arrived first at L1 and $6.9^{+0.5}_{-0.4}$ ms later at H1; for a visual comparison, the H1 data are also shown, shifted in time by this amount and inverted (to account for the detectors' relative orientations). *Second row:* Gravitational-wave strain projected onto each

PRL 116 (2016) 061102

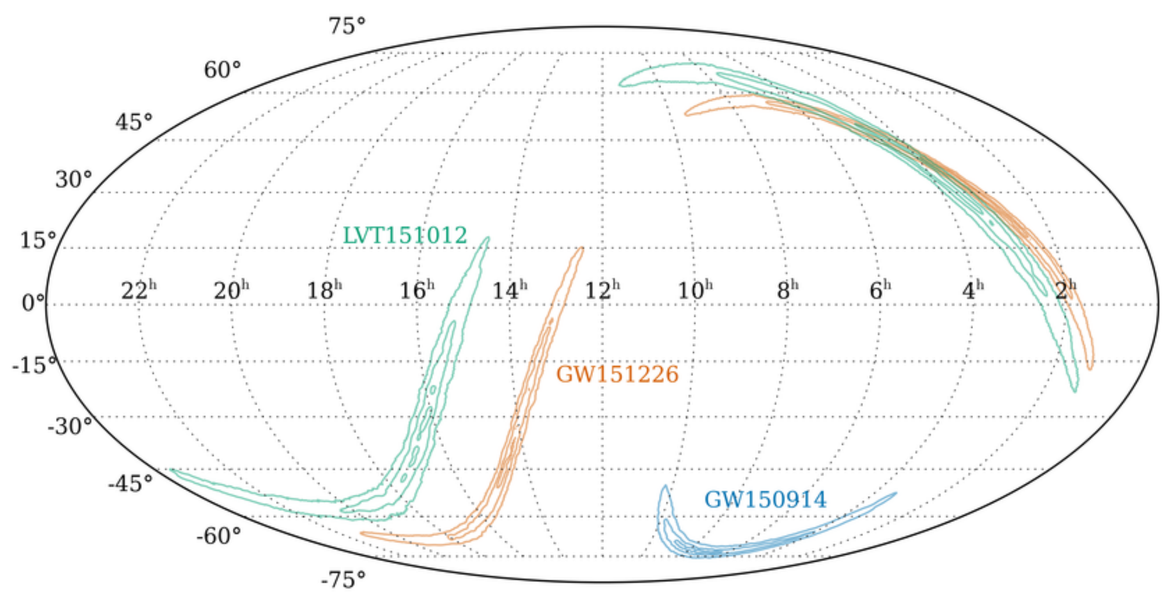

GPS: 1126259462.4

UTC Time: 2015-09-14 09:50

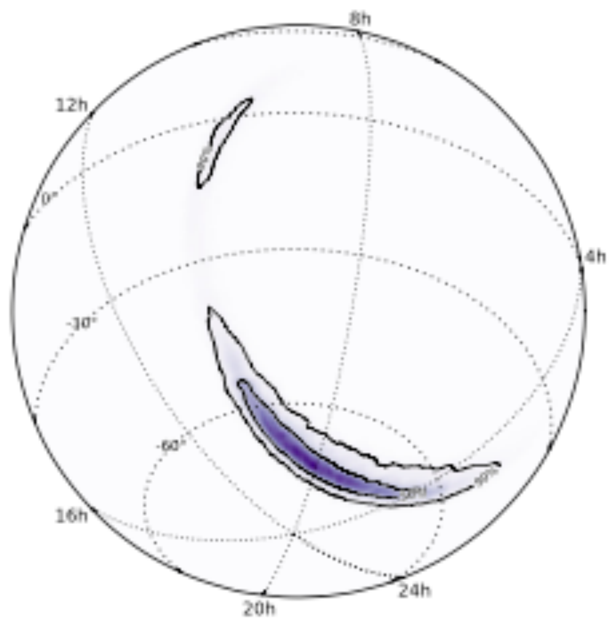

FIG. 4. An orthographic projection of the PDF for the sky location of GW150914 given in terms of right ascension α (measured in hours and labeled around the edge of the figure) and declination δ (measured in degrees and labeled inside the figure). The contours of the 50% and 90% credible regions are plotted over a color-coded PDF. The sky localization forms part of an annulus, set by the time delay of $6.9^{+0.5}_{-0.4}$ ms between the Livingston and Hanford detectors.

PRL 116 (2016) 241102

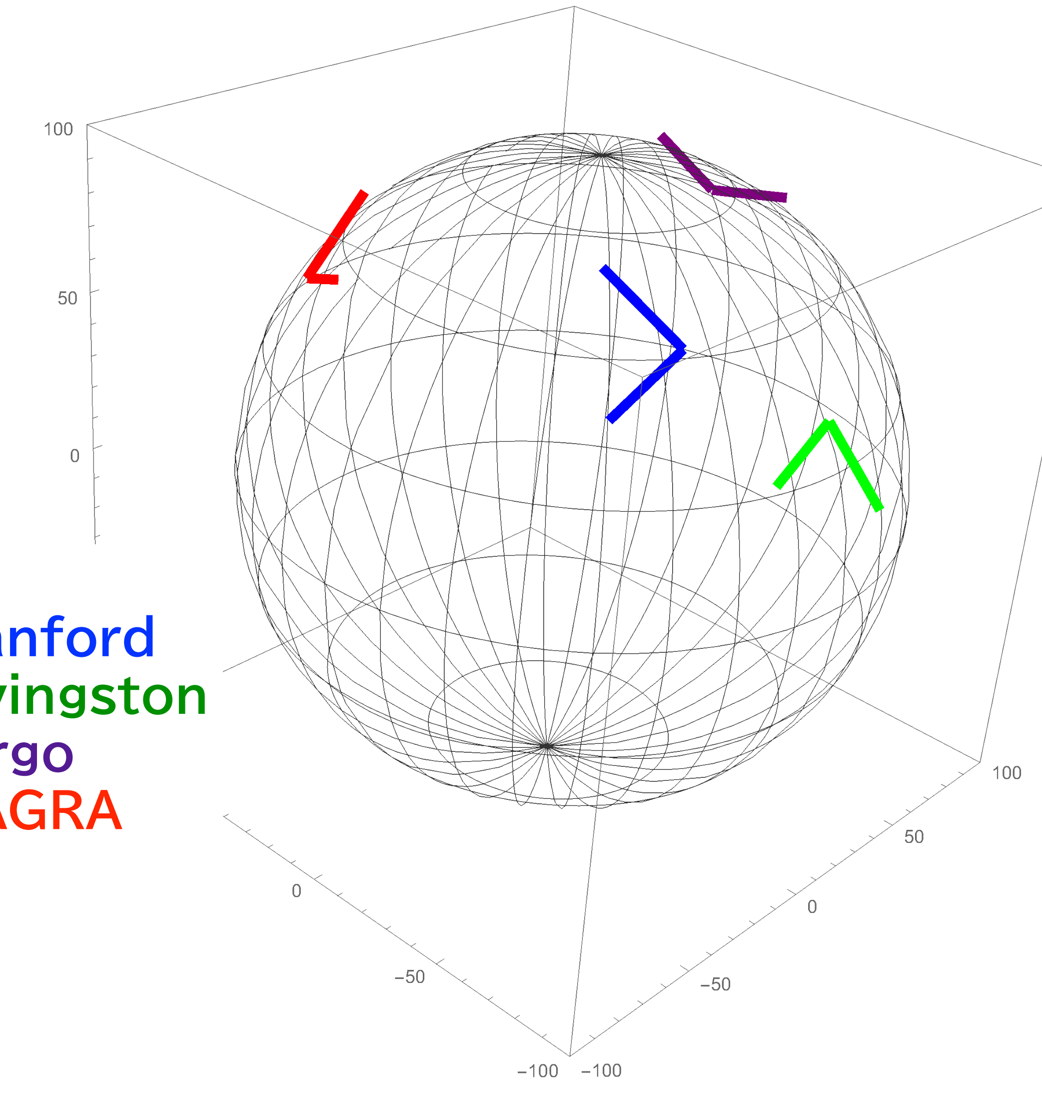

Hanford
Livingston
Virgo
KAGRA

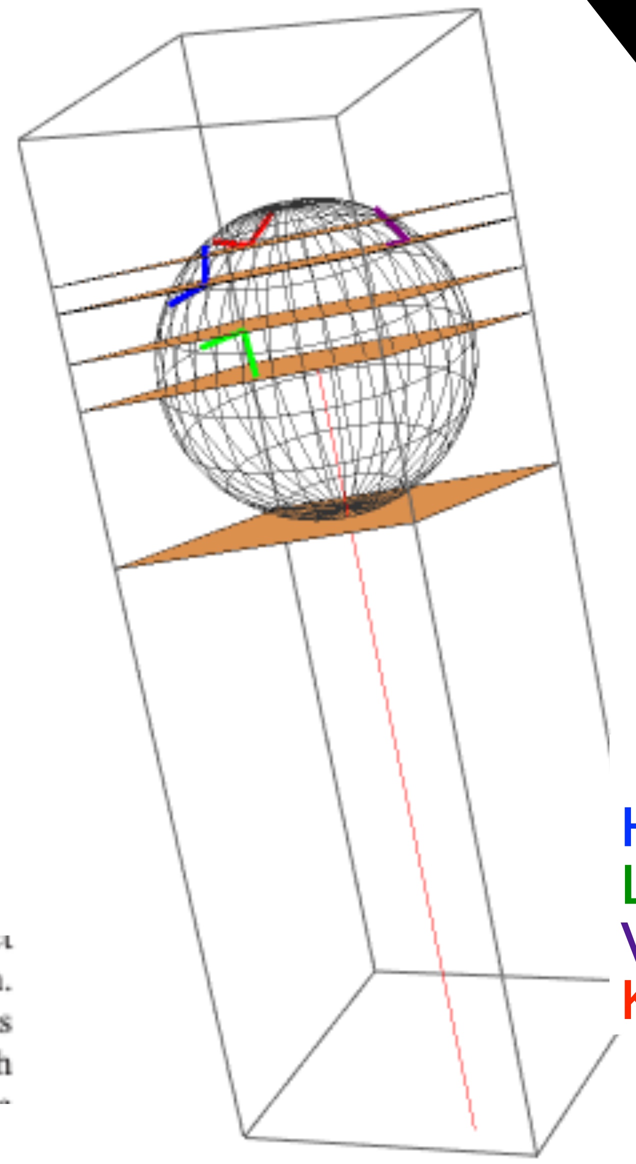

```
GW150914
delay time (msec) from t0
(+ delay, - advanced)

LHO  = 12.8483
LLO  =  6.26193
```

Hanford
Livingston
Virgo
KAGRA

PRL **116,** 221101 (2016) PHYSICAL RE

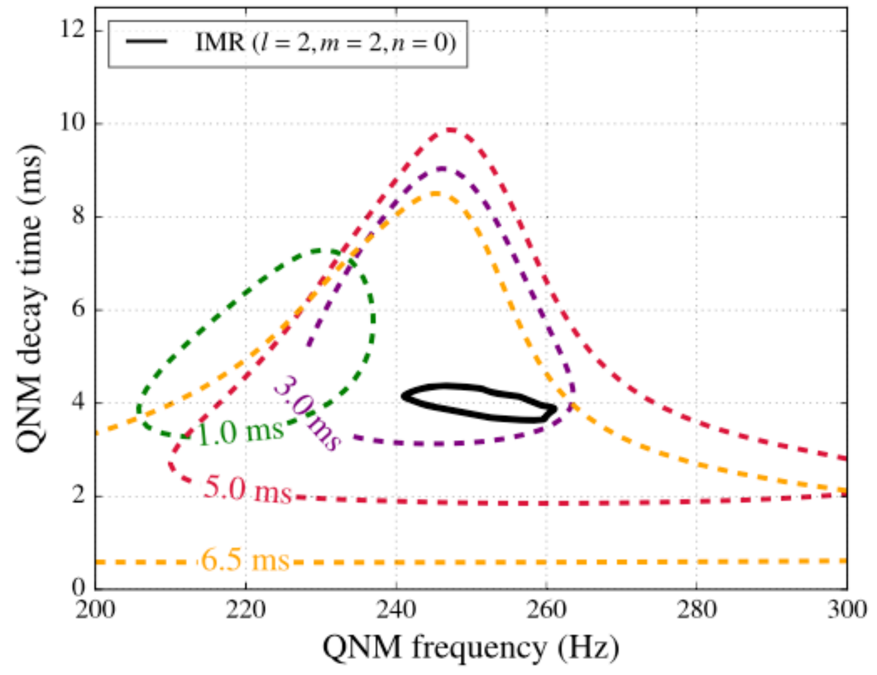

FIG. 5. 90% credible regions in the joint posterior distributions for the damped-sinusoid parameters f_0 and τ (see the main text), assuming start times $t_0 = t_M + 1, 3, 5, 6.5$ ms, where t_M is the merger time of the MAP waveform for GW150914. The black solid line shows the 90% credible region for the frequency and decay time of the $\ell = 2$, $m = 2$, $n = 0$ (i.e., the least-damped) QNM, as derived from the posterior distributions of the remnant mass and spin parameters.

https://www.gw-openscience.org/eventapi/html/GWTC-1-confident/GW150914/v3

Comparisons of the segment length

1. We show the segment time as its center, merger time = real merger time+seg. length/
2. Longer seg.length, short-lived ringdown modes hide behind the candidates
3. Shorter seg.length, we pick up many transient noises

GW150914

	1 segment = 32 points = 1/128 sec = 7.8125 ms	1 segment = 64 points = 1/64 sec = 15.625 ms	1 segment = 128 points = 1/32 sec = 31.25 ms	1 segment = 256 points = 1/16 sec = 62.5 ms

Hanford

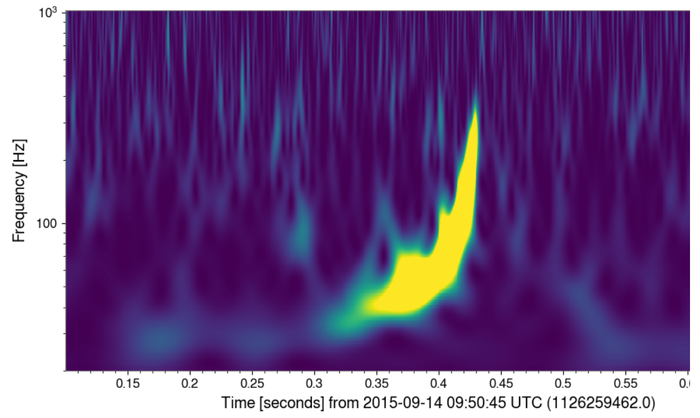

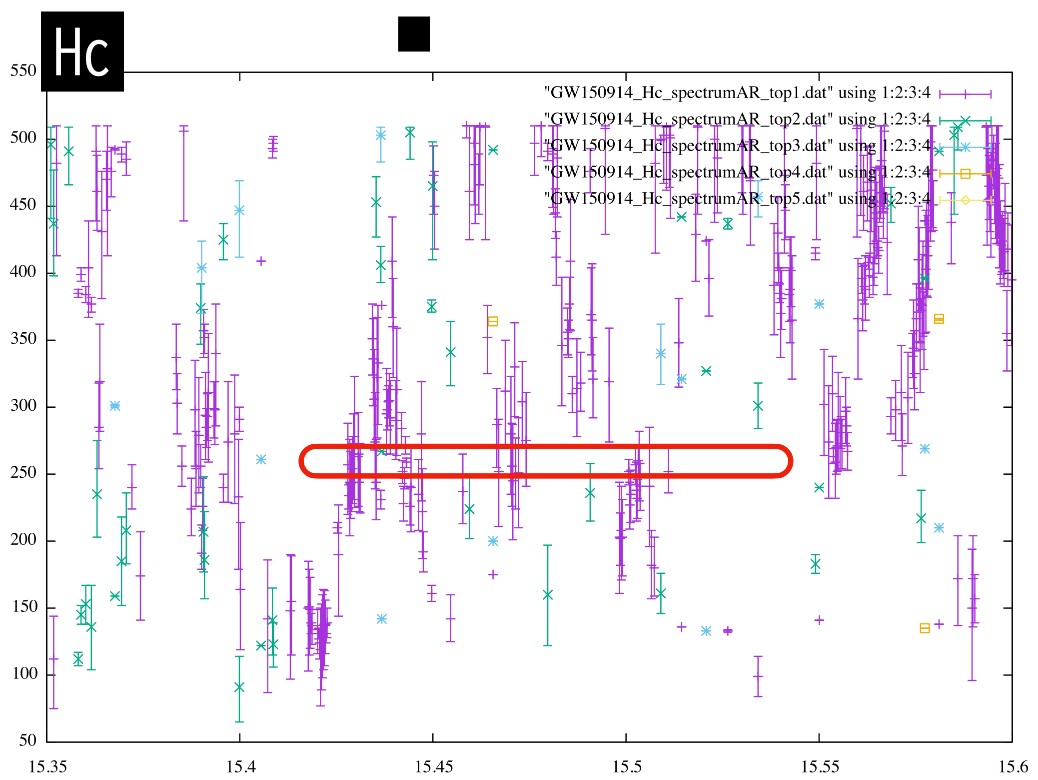

21 segments
f=251.85 +- 9.17 Hz
t=15.4285 -15.5449

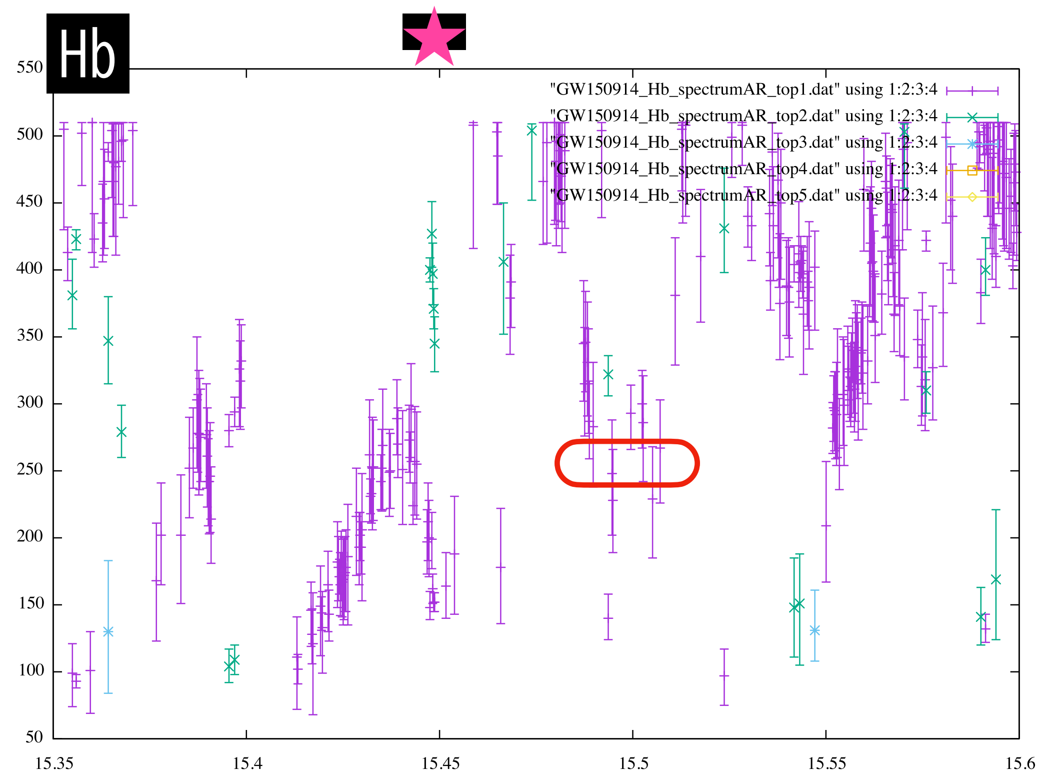

7 segments
f=251.63 +- 14.6 Hz
t=15.4705 -15.5188

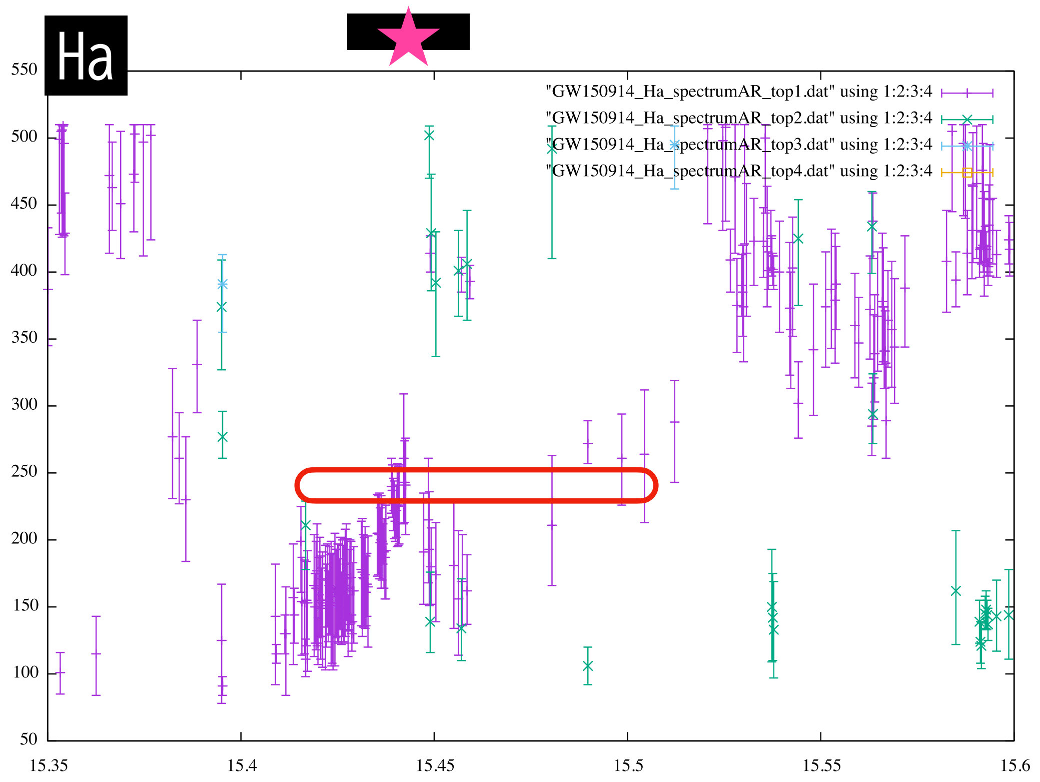

13 segments
f=242.20 +- 8.36 Hz
t=15.4351 -15.5132

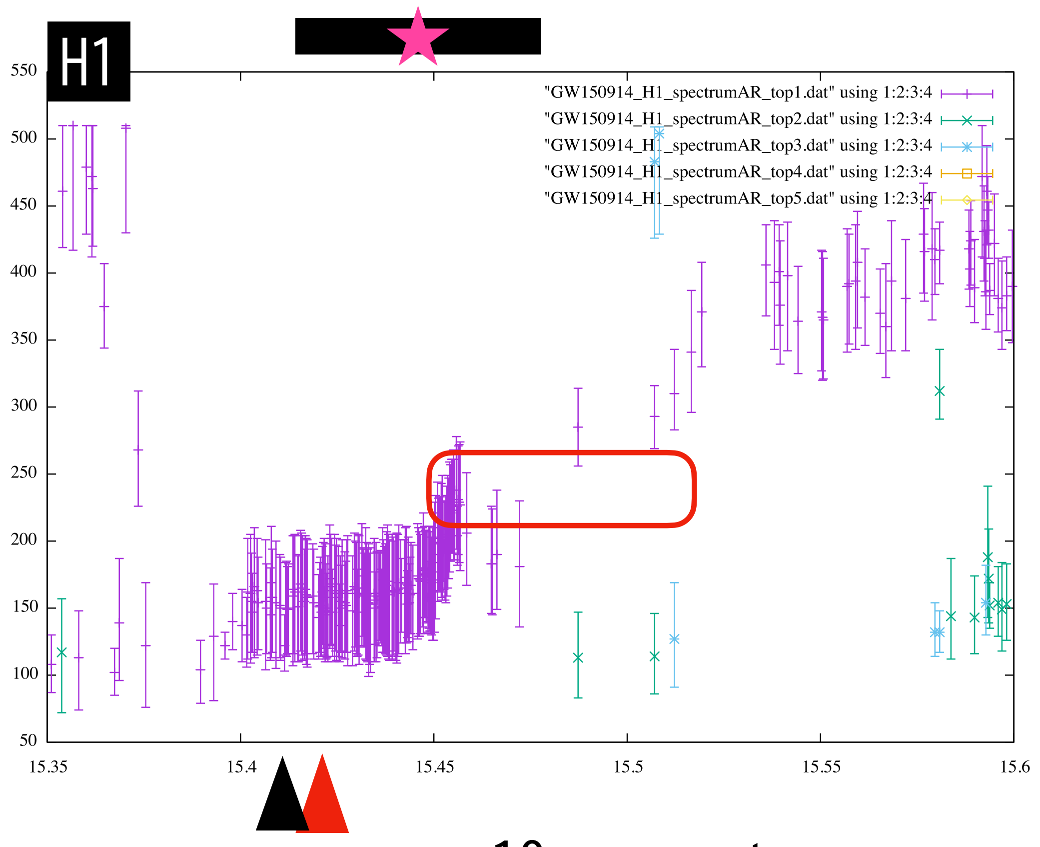

18 segments
f=249.07 +- 28.19 Hz
t=15.4578 -15.5286

Livingston

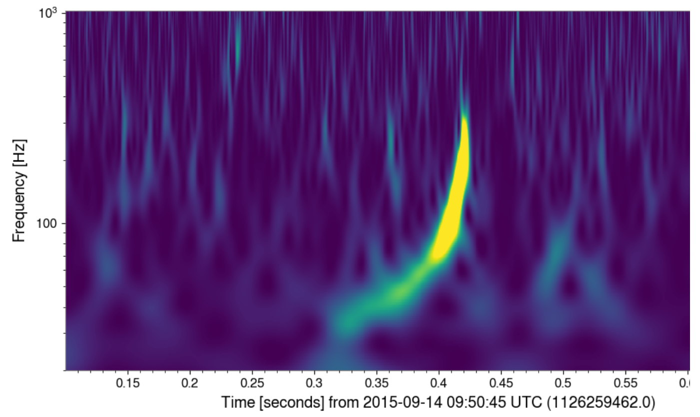

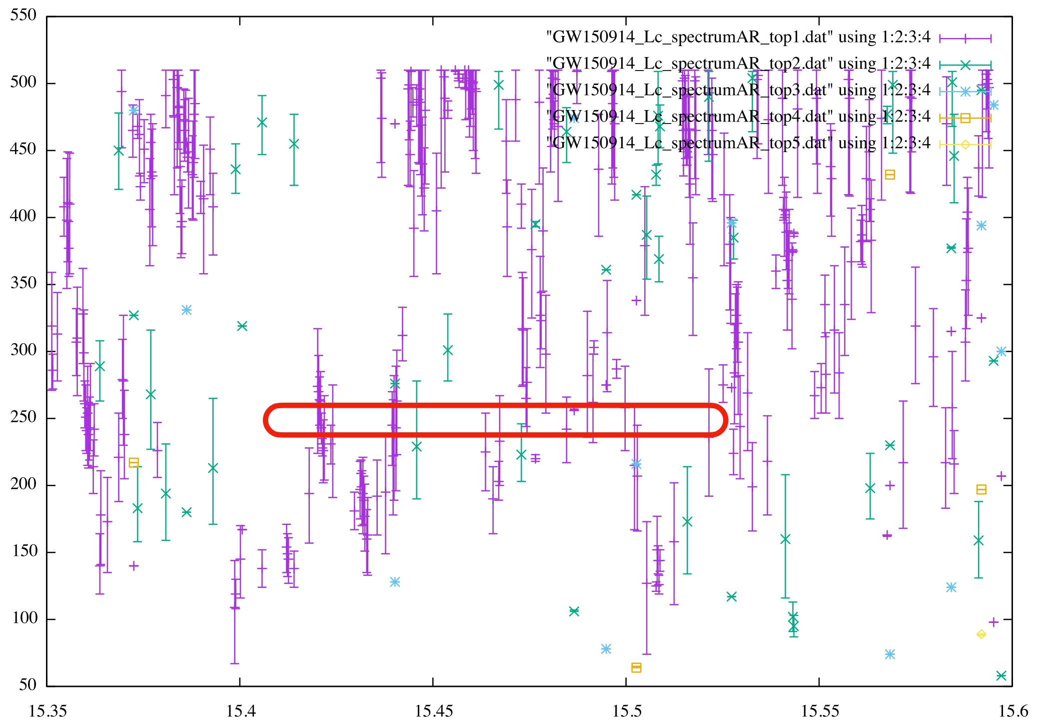

16 segments
f=251.57 +- 11.43 Hz
t=15.4177 -15.5295

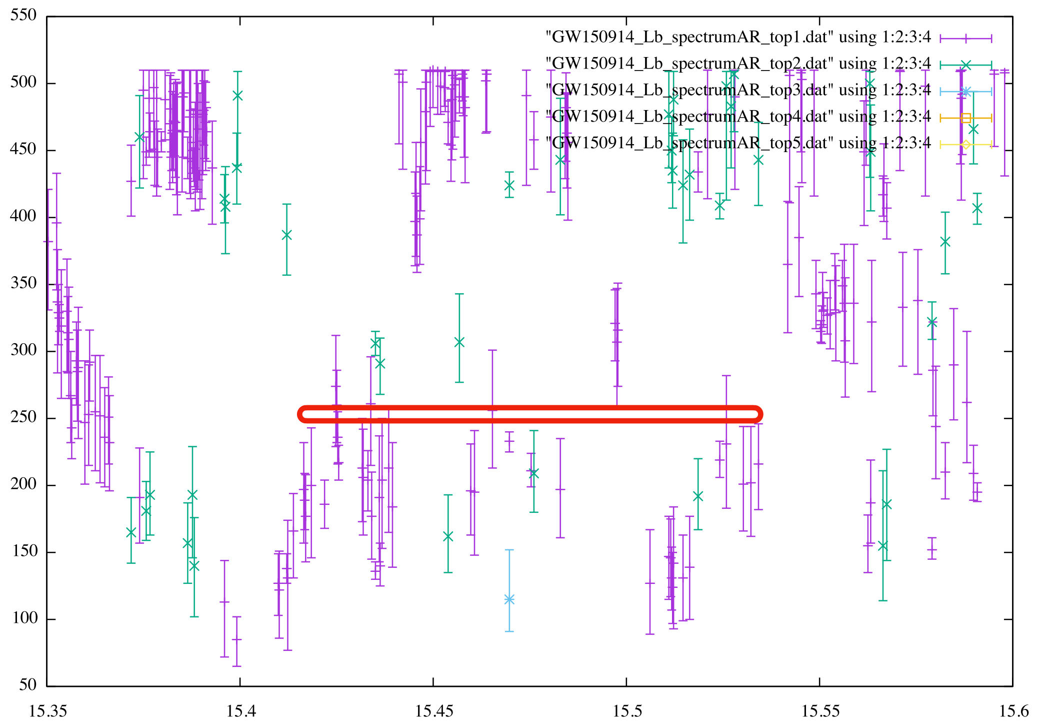

15 segments
f=248.52 +- 8.12 Hz
t=15.4199 -15.5352

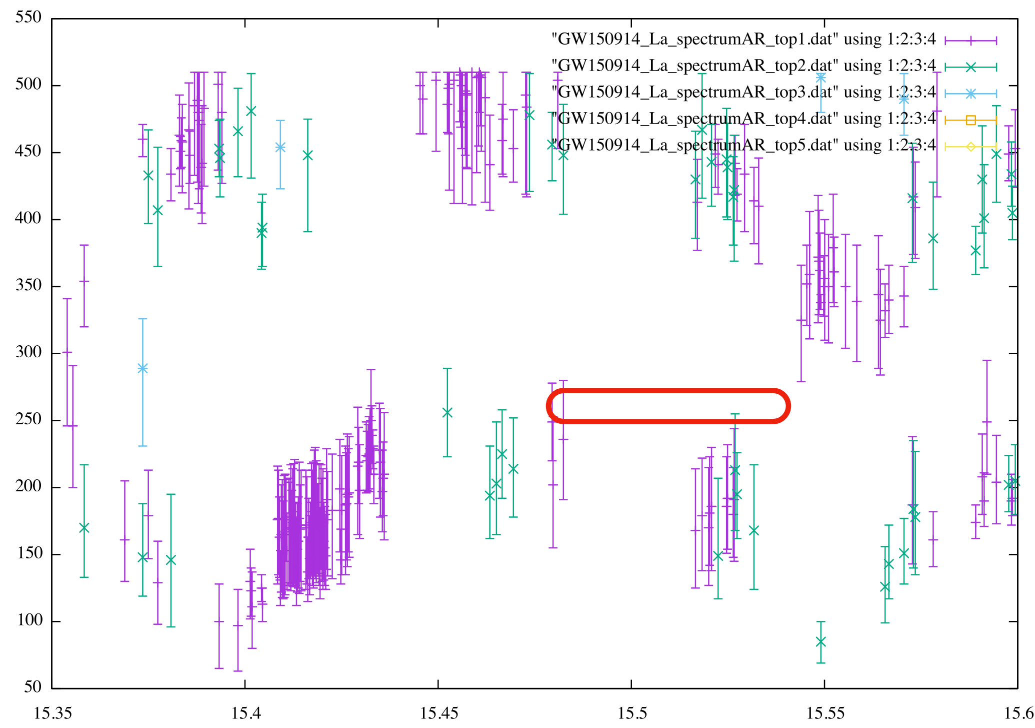

13 segments
f=254.29 +- 12.32 Hz
t=15.4763 -15.5447

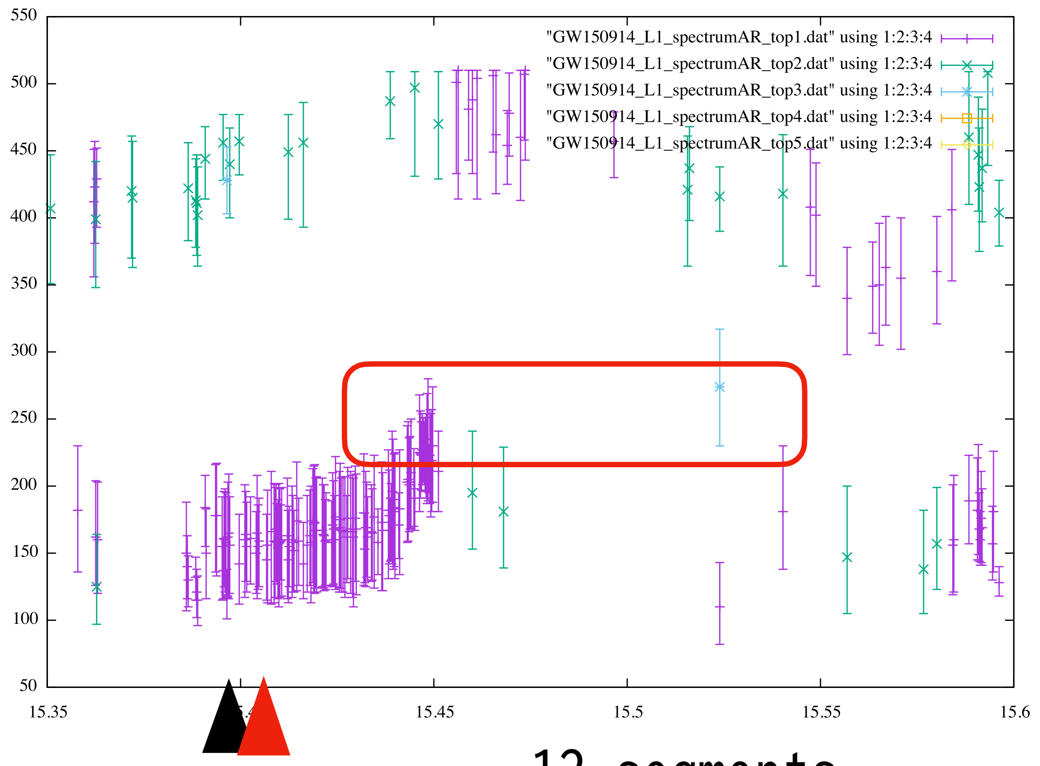

12 segments
f=248.64 +- 41.95 Hz
t=15.4443 -15.5432

GW150914

1 segment = 256 points
= 1/16 sec = 62.5 ms

LV paper ▸

$$(M, a, z) = (63.1^{+3.4}_{-3.}, 0.69^{+0.05}_{-0.04}, 0.09^{+0.03}_{-0.03})$$

f QNM
@Earth ▸

$$f_{220} = 249.4 + i\ 38.42\ \text{Hz},\ f_{221} = 244.0 + i\ 116.6\ \text{Hz},\ f_{222} = 233.7 + i\ 197.2\ \text{Hz}$$
$$f_{210} = 349.3 + i\ 62.91\ \text{Hz},\ f_{211} = 207.1 + i\ 117.5\ \text{Hz},\ f_{200} = 231.9 + i\ 49.46\ \text{Hz}$$
$$f_{330} = 395.3 + i\ 39.41\ \text{Hz},\ f_{331} = 392.1 + i\ 121.2\ \text{Hz},\ f_{332} = 386.3 + i\ 217.9\ \text{Hz}$$
$$f_{320} = 355.9 + i\ 39.73\ \text{Hz},\ f_{310} = 322.1 + i\ 53.2\ \text{Hz},\ f_{300} = 293.9 + i\ 41.37\ \text{Hz}$$

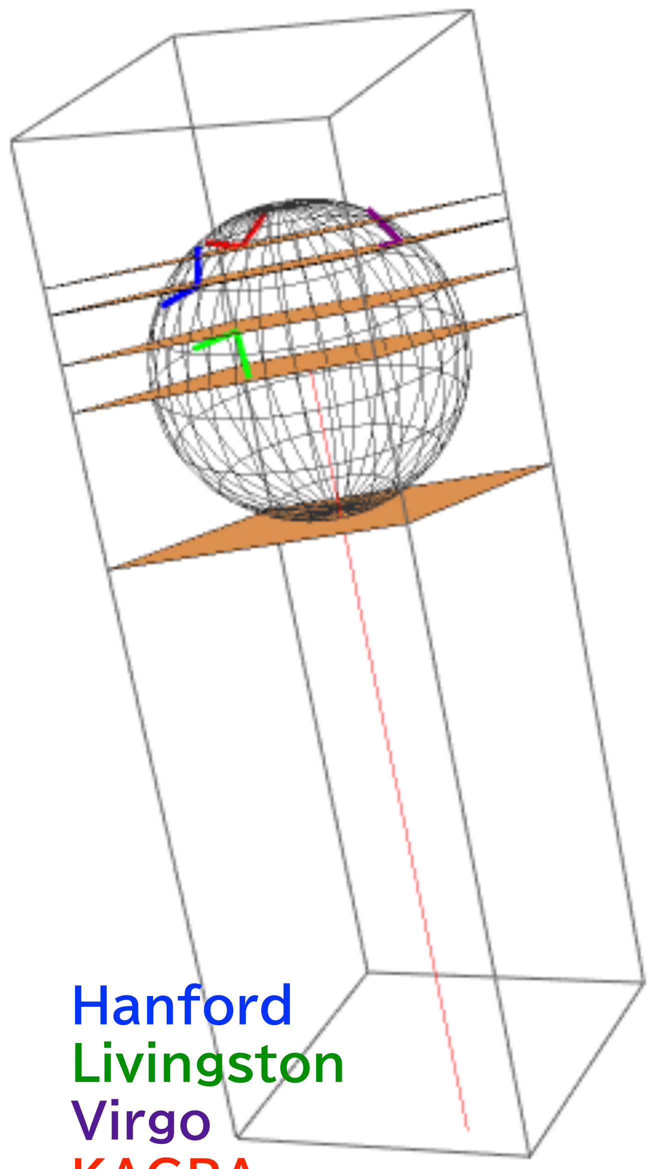

Hanford
Livingston
Virgo
KAGRA

Hanford

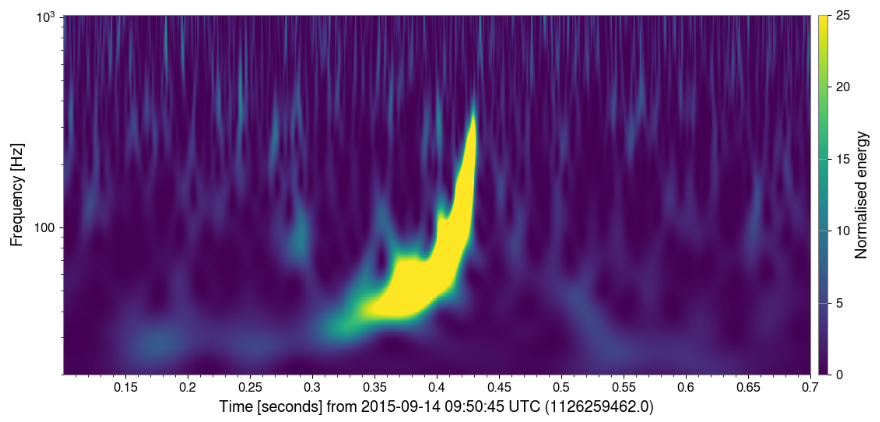

Hanford (SNR=20.6)

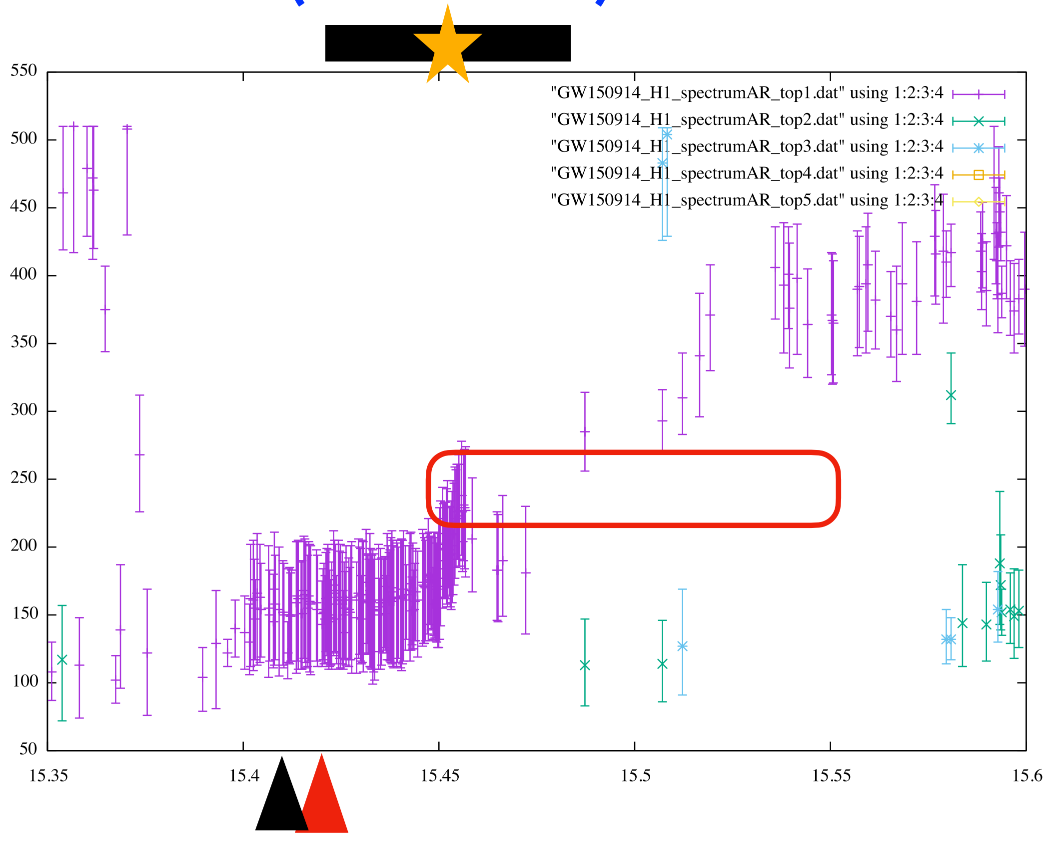

18 segments
f=249.07 +- 28.19 Hz
t=15.4578 -15.5286

Livingston

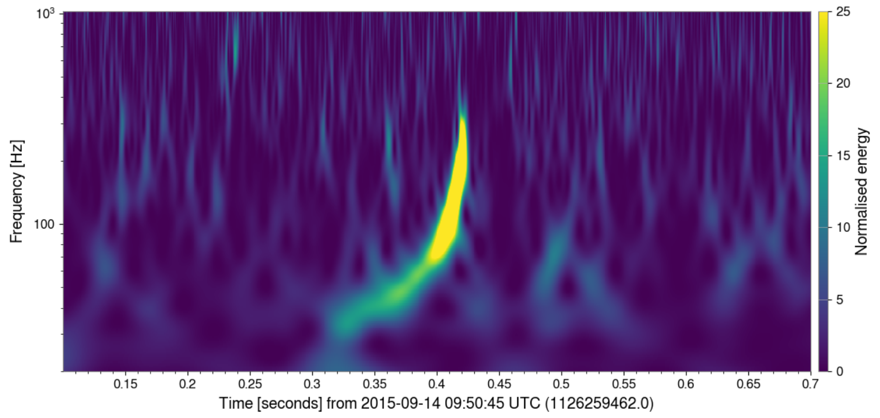

Livingston (SNR=14.2)

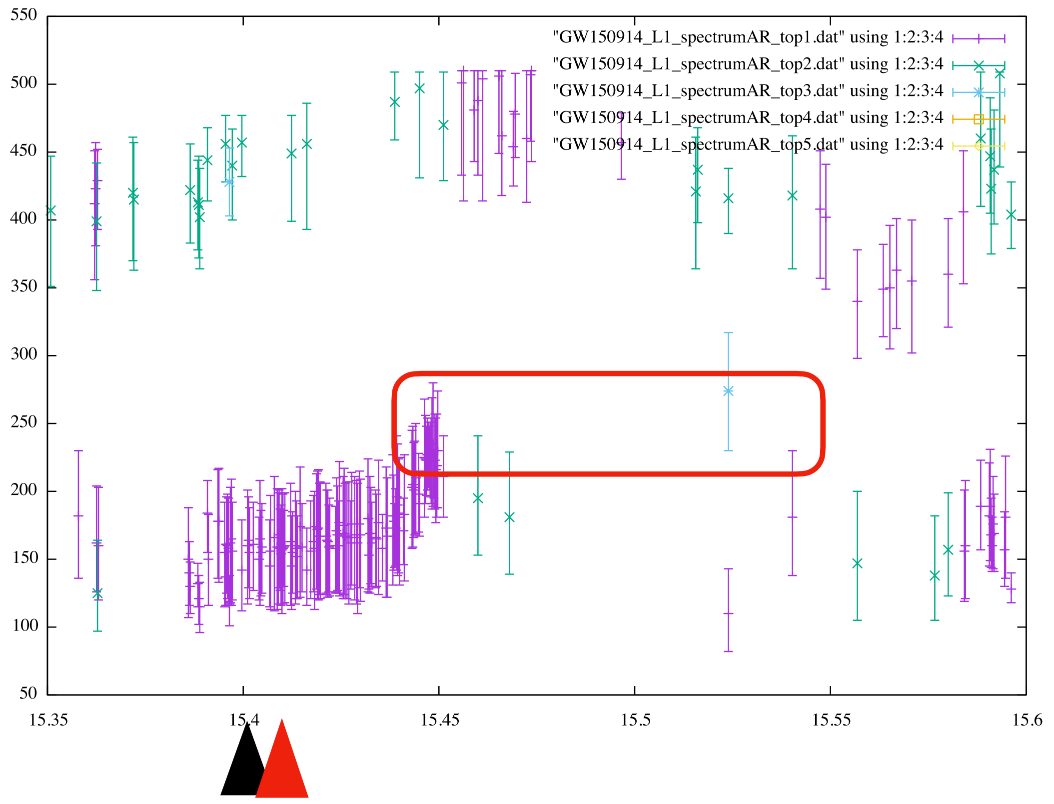

12 segments
f=248.64 +- 41.95 Hz
t=15.4443 -15.5432

1 segment = 256 points
= 1/16 sec = 62.5 ms

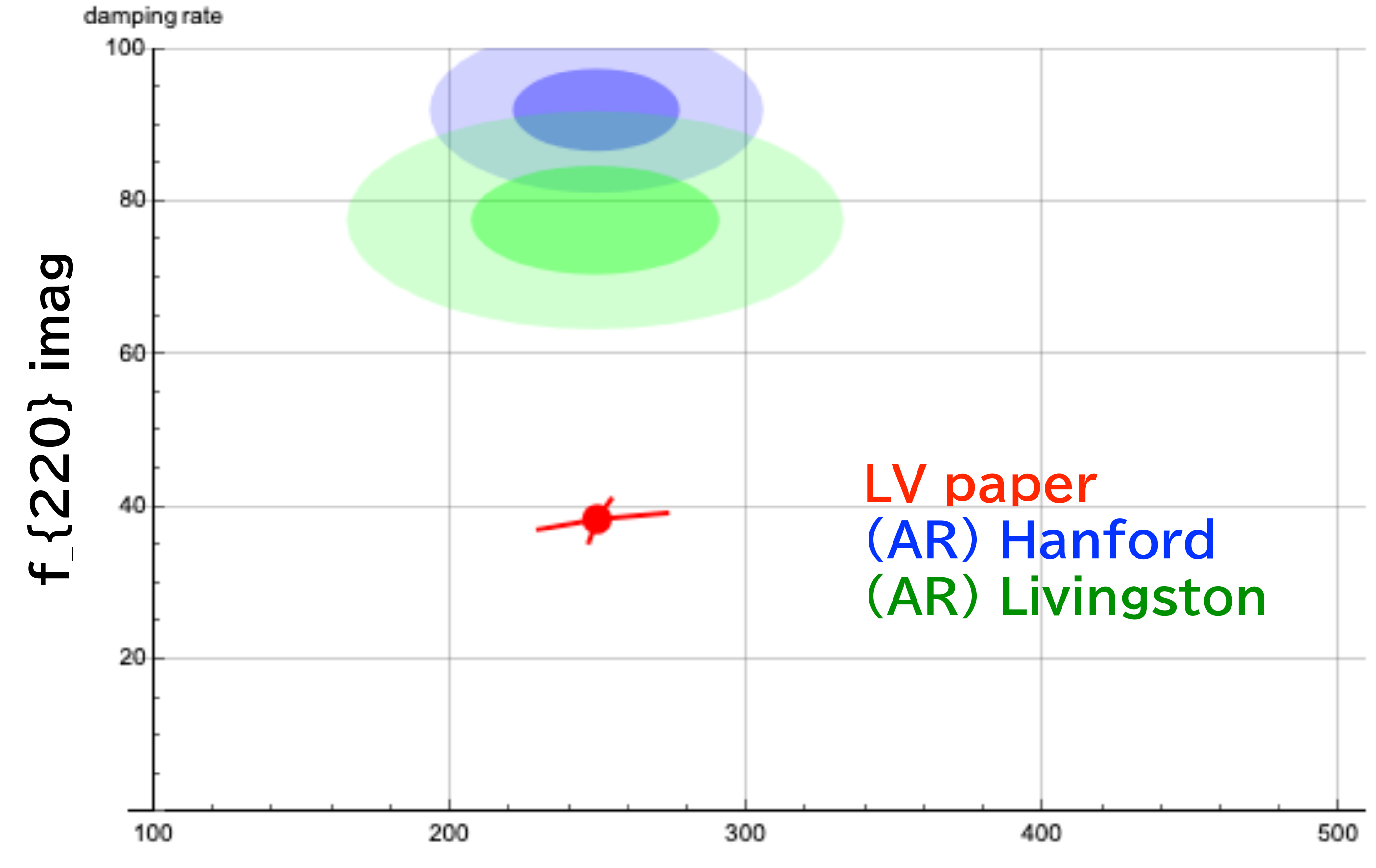

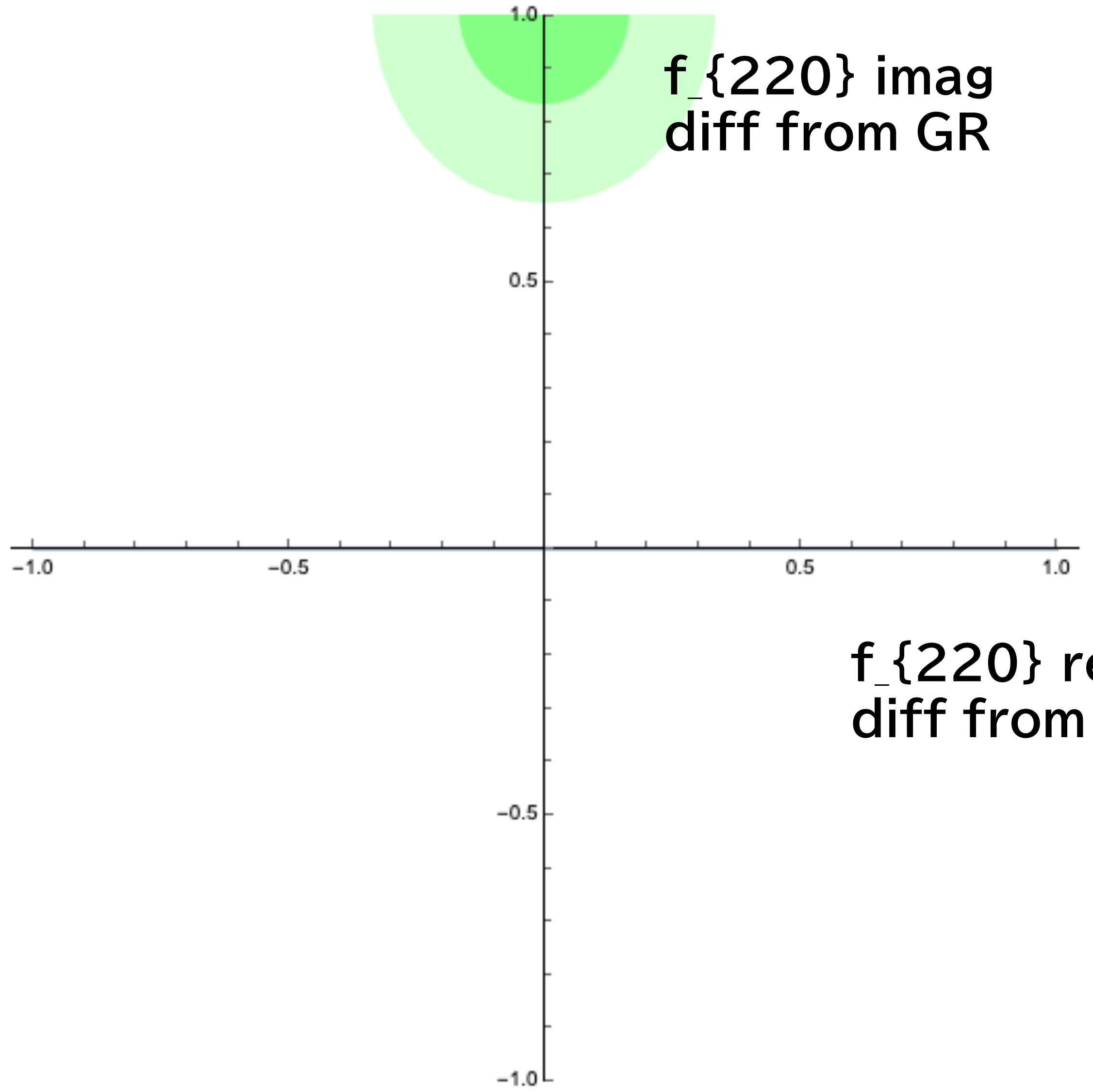

GW150914
delay time (msec) from t0
(+ delay, - advanced)

LHO = 12.8483
LLO = 6.26193

t_merger = 15.4 s
t_mergerH = 15.413
t_mergerL = 15.406

GW150914

1 segment = 32 points
= 1/128 sec = 7.8125 ms

LV paper

$$(M, a, z) = (63.1^{+3.4}_{-3.}, 0.69^{+0.05}_{-0.04}, 0.09^{+0.03}_{-0.03})$$

fQNM @Earth

$f_{220} = 249.4 + i\ 38.42$ Hz, $f_{221} = 244.0 + i\ 116.6$ Hz, $f_{222} = 233.7 + i\ 197.2$ Hz
$f_{210} = 349.3 + i\ 62.91$ Hz, $f_{211} = 207.1 + i\ 117.5$ Hz, $f_{200} = 231.9 + i\ 49.46$ Hz
$f_{330} = 395.3 + i\ 39.41$ Hz, $f_{331} = 392.1 + i\ 121.2$ Hz, $f_{332} = 386.3 + i\ 217.9$ Hz
$f_{320} = 355.9 + i\ 39.73$ Hz, $f_{310} = 322.1 + i\ \ 53.2$ Hz, $f_{300} = 293.9 + i\ 41.37$ Hz

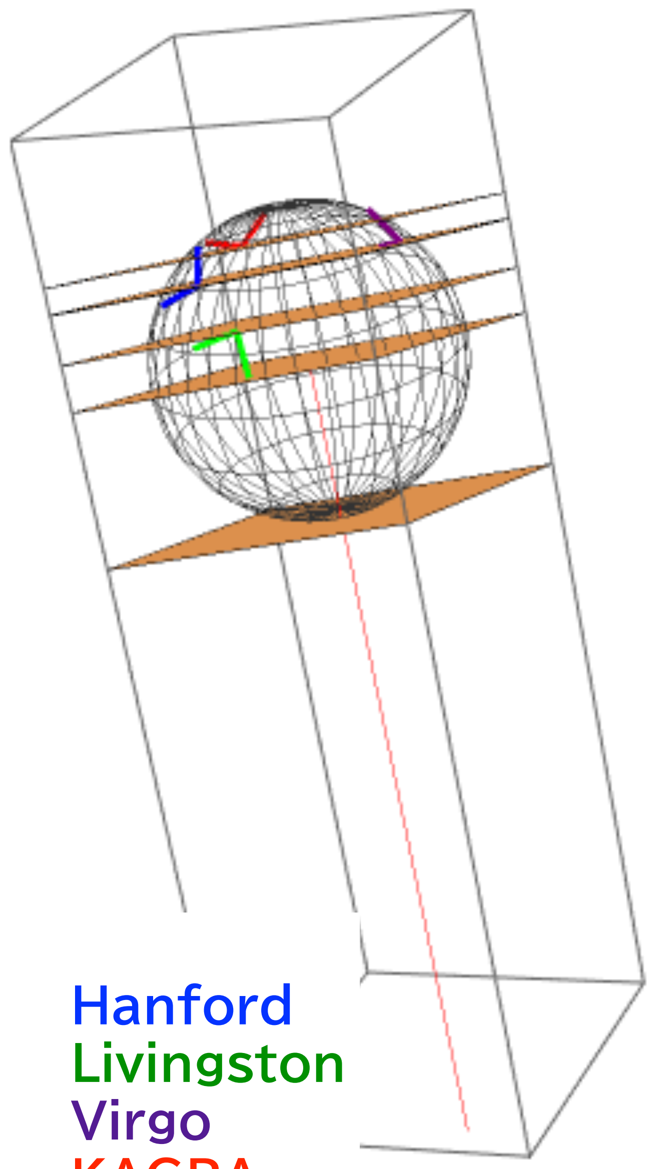

Hanford
Livingston
Virgo
KAGRA

Hanford

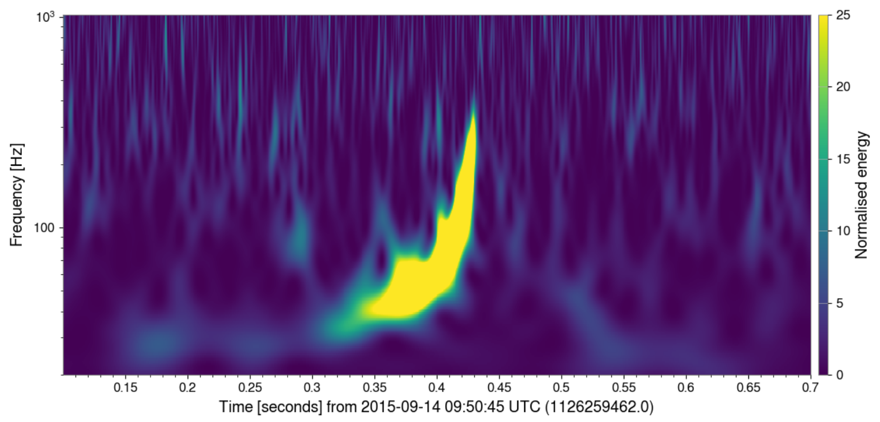

Livingston

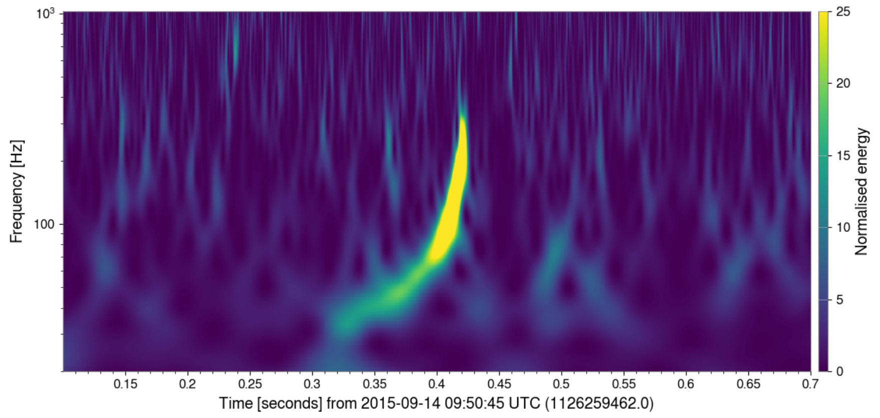

Hanford (SNR=20.6)

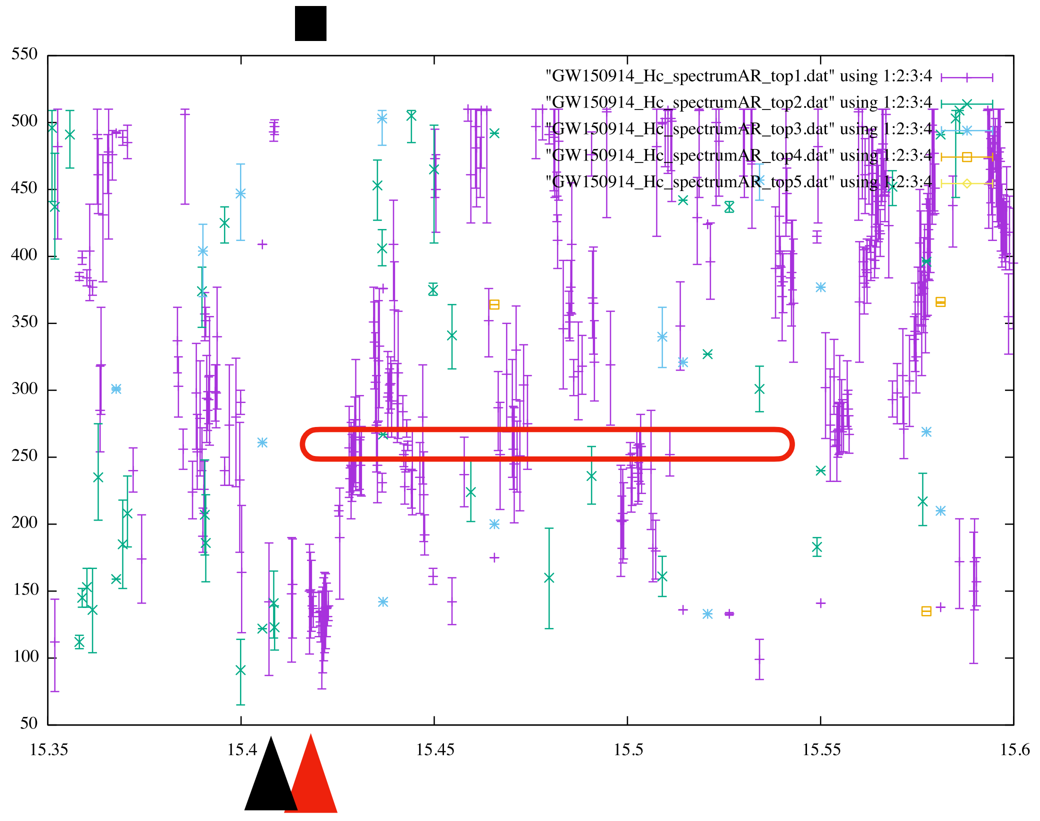

21 segments
f=251.85 +- 9.17 Hz
t=15.4285 -15.5449

f_{220} starts 8ms after t_merger

Livingston (SNR=14.2)

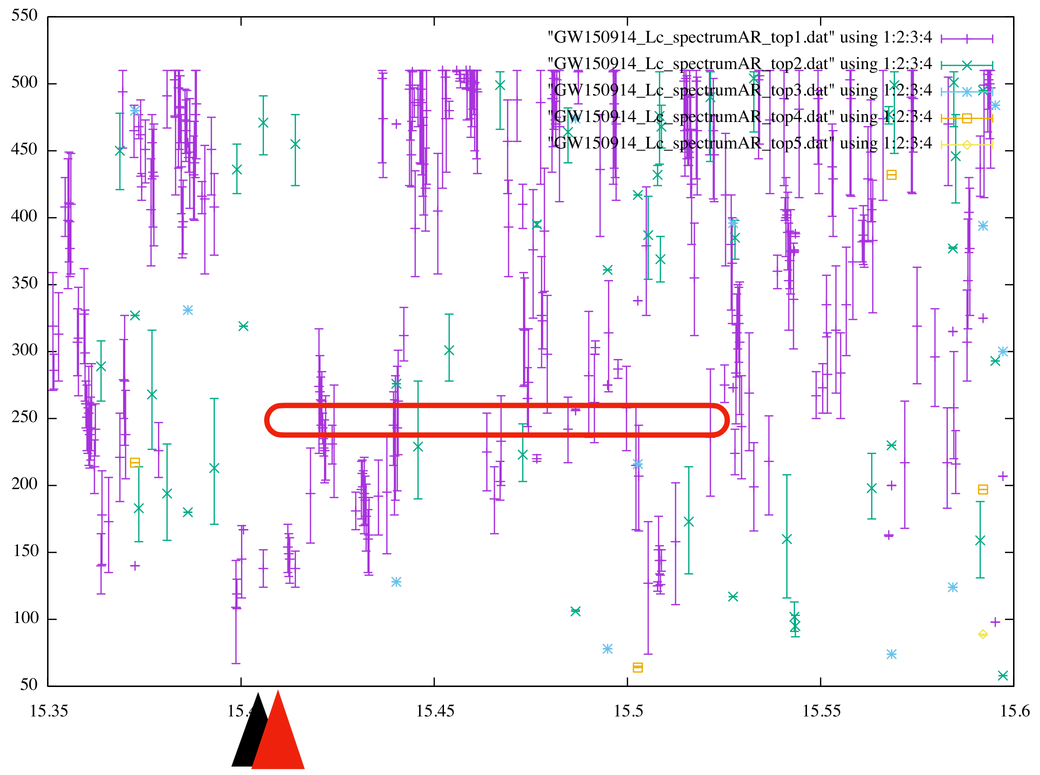

16 segments
f=251.57 +- 11.43 Hz
t=15.4177 -15.5295

f_{220} starts 11ms after t_merger

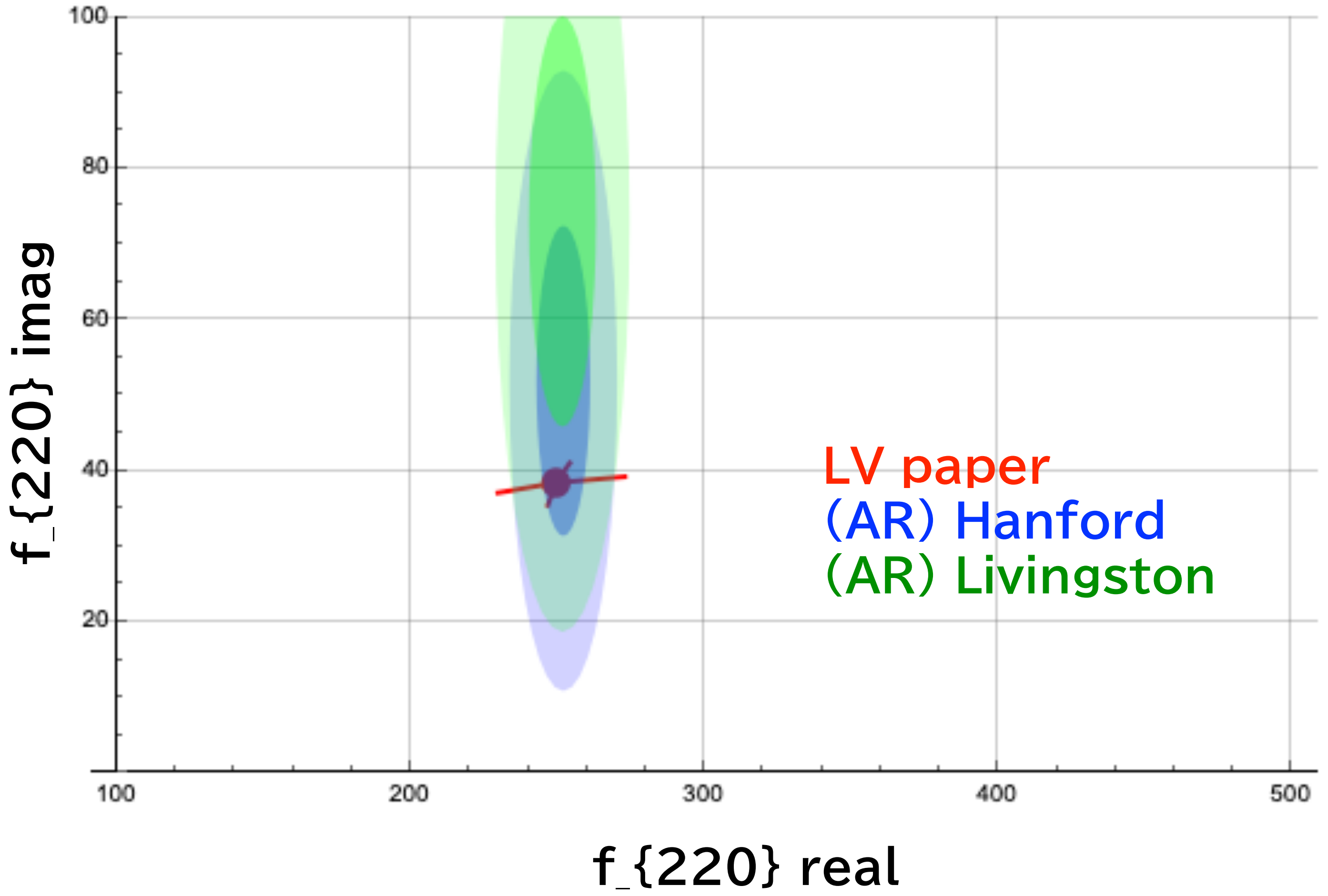

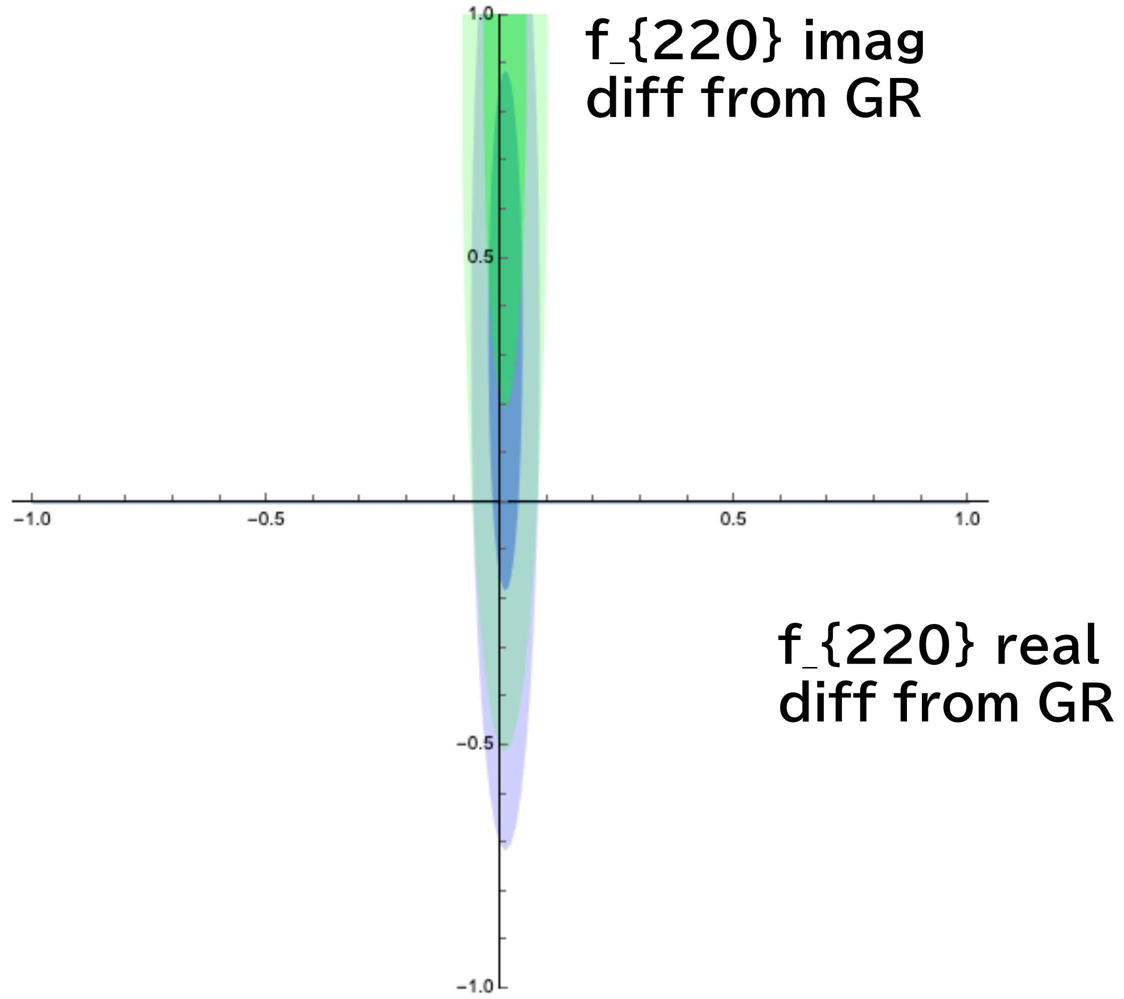

GW150914
delay time (msec) from t0
(+ delay, - advanced)

LHO = 12.8483
LLO = 6.26193

t_merger = 15.4 s
t_mergerH = 15.413
t_mergerL = 15.406

+3.9ms
t_mergerH = 15.417
t_mergerL = 15.410

For both, we picked up 251.6 Hz
Livingston picks up 11ms earlier than Hanford
We see ringdown 8ms after the merger @Livingston, 11ms @Hanford

GW190412

Network SNR=18.9

1 segment = 64 points
= 1/64 sec = 15.625 ms

LV paper ▶

$(M, a, z) = (37.3^{+3.9}_{-3.8}, 0.67^{+0.06}_{-0.07}, 0.15^{+0.03}_{-0.03})$

fQNM @Earth ▶

$f_{220} = 393.7 + i\ 62.17$ Hz, $f_{221} = 384.7 + i\ 188.9$ Hz, $f_{222} = 367.4 + i\ 319.9$ Hz
$f_{210} = 562.9 + i\ 103.0$ Hz, $f_{211} = 328.9 + i\ 190.0$ Hz, $f_{200} = 372.7 + i\ 79.98$ Hz
$\boxed{f_{330} = 624.8 + i\ 63.84 \text{ Hz}}$, $f_{331} = 619.4 + i\ 196.1$ Hz, $f_{332} = 609.5 + i\ 354.1$ Hz
$f_{320} = 565.1 + i\ 64.26$ Hz, $f_{310} = 513.6 + i\ 84.68$ Hz, $f_{300} = 470.2 + i\ 66.54$ Hz

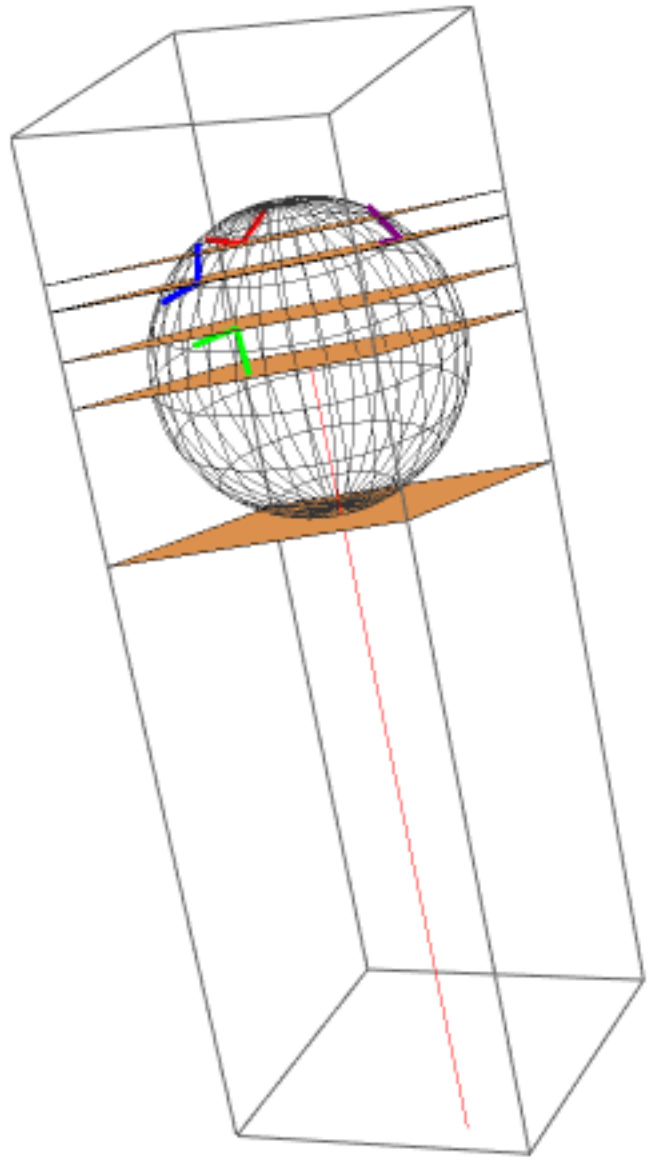

Hanford

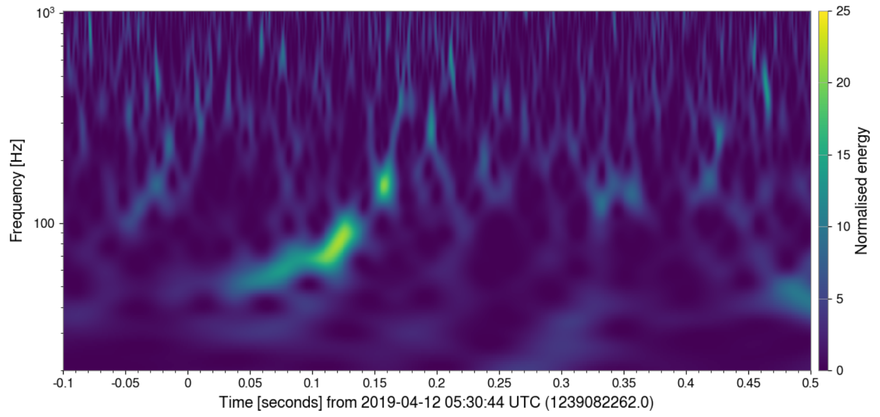

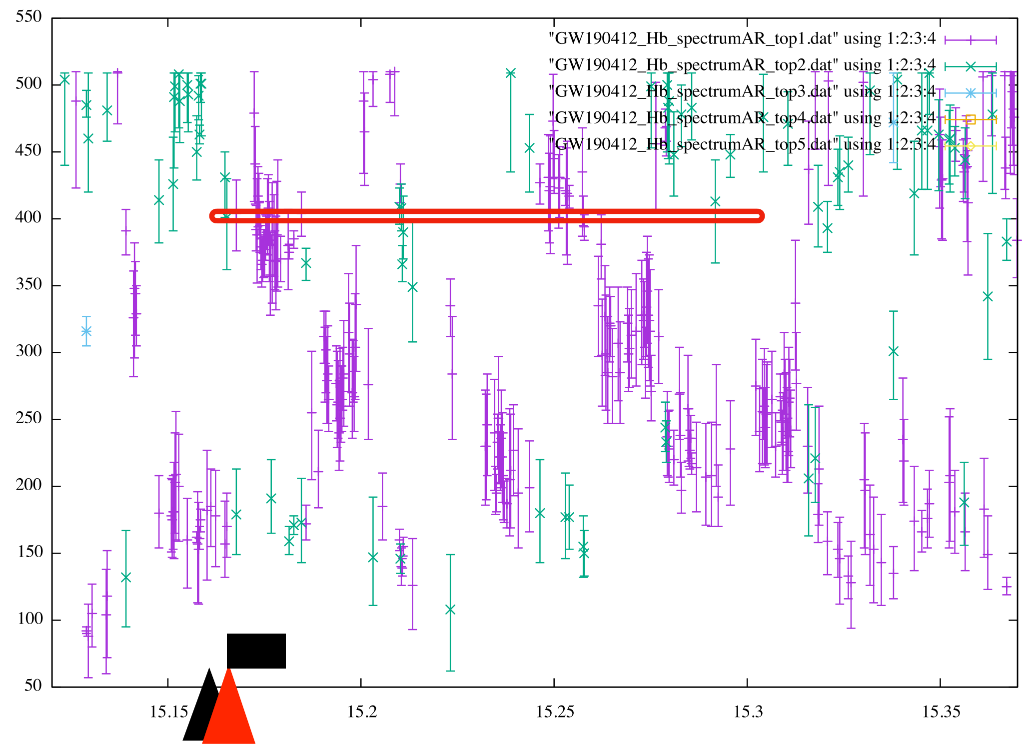

21 segments
f=394.97 +- 5.74 Hz
t=15.1675 -15.3018

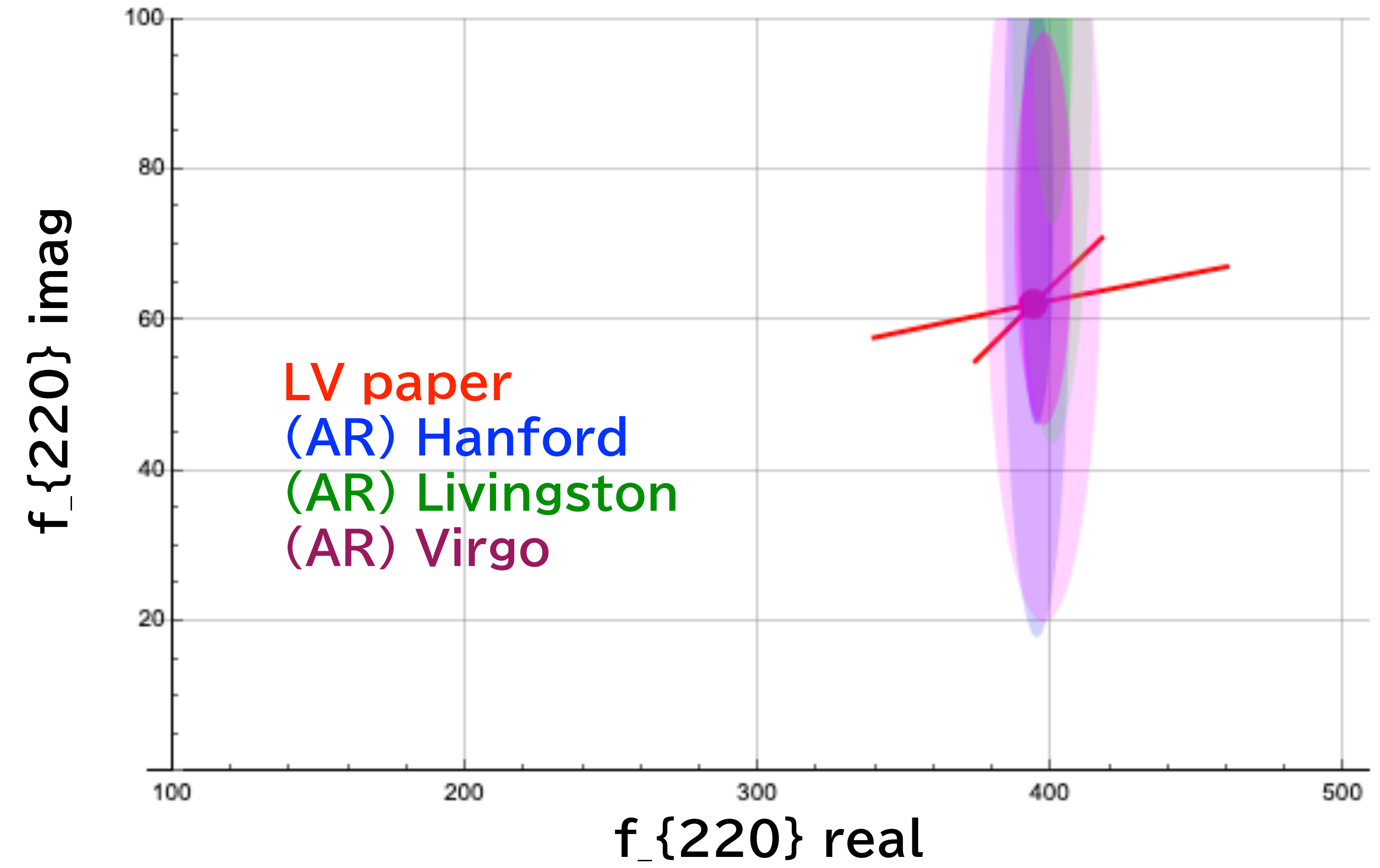

Livingston

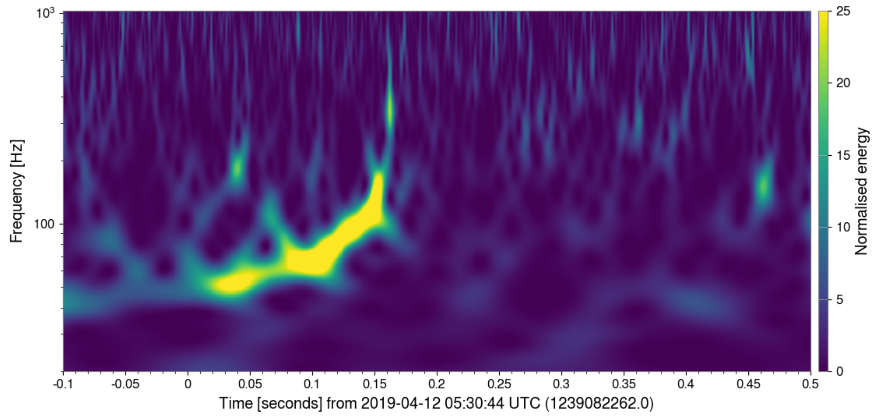

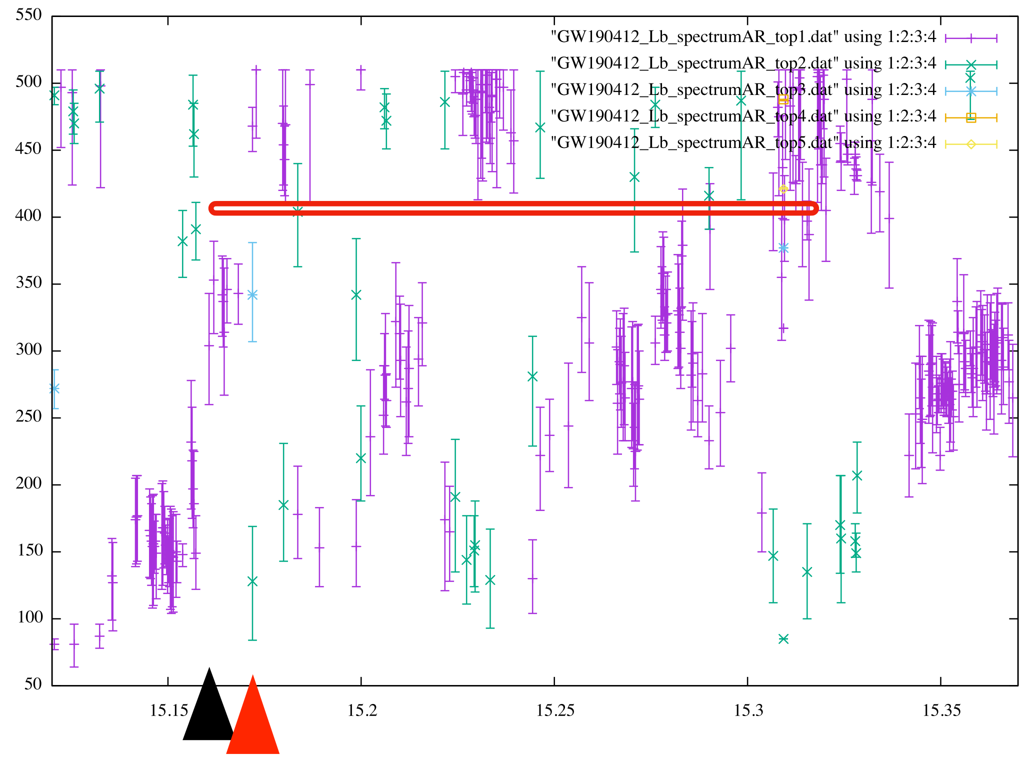

19 segments
f=400.28 +- 6.93 Hz
t=15.1660 -15.3159

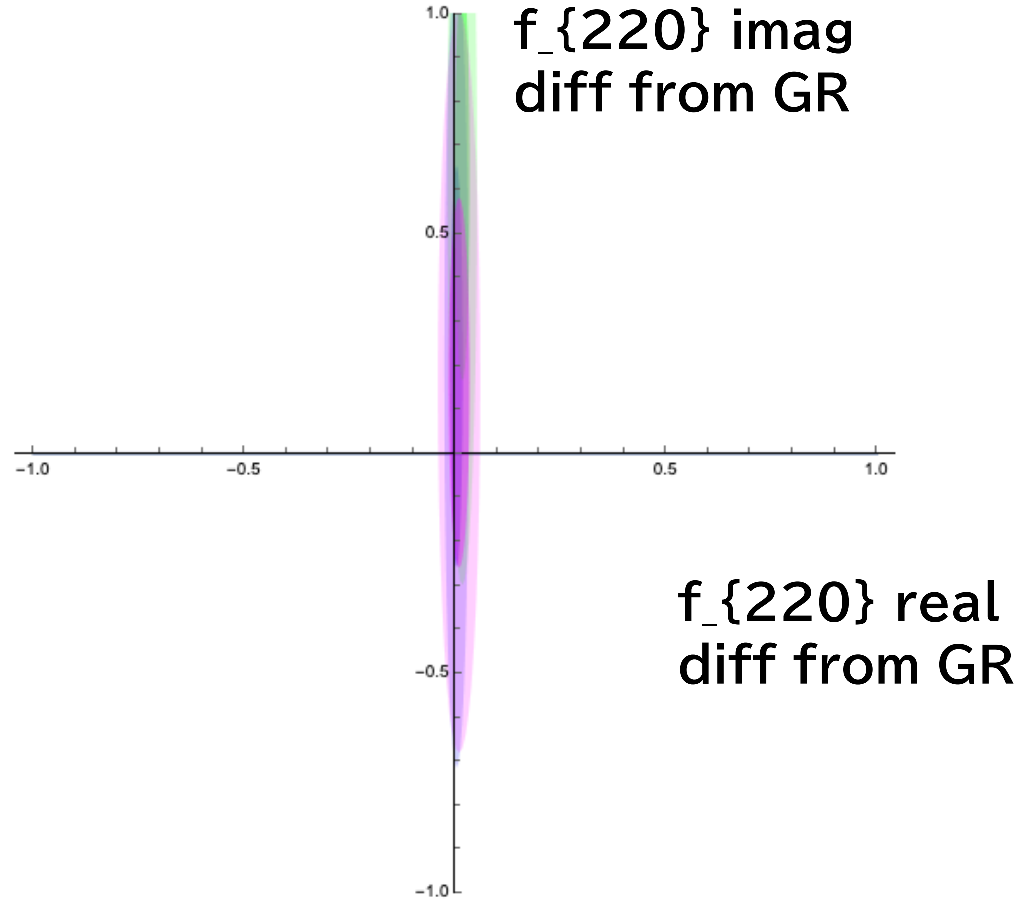

GW190412
delay time (msec) from t0
(+ delay, - advanced)

LHO = 0.87046
LLO = 7.94444
Virgo= -11.2685

t_merger = 15.166
t_mergerH = 15.167
t_mergerL = 15.174
t_mergerV = 15.105

Virgo

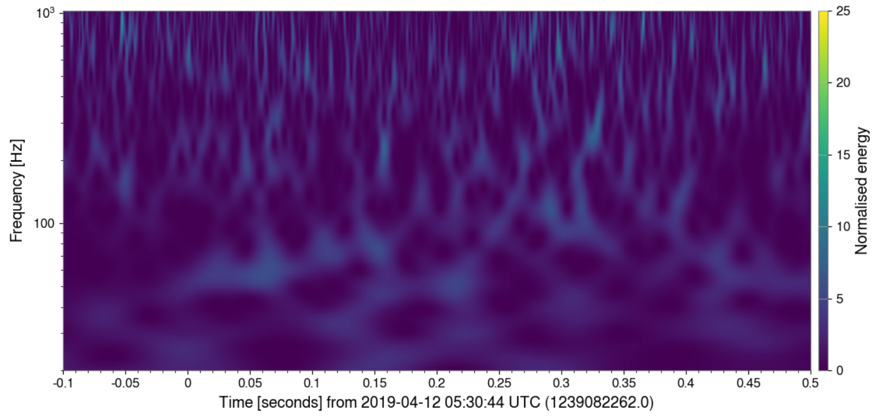

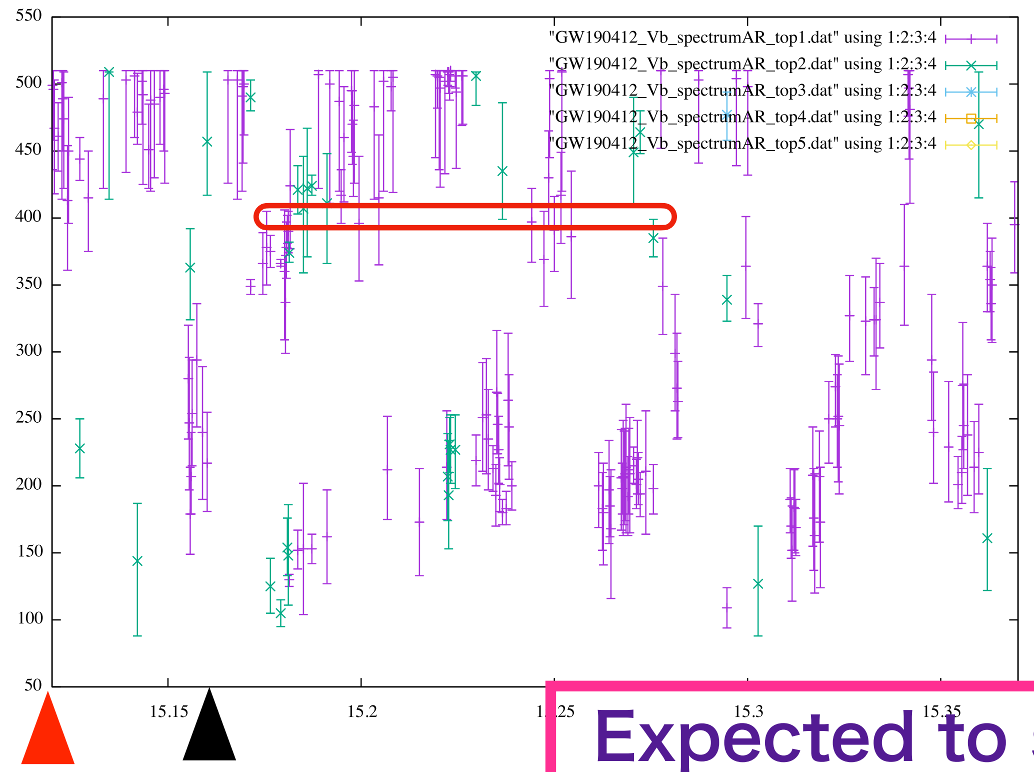

12 segments
f=397.33 +- 9.90 Hz
t=15.1699 -15.2835

Expected to see 3-3 mode, but N/A due to large noise in higher freq.

GW190521

Network SNR=14.2

1 segment = 64 points
= 1/64 sec = 15.625 ms

LV paper ▶

$$(M, a, z) = (150.3^{+35.8}_{-20.}, 0.73^{+0.11}_{-0.14}, 0.72^{+0.29}_{-0.29})$$

fQNM @Earth ▶

$f_{220} = 68.54 + i\ 10.00$ Hz, $f_{221} = 67.28 + i\ 30.31$ Hz, $f_{222} = 64.79 + i\ 51.07$ Hz
$f_{210} = 91.92 + i\ 15.99$ Hz, $f_{211} = 56.20 + i\ 30.67$ Hz, $f_{200} = 61.42 + i\ 12.92$ Hz
$f_{330} = 108.4 + i\ 10.23$ Hz, $f_{331} = 107.7 + i\ 31.52$ Hz, $f_{332} = 106.3 + i\ 56.17$ Hz
$f_{320} = 96.67 + i\ 10.35$ Hz, $f_{310} = 86.73 + i\ 14.37$ Hz, $f_{300} = 78.55 + i\ 10.93$ Hz

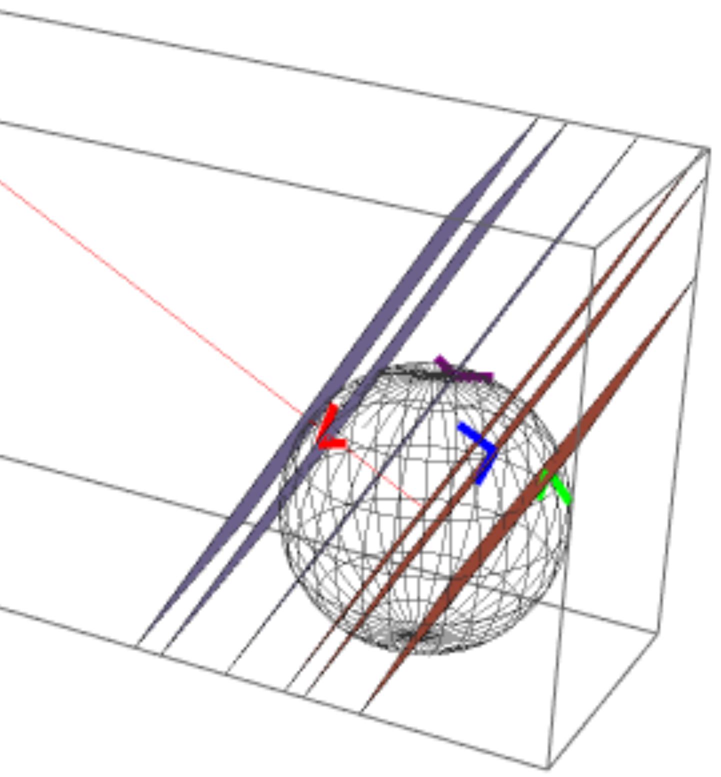

Hanford

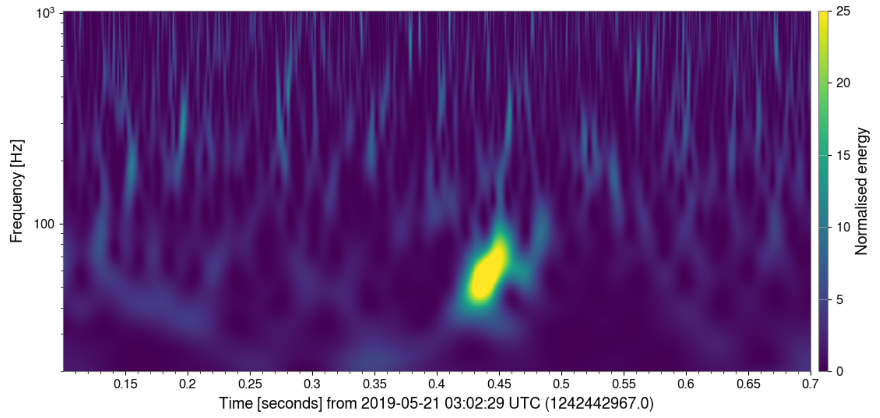

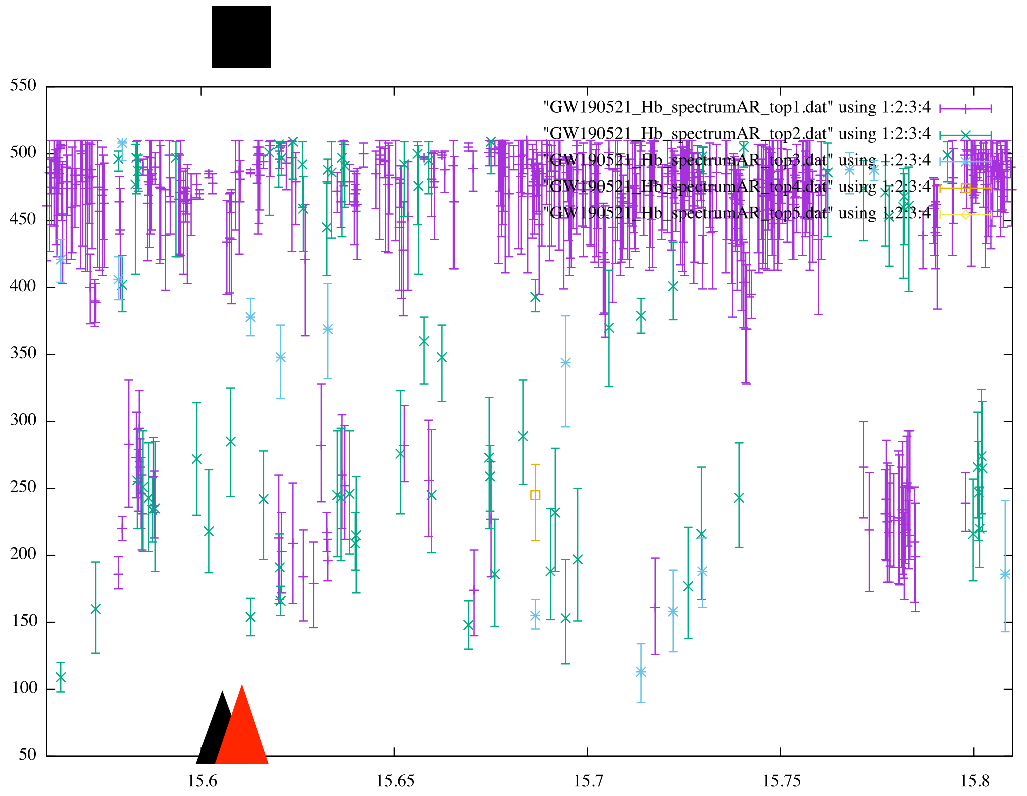

Livingston

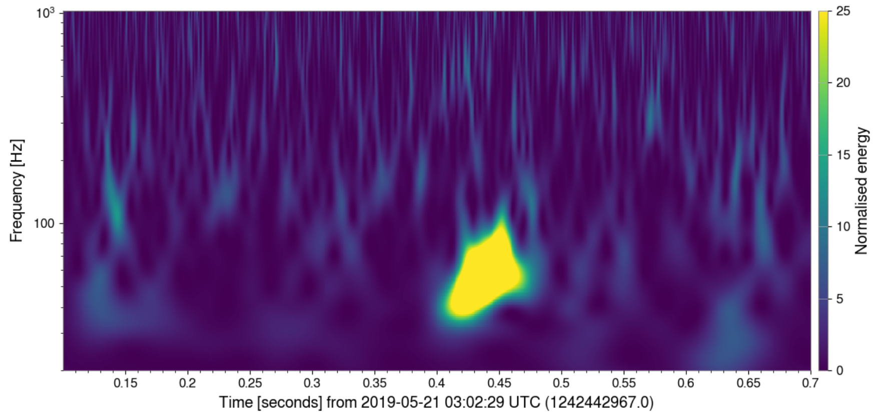

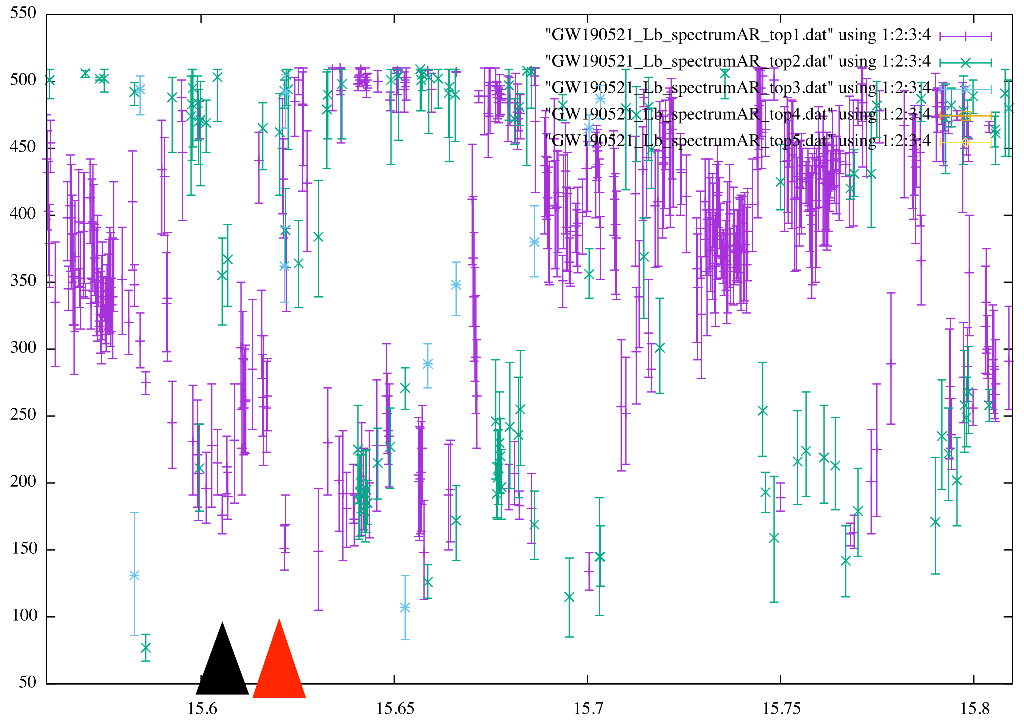

Full of noises at lower freq.

Virgo

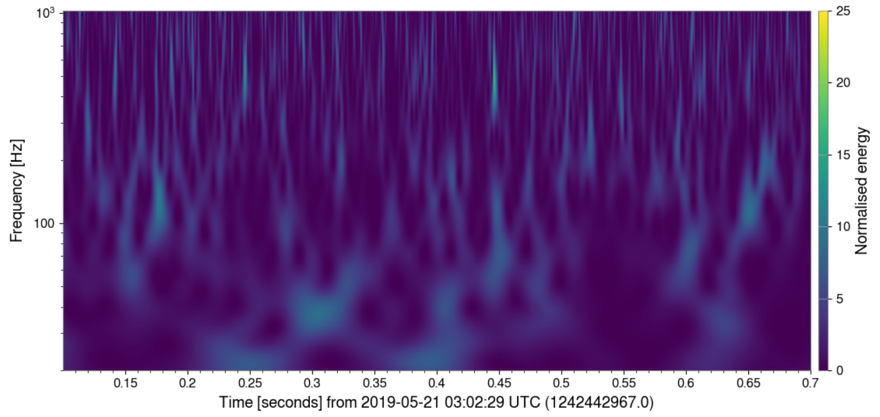

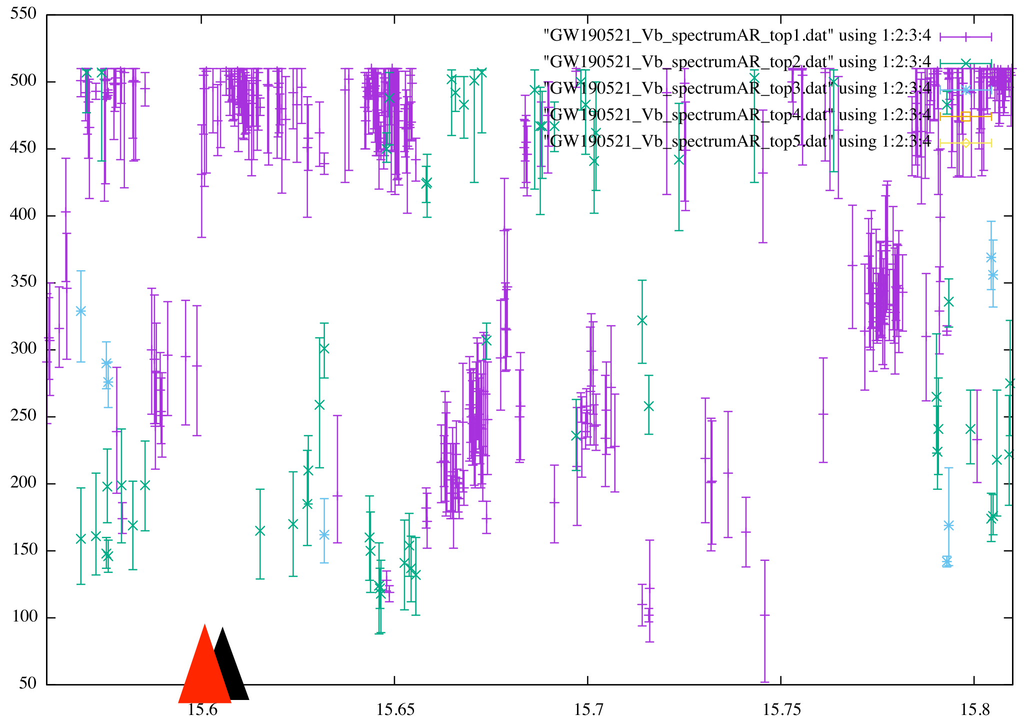

```
GW190521
delay time (msec) from tʊ
(+ delay, - advanced)

LHO  =  2.6754
LLO  = 10.3767
Virgo= -8.27122
```

t_merger = 15.61 s
t_mergerH = 15.613
t_mergerL = 15.620
t_mergerV = 15.602

GW190521_074359

Network SNR=25.8

1 segment = 64 points
= 1/64 sec = 15.625 ms

LV paper ▶

$$(M, a, z) = (70.7^{+6.4}_{-4.2}, 0.72^{+0.05}_{-0.07}, 0.25^{+0.06}_{-0.1})$$

fQNM
@Earth ▶

$f_{220} = 198.8 + i\ 29.43$ Hz, $f_{221} = 195.0 + i\ 89.23$ Hz, $f_{222} = 187.5 + i\ 150.5$ Hz
$f_{210} = 269.7 + i\ 47.34$ Hz, $f_{211} = 163.6 + i\ 90.18$ Hz, $f_{200} = 179.9 + i\ 37.98$ Hz
$f_{330} = 314.7 + i\ 30.14$ Hz, $f_{331} = 312.5 + i\ 92.78$ Hz, $f_{332} = 308.3 + i\ 165.7$ Hz
$f_{320} = 281.3 + i\ 30.46$ Hz, $f_{310} = 252.9 + i\ 41.88$ Hz, $f_{300} = 229.5 + i\ 32.02$ Hz

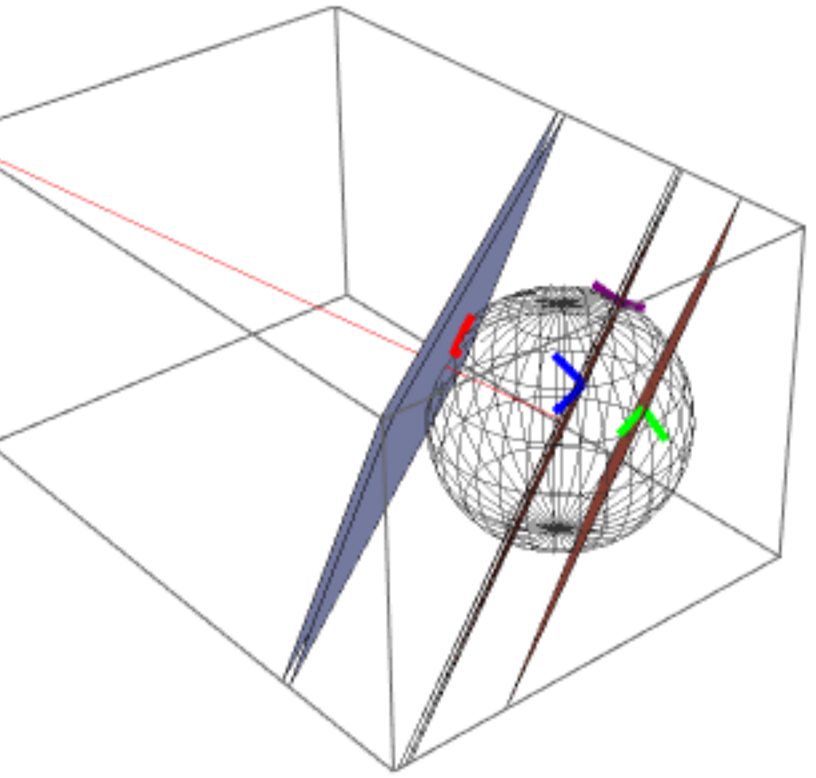

Hanford

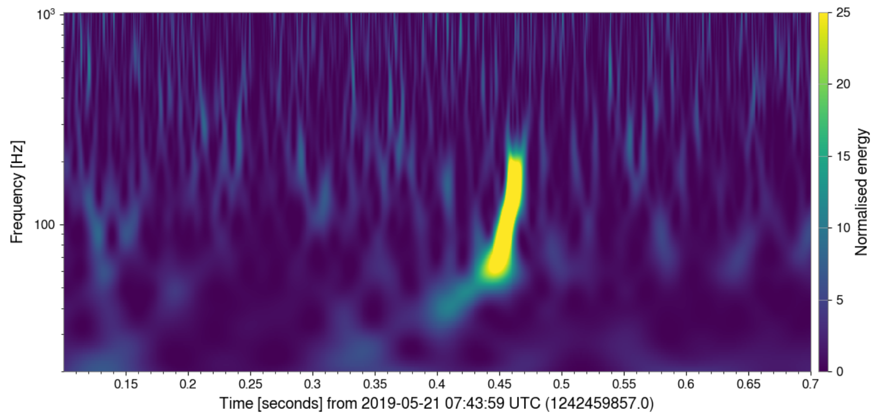

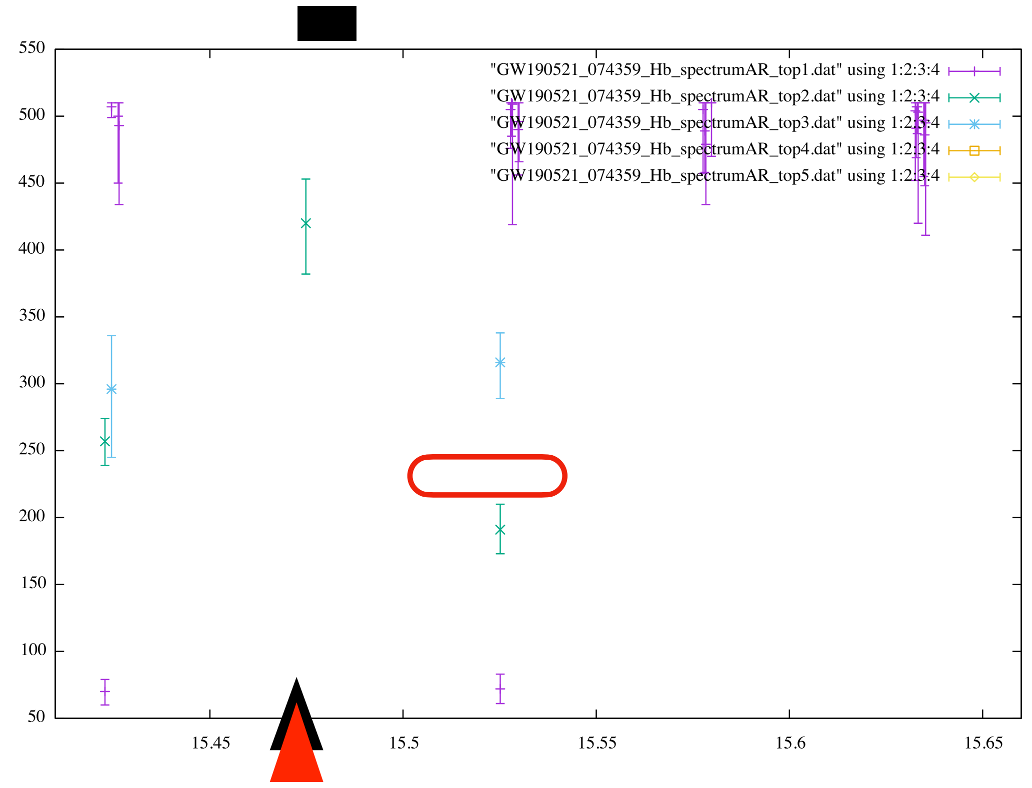

2 segments
f= 233.66 +- 22.164 Hz
t= 15.5256 --15.5266

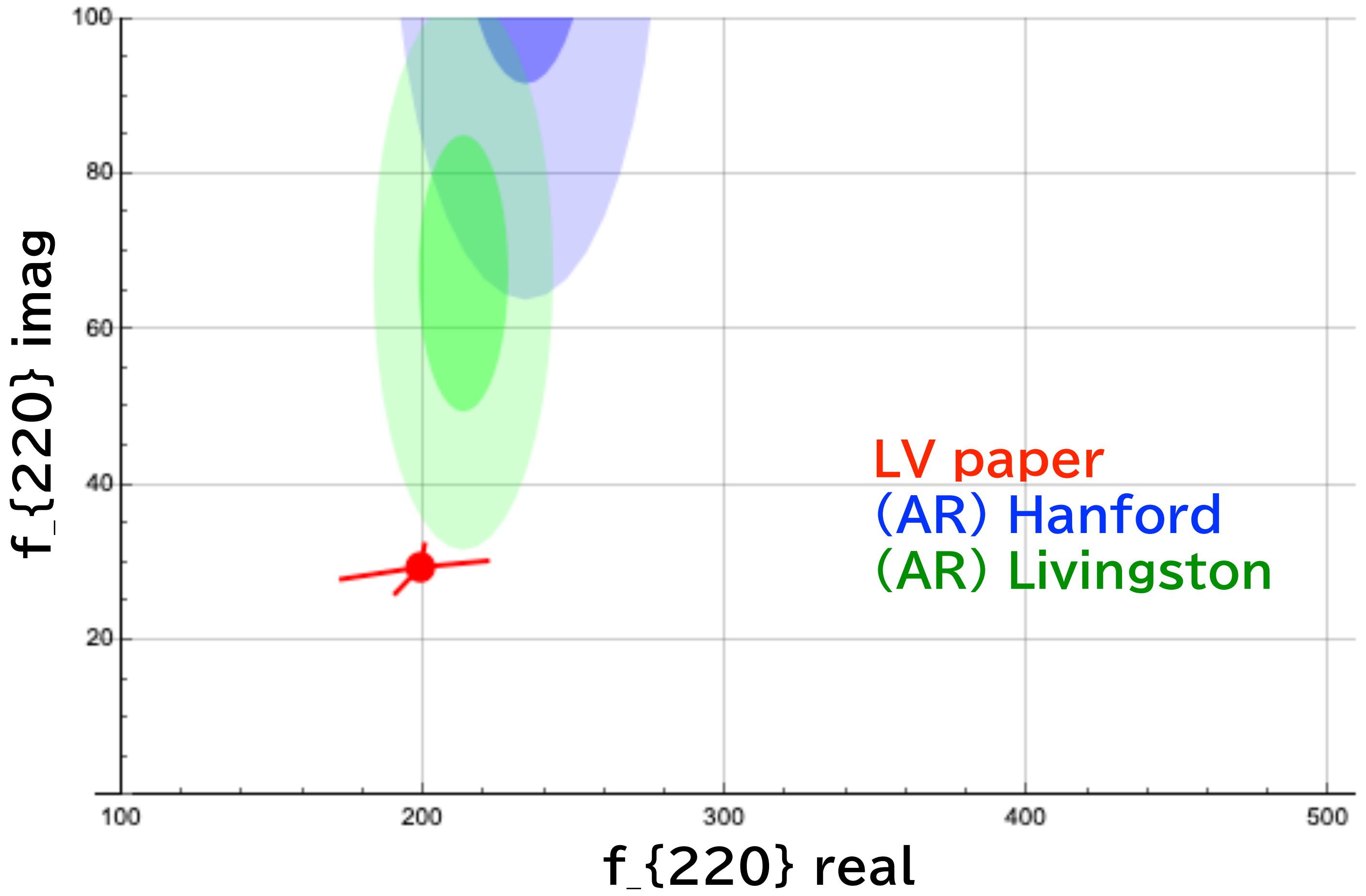

Livingston

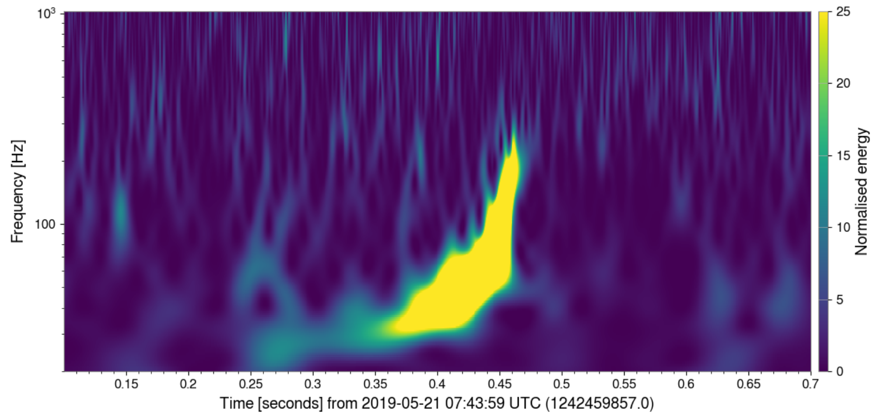

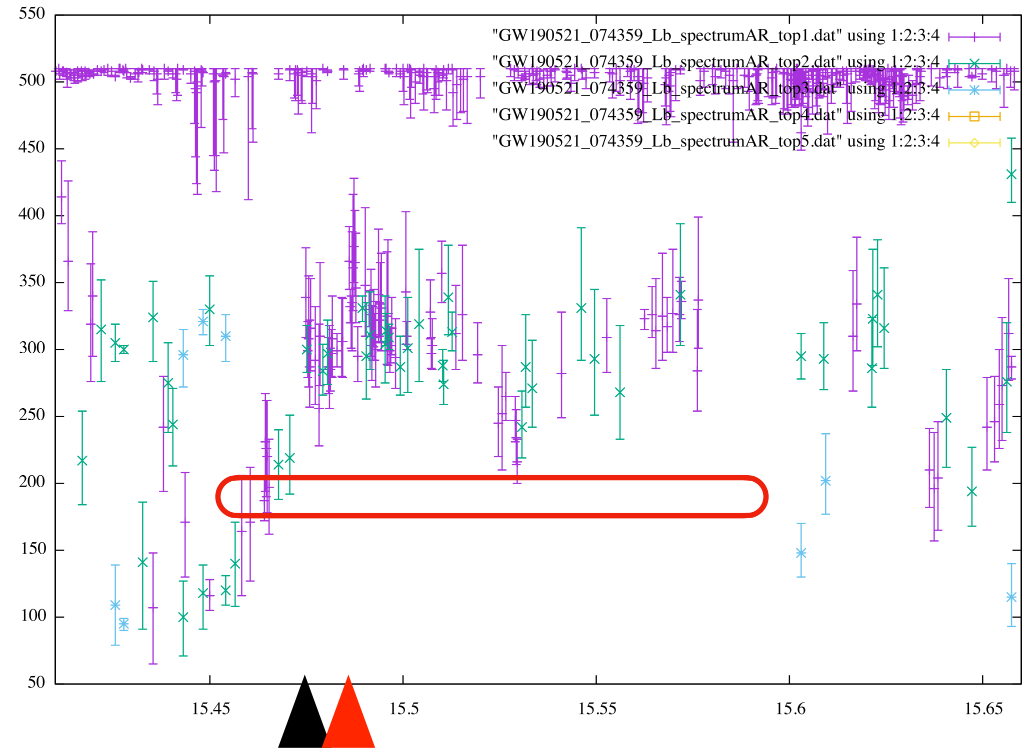

6 segments
f=213.03 +- 14.90 Hz
t=15.4639 -15.5928

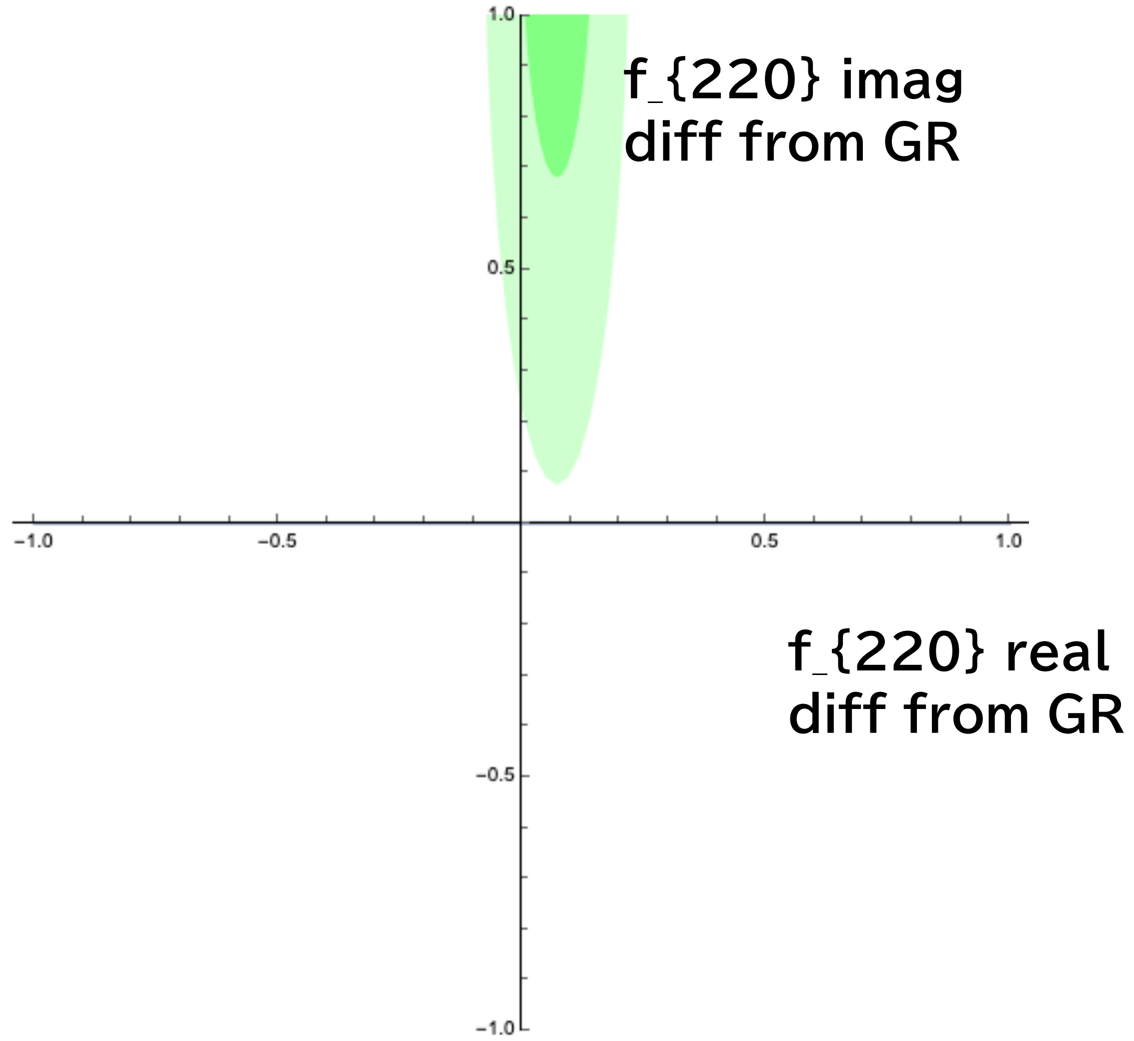

GW190521_074359
delay time (msec) from t
(+ delay, - advanced)

LHO = 1.11895
LLO = 10.7412
Virgo= 0.690039

Virgo X

t_merger = 15.463 s
t_mergerH = 15.464
t_mergerL = 15.474
t_mergerV = 15.457

No detections on this event.

GW200112_155838

Network SNR=19.8

1 segment = 64 points
= 1/64 sec = 15.625 ms

LV paper

$(M, a, z) = (60.8^{+5.3}_{-4.3}, 0.71^{+0.06}_{-0.06}, 0.24^{+0.07}_{-0.08})$

$f_{\rm QNM}$ @Earth

$f_{220} = 231.1 + i\ 34.69$ Hz, $f_{221} = 226.5 + i\ 105.2$ Hz, $f_{222} = 217.5 + i\ 177.6$ Hz
$f_{210} = 317.0 + i\ 56.13$ Hz, $f_{211} = 190.8 + i\ 106.2$ Hz, $f_{200} = 211.1 + i\ 44.72$ Hz
$f_{330} = 366.1 + i\ 35.55$ Hz, $f_{331} = 363.3 + i\ 109.4$ Hz, $f_{332} = 358.3 + i\ 195.8$ Hz
$f_{320} = 328.0 + i\ 35.89$ Hz, $f_{310} = 295.6 + i\ 48.9$ Hz, $f_{300} = 268.7 + i\ 37.61$ Hz

Hanford X

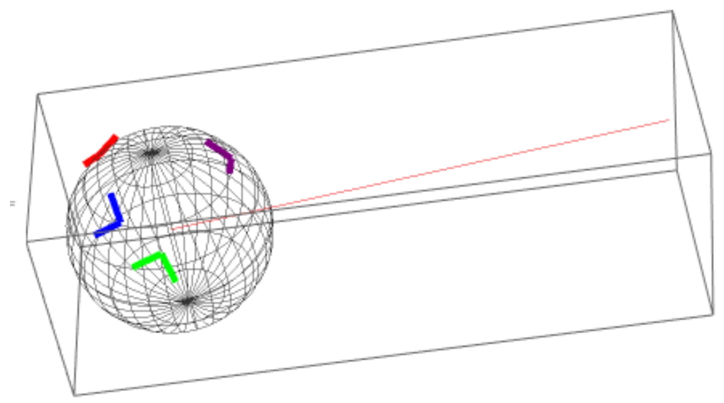

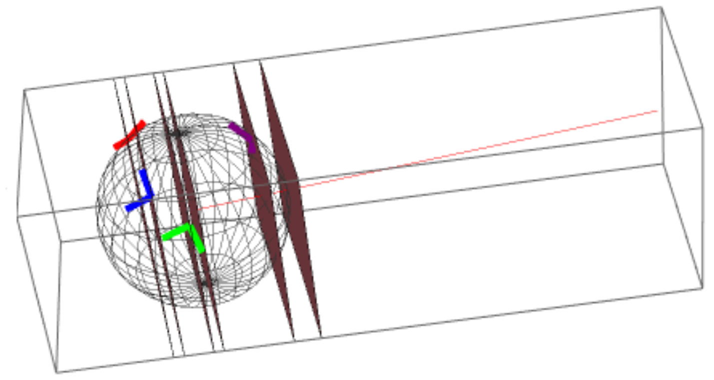

Livingston

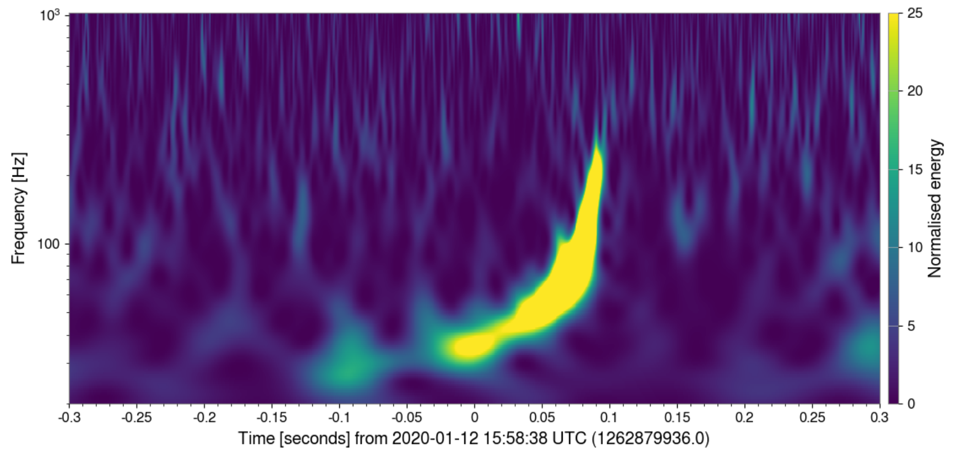

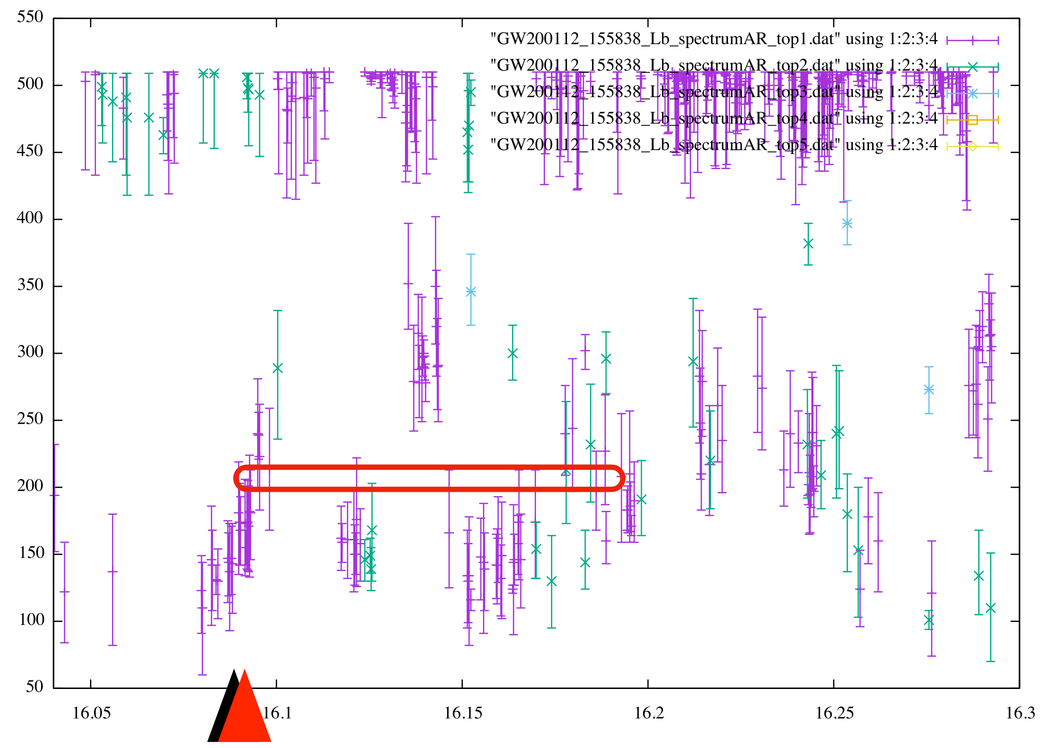

31 segments
f= 226.88 +- 10.95 Hz
t= 16.0950 --16.1992

Virgo

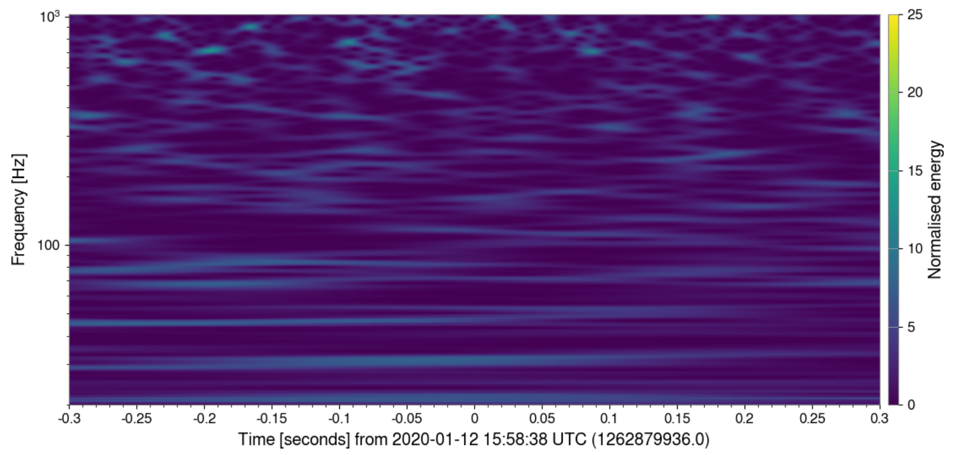

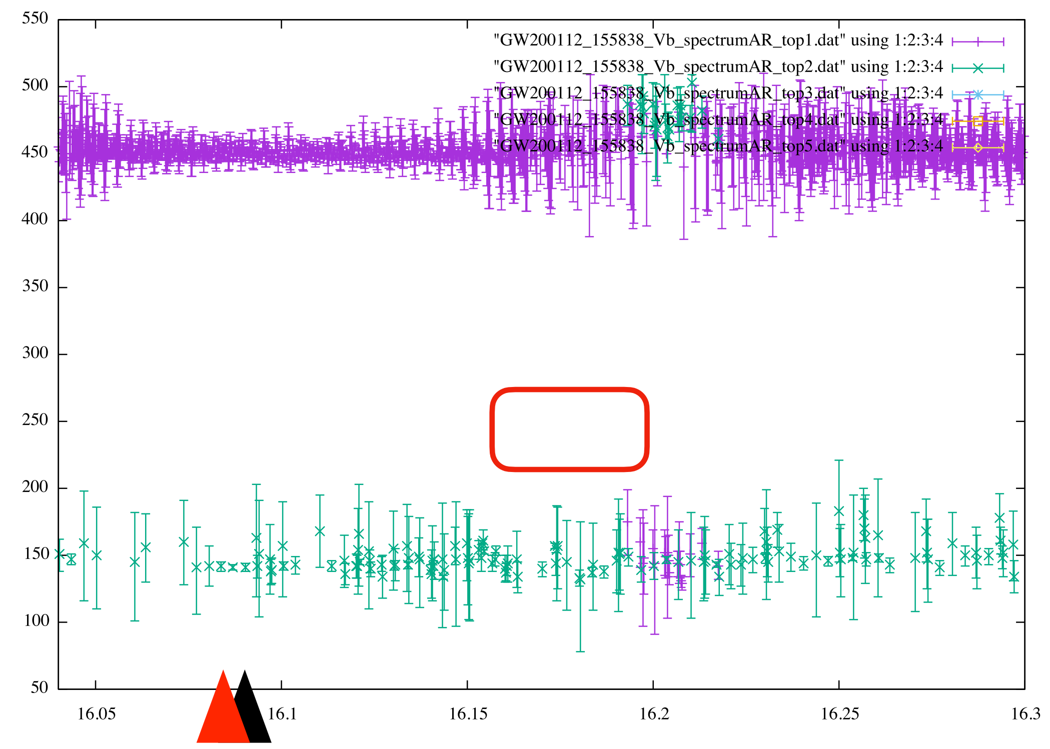

2 segments
f= 276.78 +- 76.15 Hz
t= 16.1528 -- 16.1992

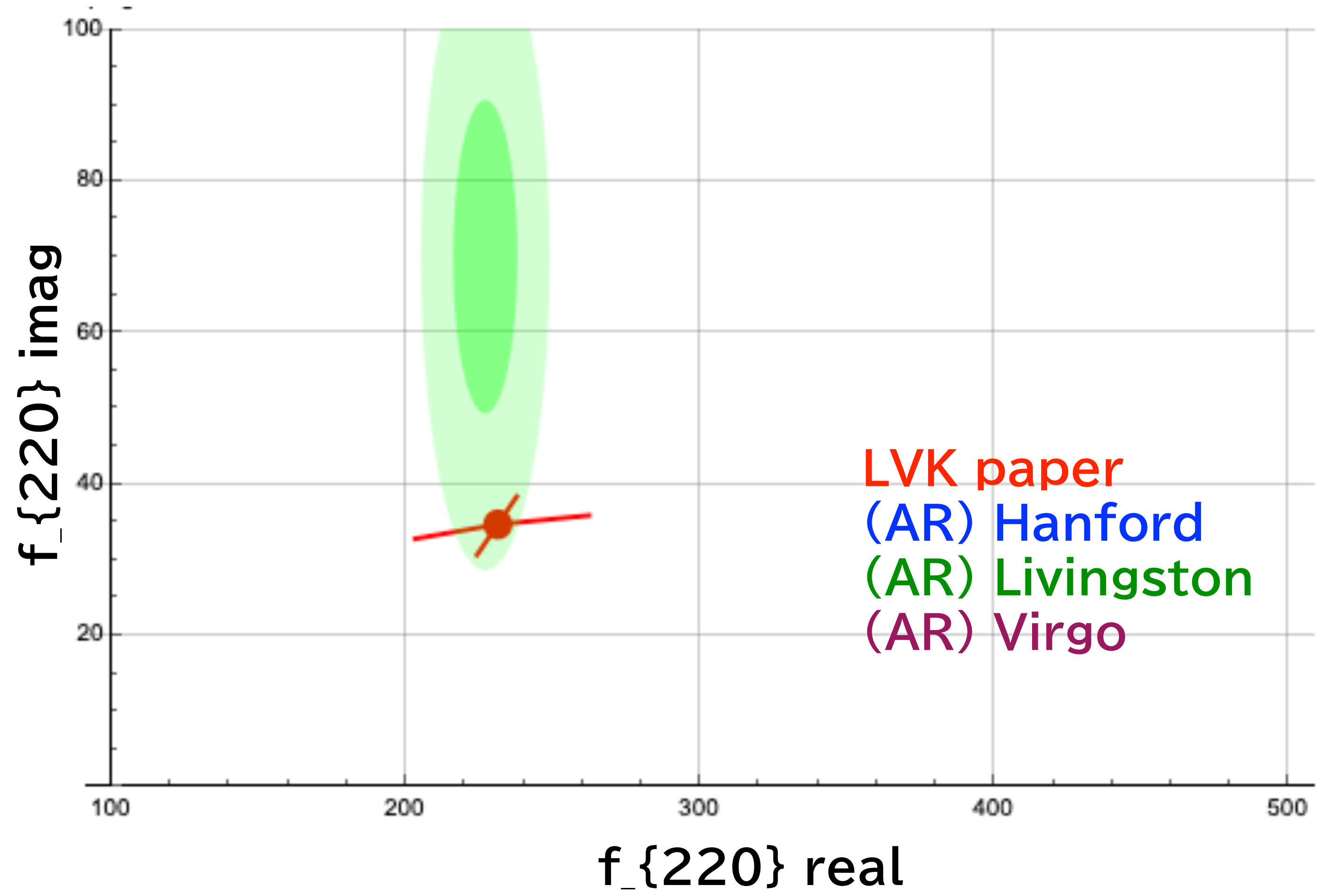

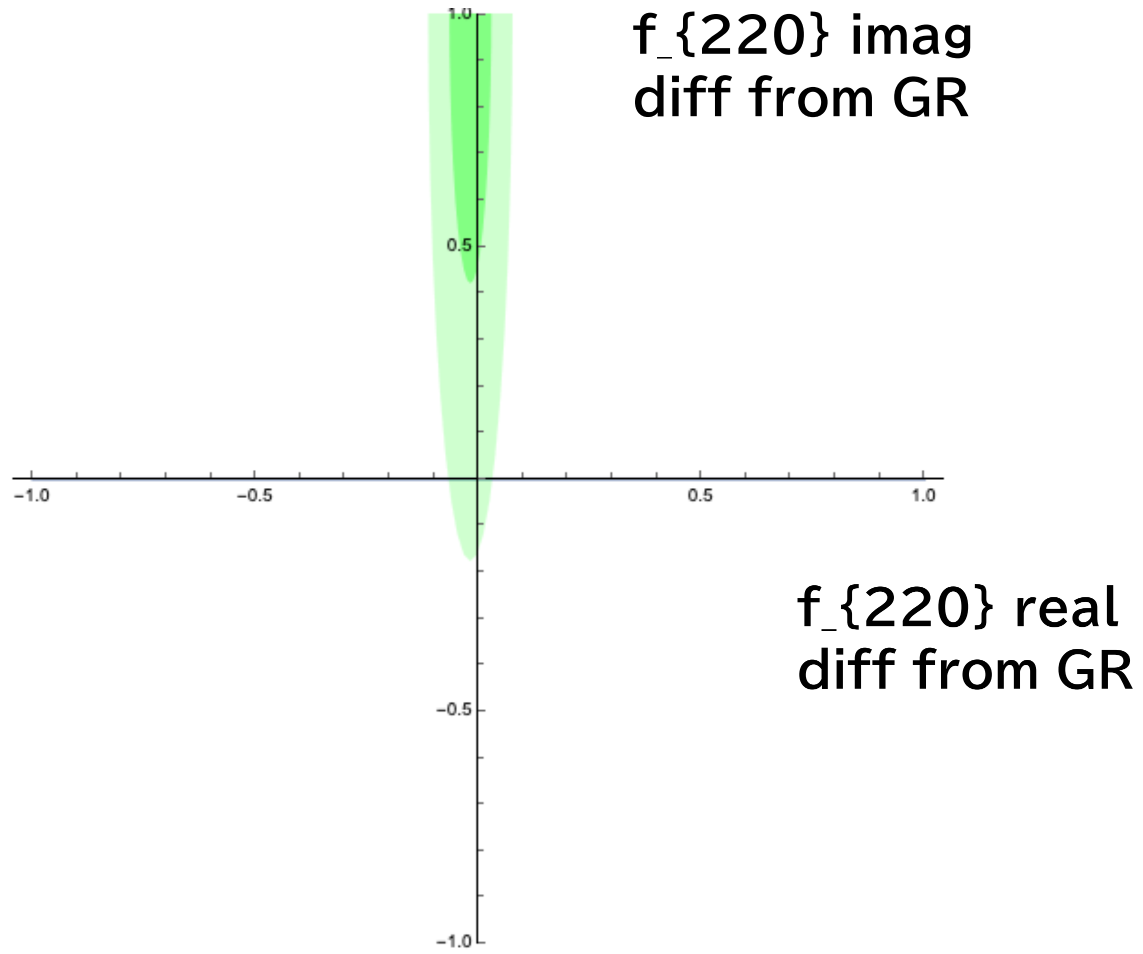

GW200112
delay time (msec) from t0
(+ delay, - advanced)

LHO = 8.634
LLO = 2.1455
Virgo= -15.3773

t_merger = 16.094 s
t_mergerH = 16.103
t_mergerL = 16.096
t_mergerV = 16.080

GW200129_065458

Network SNR=26.8

1 segment = 256 points
= 1/16 sec = 62.5 ms

LV paper ▶

$$(M, a, z) = (60.3^{+4.0}_{-3.3}, 0.73^{+0.06}_{-0.05}, 0.18^{+0.05}_{-0.07})$$

f_{QNM} @Earth ▶

$f_{220} = 249.0 + i\ 36.34$ Hz, $f_{221} = 244.4 + i\ 110.1$ Hz, $f_{222} = 235.4 + i\ 185.5$ Hz,
$f_{210} = 334.0 + i\ 58.09$ Hz, $f_{211} = 204.2 + i\ 111.4$ Hz, $f_{200} = 223.1 + i\ 46.94$ Hz,
$f_{330} = 394.0 + i\ 37.18$ Hz, $f_{331} = 391.3 + i\ 114.5$ Hz, $f_{332} = 386.3 + i\ 204.1$ Hz,
$f_{320} = 351.2 + i\ 37.62$ Hz, $f_{310} = 315.1 + i\ 52.23$ Hz, $f_{300} = 285.4 + i\ 39.7$ Hz,

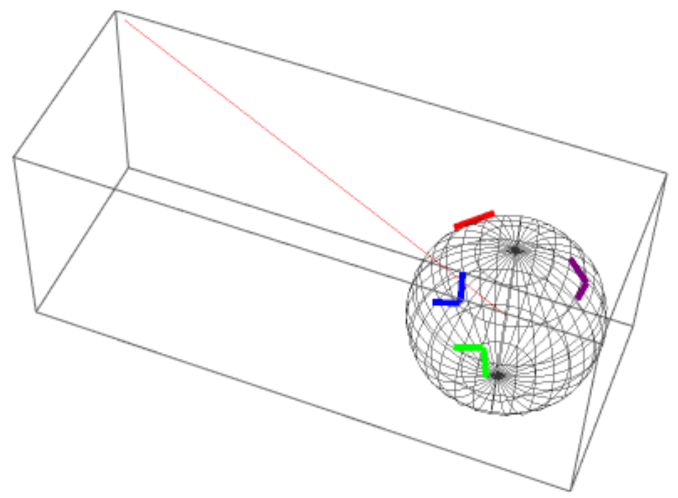

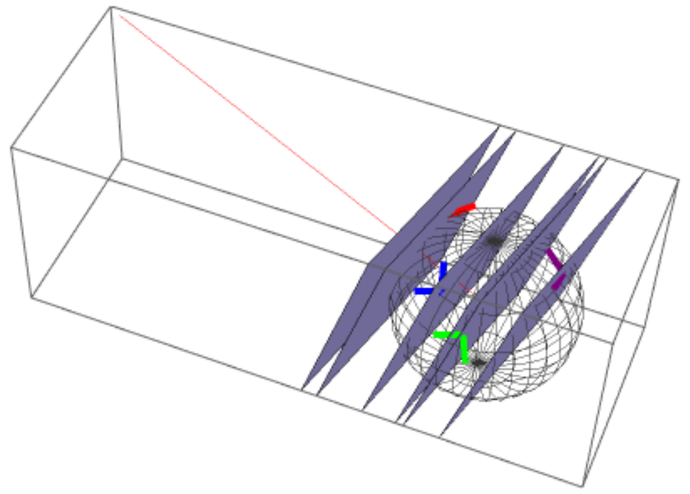

Hanford

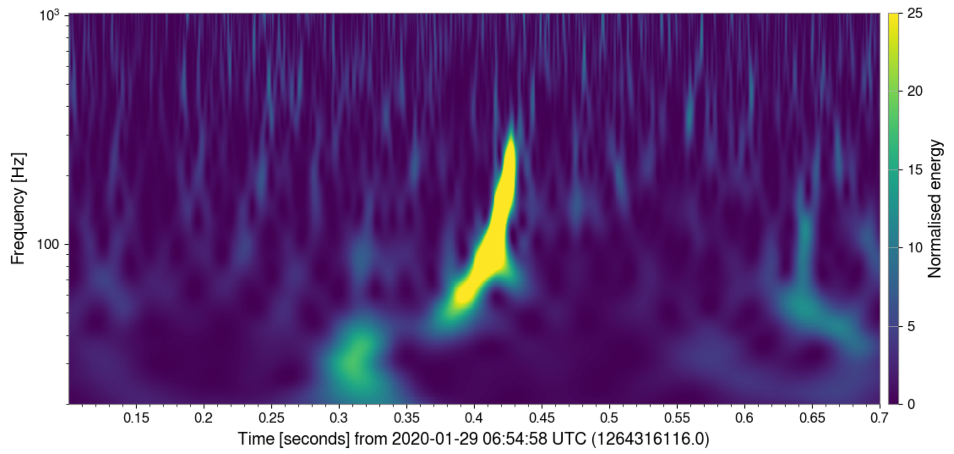

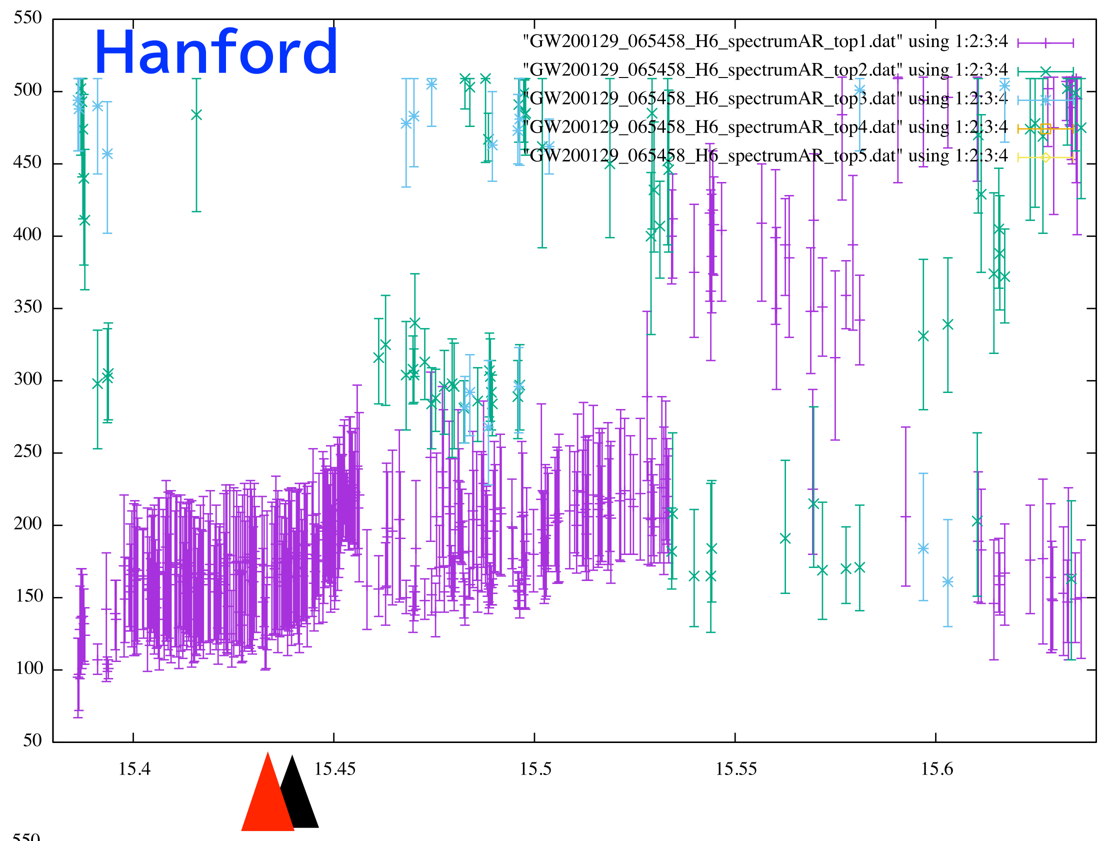

5 segments
f= 296.12+-8.29 Hz
t= 15.4736-15.5012

10 segments
f= 258.19+-3.90 Hz
t= 15.4607-15.5081

73 segments
f= 246.45+-10.08 Hz
t= 15.4556-15.5493

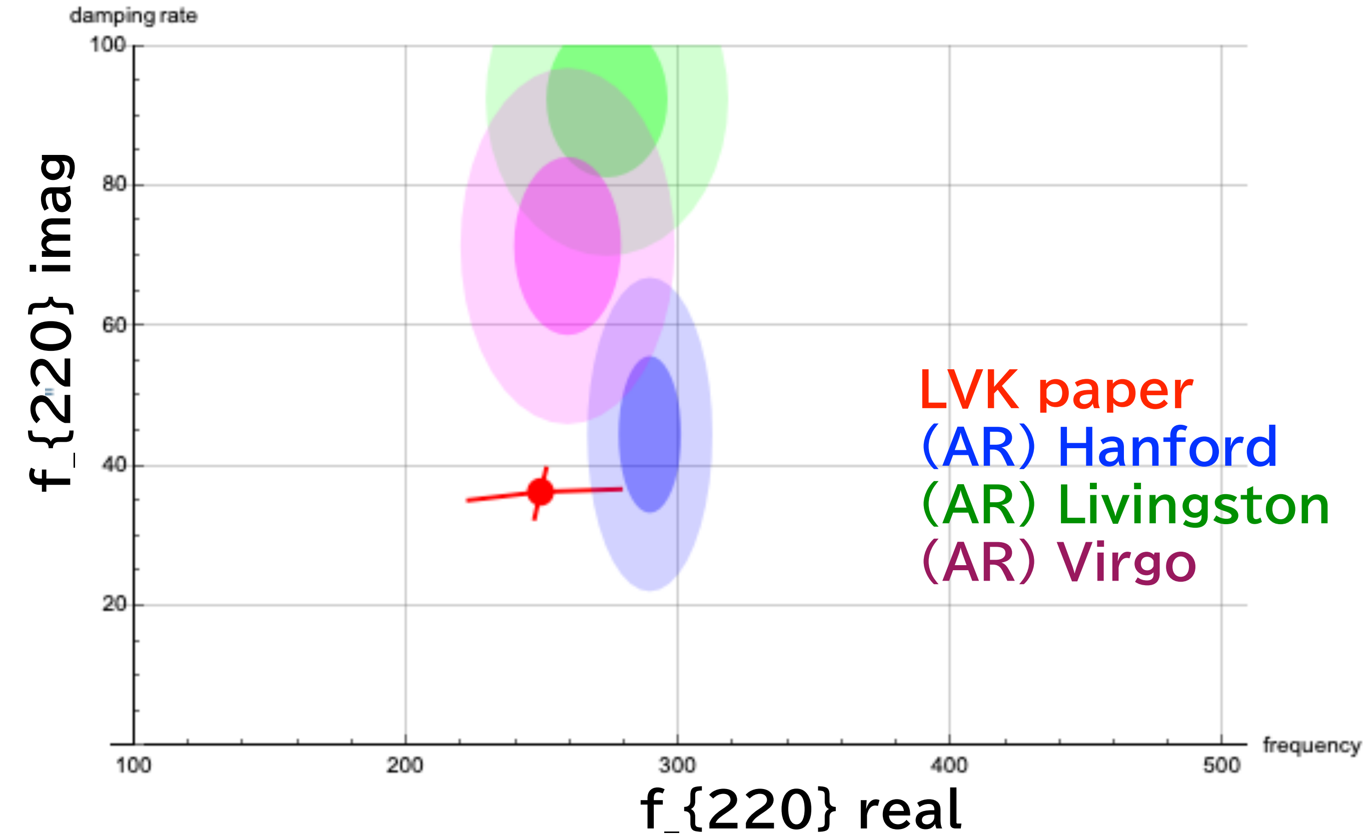

Livingston

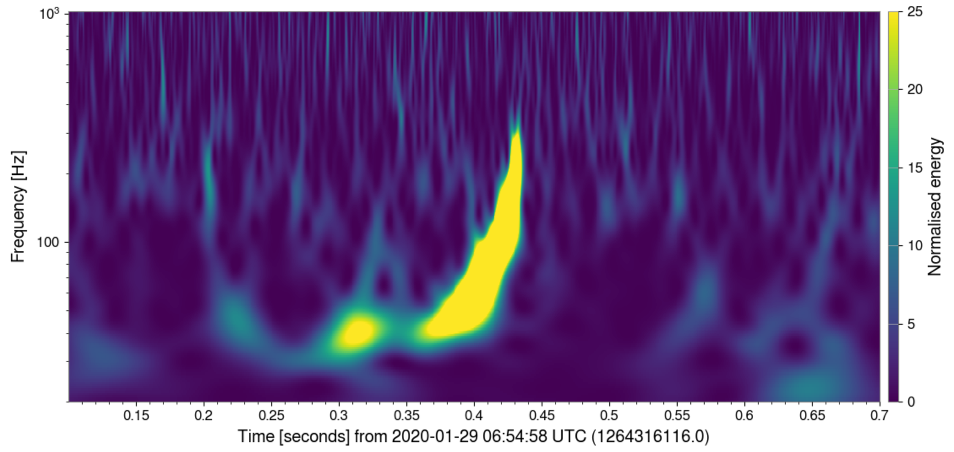

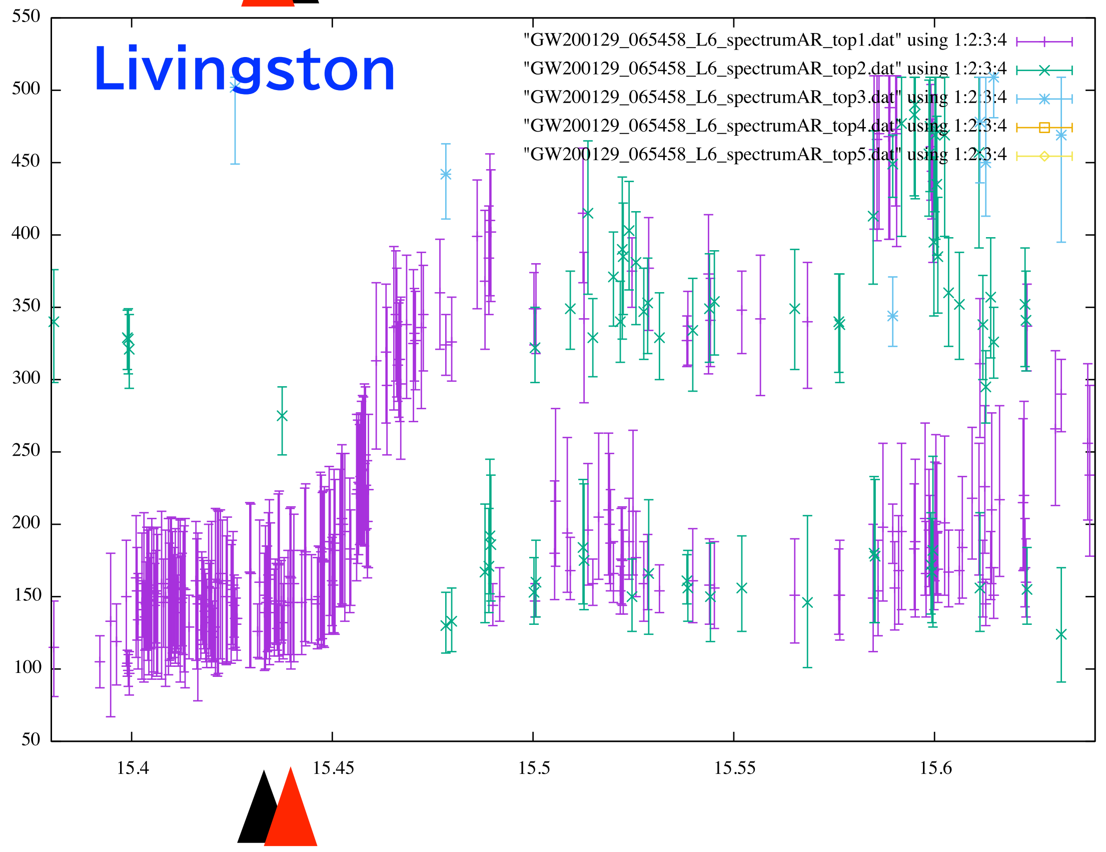

29 segments
f= 316.65+-10.77 Hz
t= 15.4609-15.4993

39 segments
f= 259.97+-11.16 Hz
t= 15.4553-15.5461

GW200129
delay time (msec) from t0
(+ delay, - advanced)

LHO = - 7.5579
LLO = 1.71251
Virgo= 9.73468

t_merger = 15.435 s
t_mergerH = 15.427
t_mergerL = 15.437
t_mergerV = 15.445

Virgo

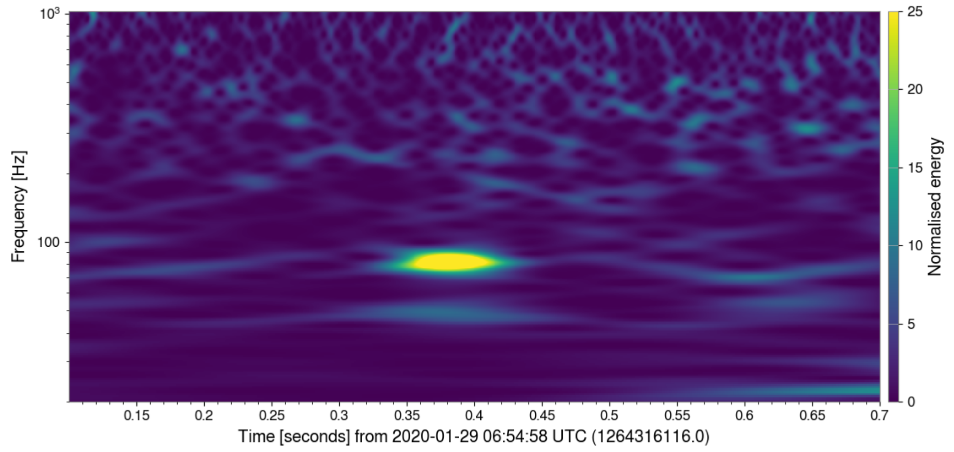

GW200129_065458

Network SNR=26.8

1 segment = 64 points
= 1/64 sec = 15.625 ms

LV paper ▶ $(M, a, z) = (60.3^{+4.0}_{-3.3}, 0.73^{+0.06}_{-0.05}, 0.18^{+0.05}_{-0.07})$

fQNM @Earth ▶

$f_{220} = 249.0 + i\ 36.34$ Hz, $f_{221} = 244.4 + i\ 110.1$ Hz, $f_{222} = 235.4 + i\ 185.5$ Hz,
$f_{210} = 334.0 + i\ 58.09$ Hz, $f_{211} = 204.2 + i\ 111.4$ Hz, $f_{200} = 223.1 + i\ 46.94$ Hz,
$f_{330} = 394.0 + i\ 37.18$ Hz, $f_{331} = 391.3 + i\ 114.5$ Hz, $f_{332} = 386.3 + i\ 204.1$ Hz,
$f_{320} = 351.2 + i\ 37.62$ Hz, $f_{310} = 315.1 + i\ 52.23$ Hz, $f_{300} = 285.4 + i\ 39.7$ Hz,

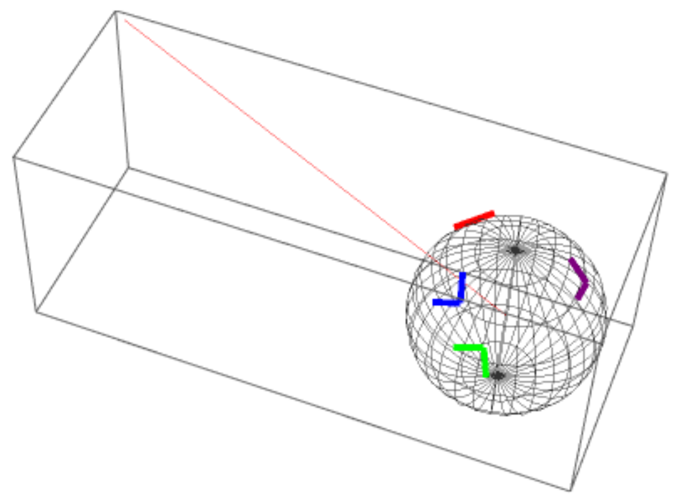

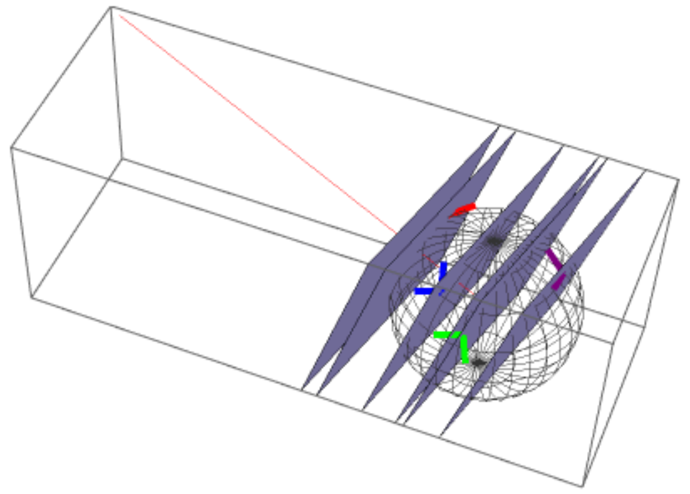

Hanford

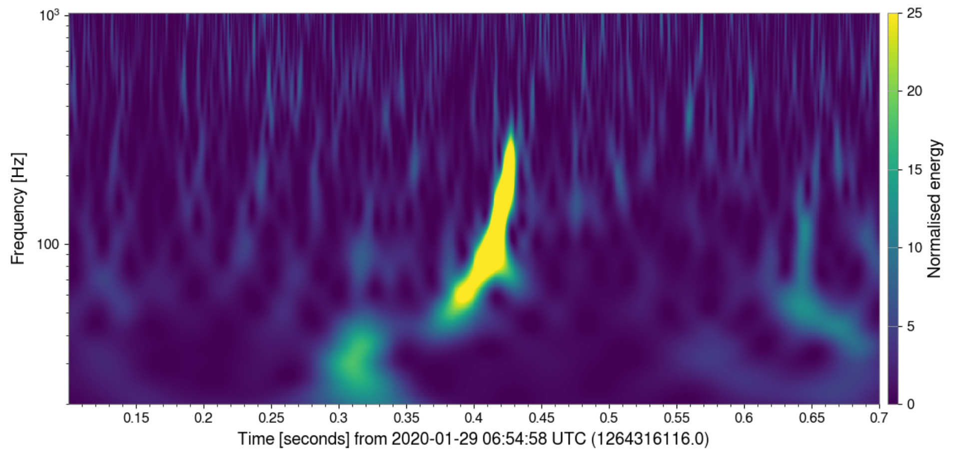

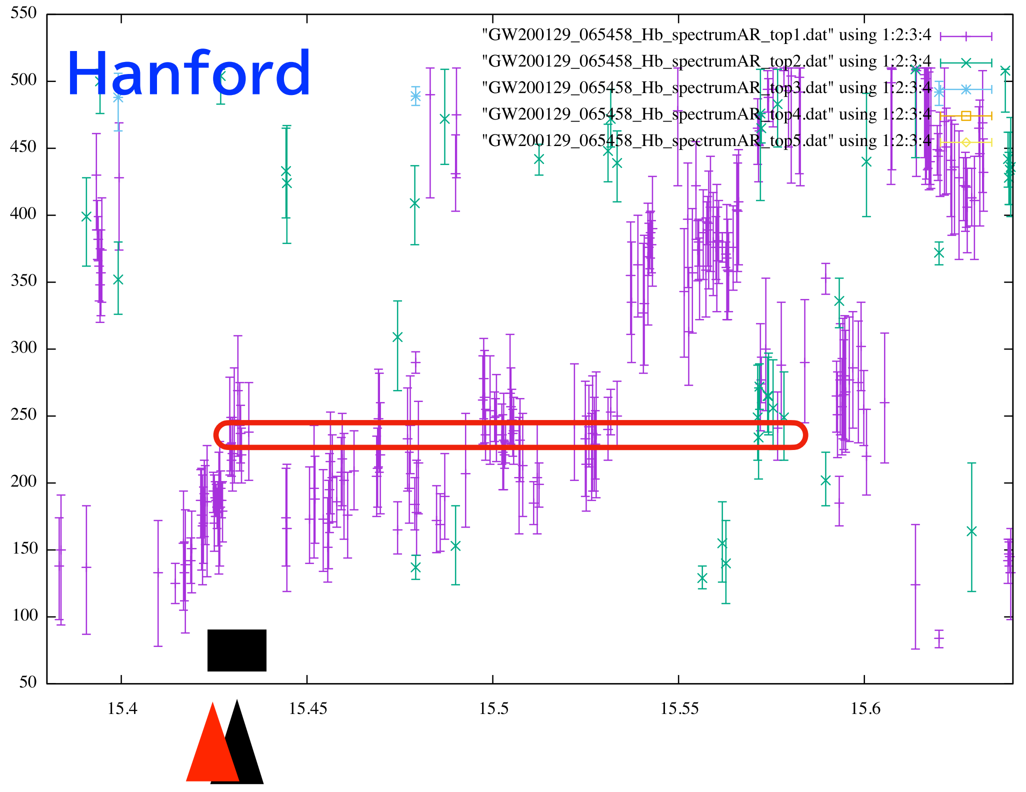

45 segments
f= 244.68+-10.90 Hz
t= 15.4399 --15.5796

f_{220} starts 5ms after t_merger

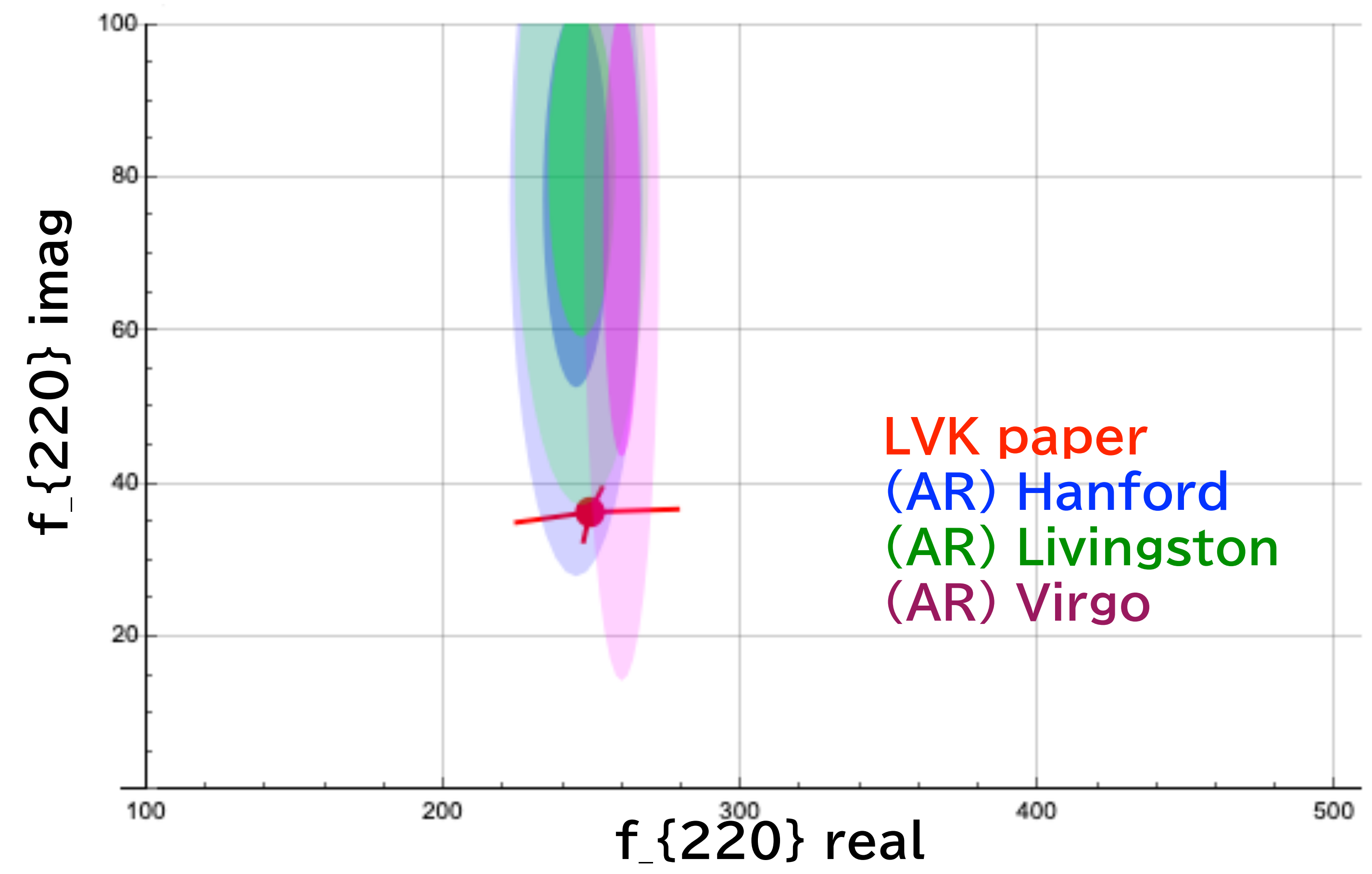

Livingston

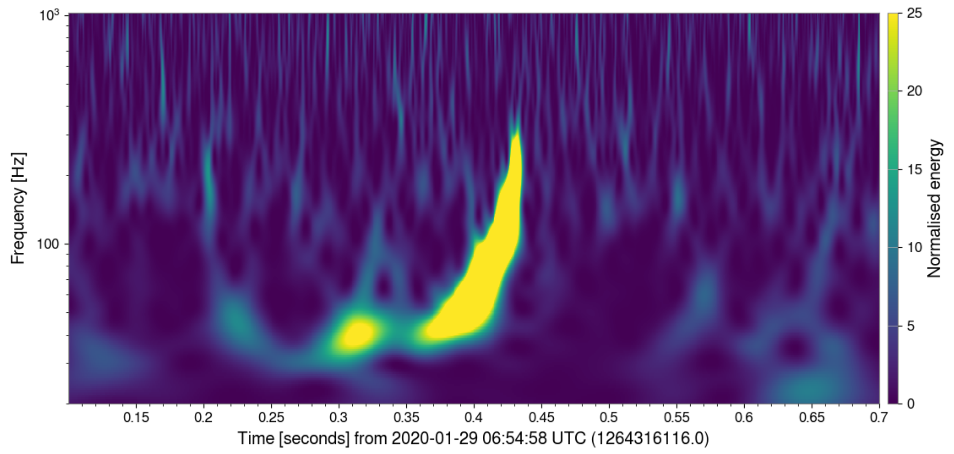

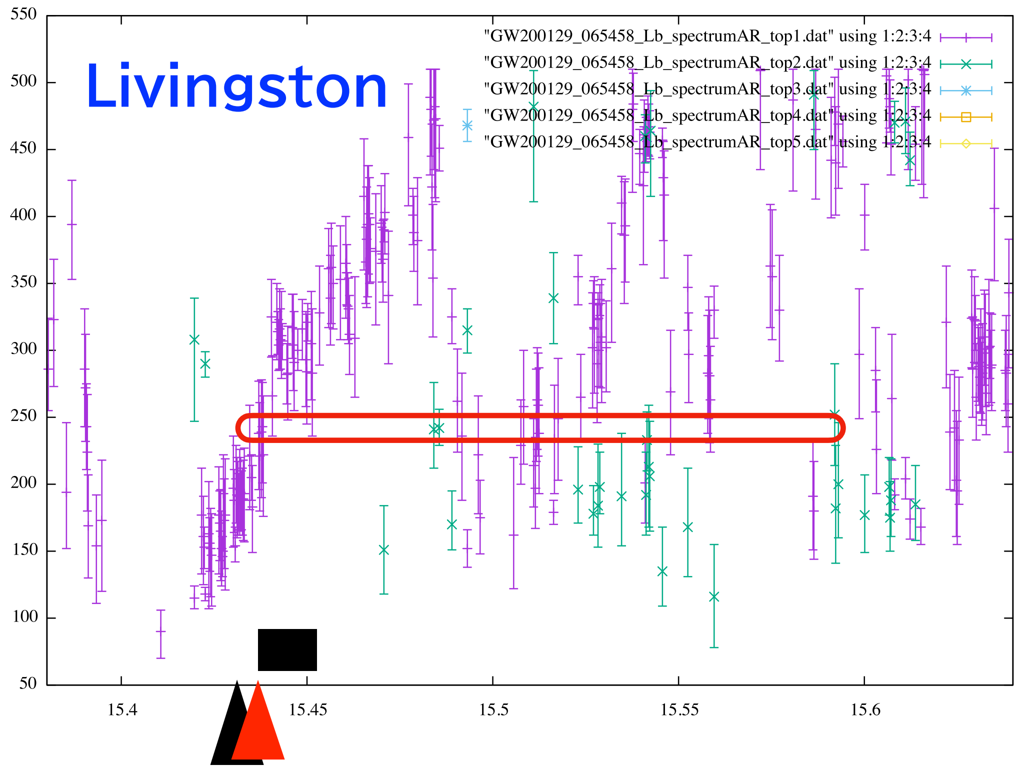

31 segments
f= 246.20 +- 11.28 Hz
t= 15.4370 -- 15.5840

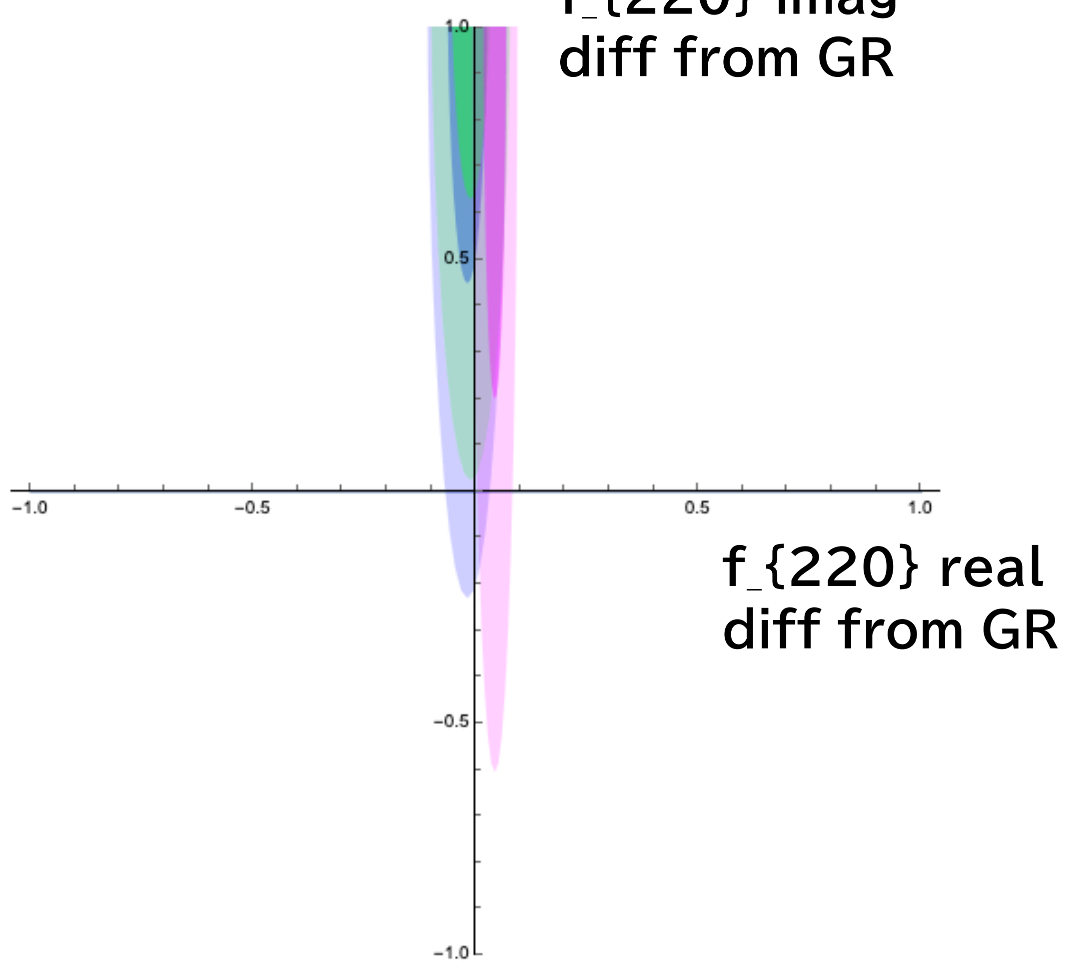

GW200129
delay time (msec) from t0
(+ delay, - advanced)

LHO = - 7.5579
LLO = 1.71251
Virgo= 9.73468

t_merger = 15.435 s
t_mergerH = 15.427
t_mergerL = 15.437
t_mergerV = 15.445

+ 7.8125s
t_mergerH = 15.435
t_mergerL = 15.445
t_mergerV = 15.452

Virgo

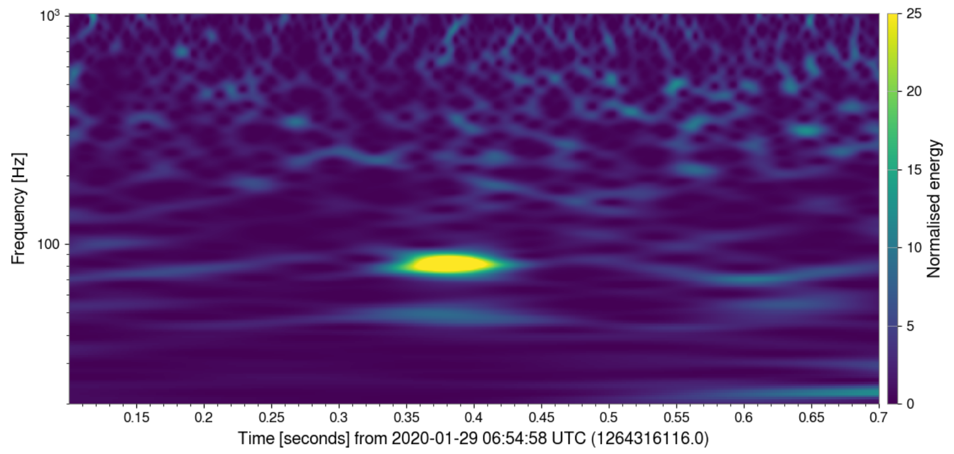

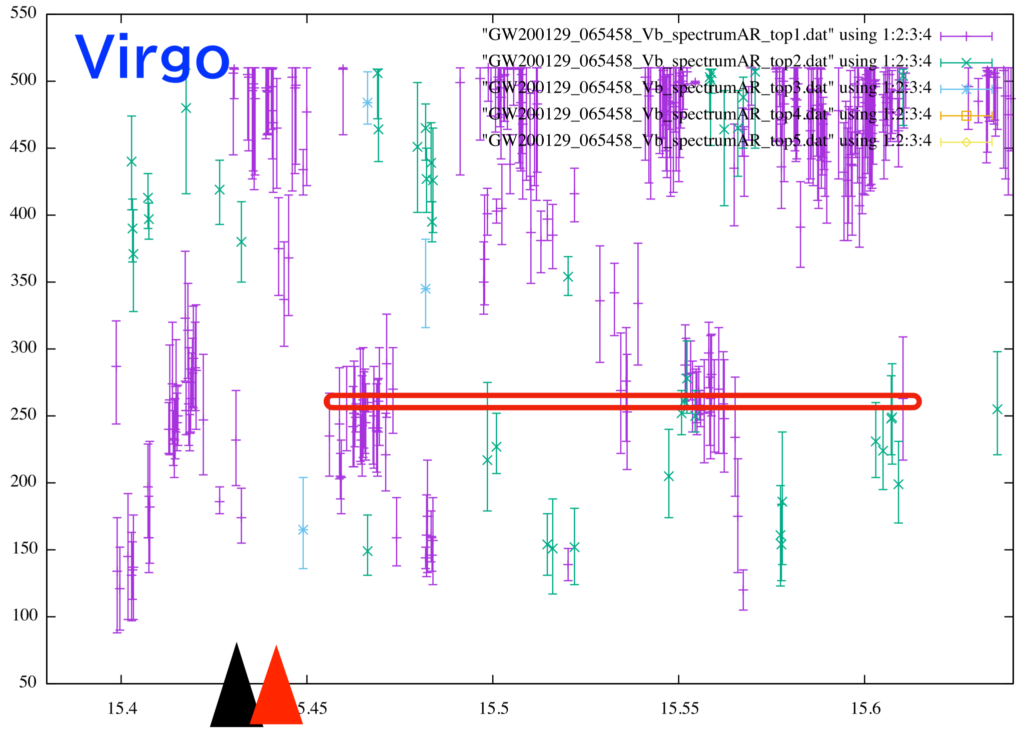

33 segments
f= 259.69 +- 6.31 Hz
t= 15.4548-15.6497

f_{220} starts 3ms after t_merger

GW200224_222234

Network SNR=20.0

1 segment = 64 points
= 1/64 sec = 15.625 ms

LV paper

$(M, a, z) = (68.6^{+6.6}_{-4.7}, 0.73^{+0.07}_{-0.07}, 0.32^{+0.08}_{-0.11})$

fQNM @Earth

$f_{220} = 195.7 + i\,28.55$ Hz, $f_{221} = 192.1 + i\,86.53$ Hz, $f_{222} = 185.0 + i\,145.8$ Hz
$f_{210} = 262.4 + i\,45.65$ Hz, $f_{211} = 160.4 + i\,87.55$ Hz, $f_{200} = 175.3 + i\,36.89$ Hz
$f_{330} = 309.6 + i\,29.22$ Hz, $f_{331} = 307.4 + i\,89.99$ Hz, $f_{332} = 303.5 + i\,160.3$ Hz
$f_{320} = 276.0 + i\,29.56$ Hz, $f_{310} = 247.6 + i\,41.04$ Hz, $f_{300} = 224.3 + i\,31.2$ Hz

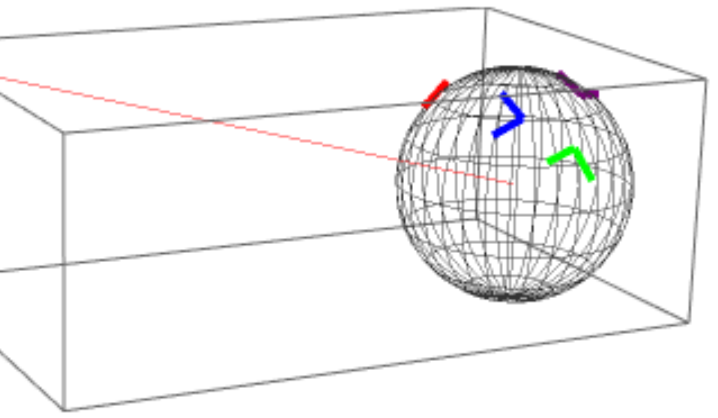

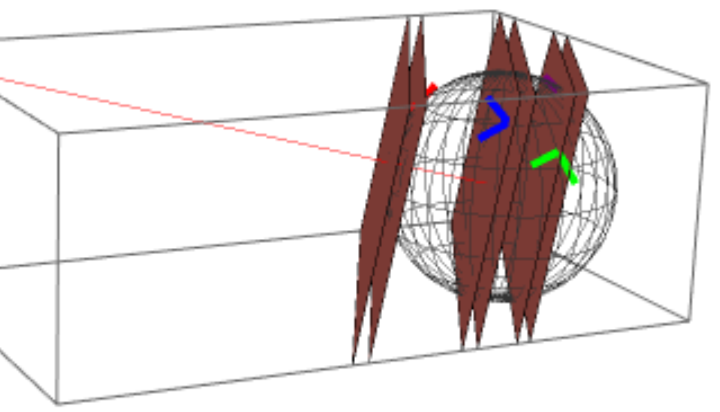

Hanford

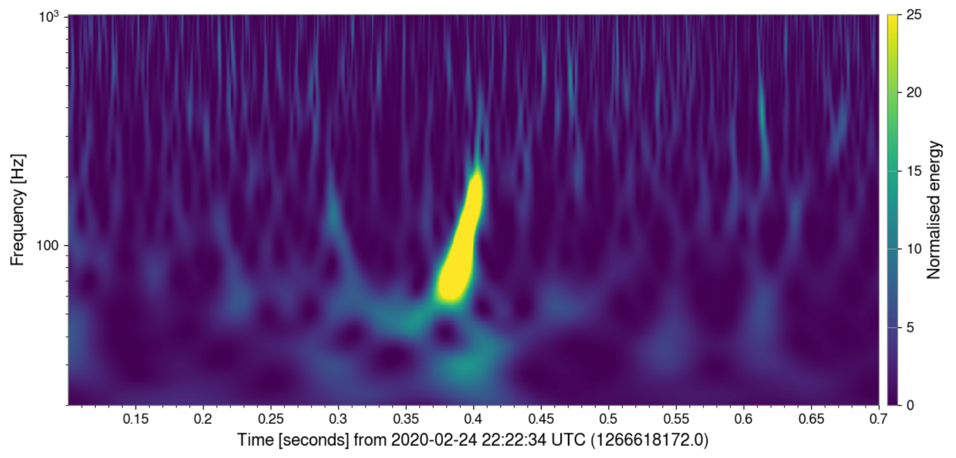

Hanford

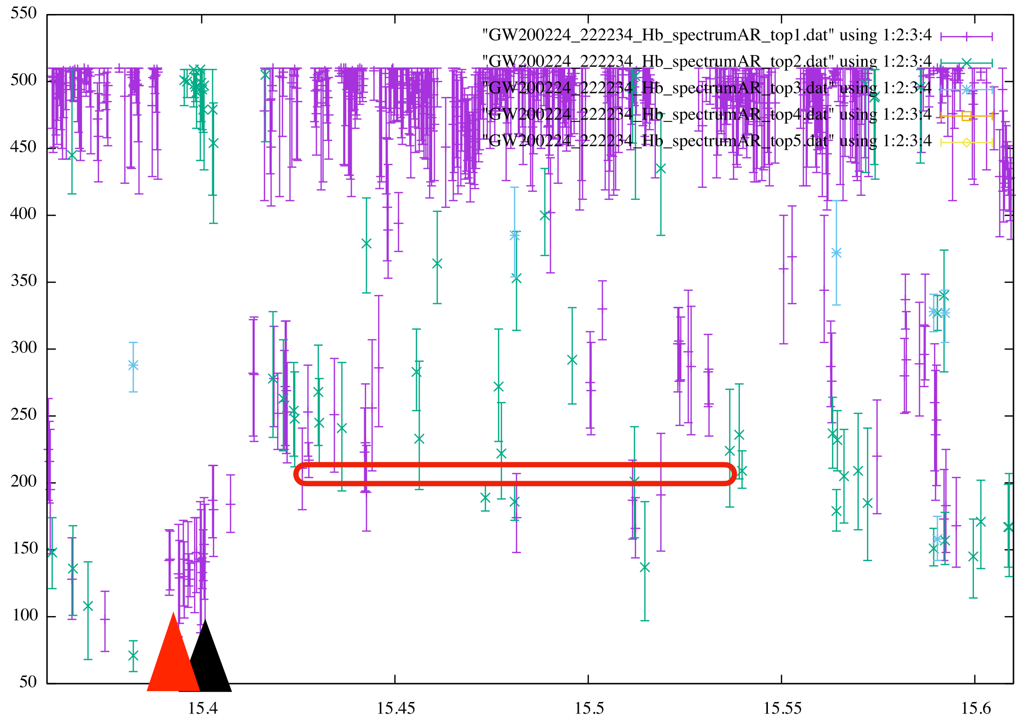

9 segments
f= 215.82 +- 9.65 Hz
t= 15.4395 --15.5396

Livingston

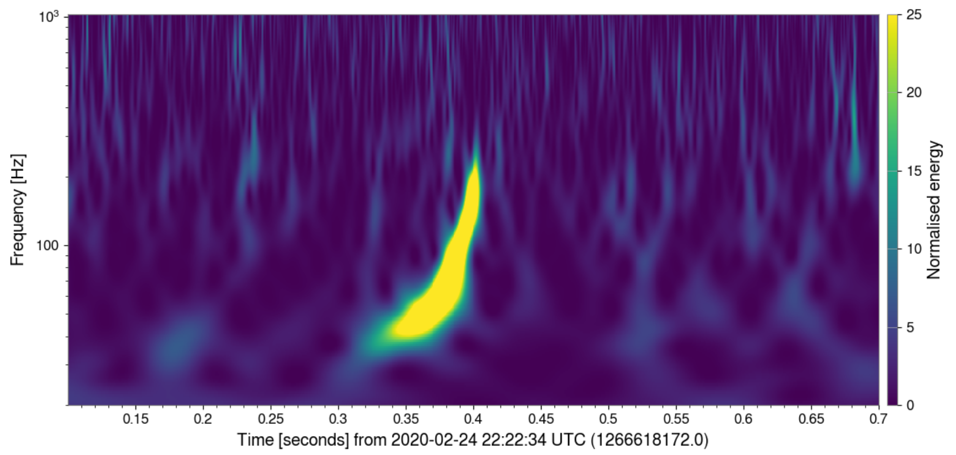

Livingston

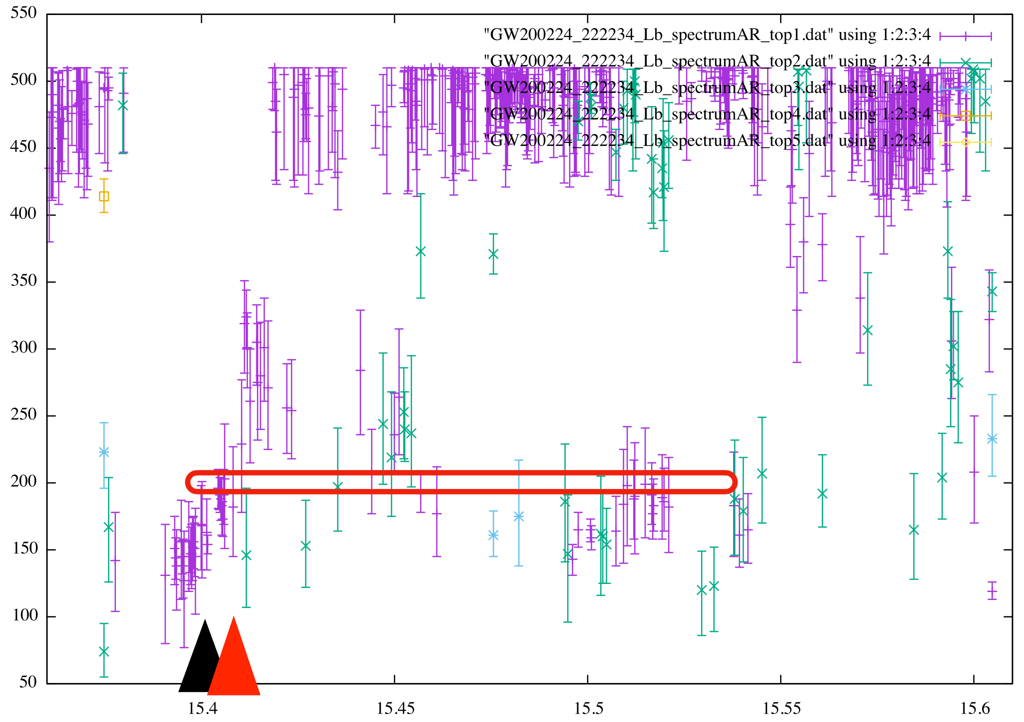

28 segments
f= 199.68 +-11.82 Hz
t= 15.4060 -- 15.5452

Virgo

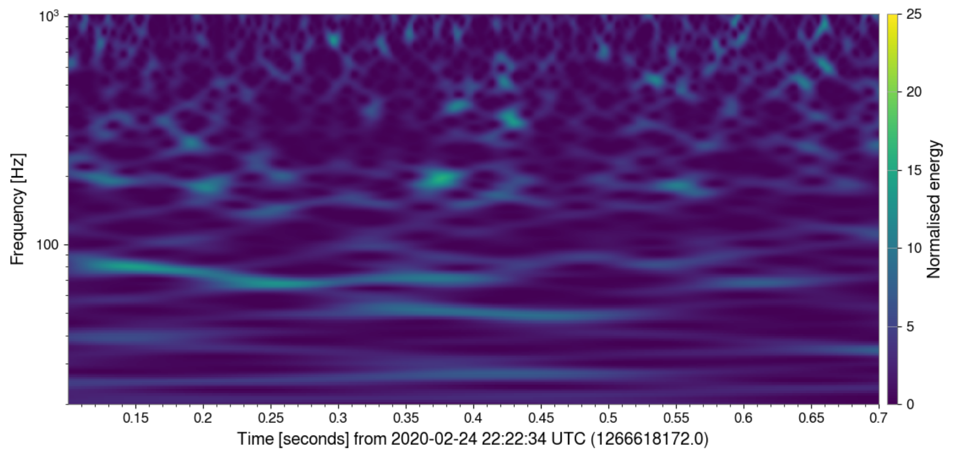

Virgo

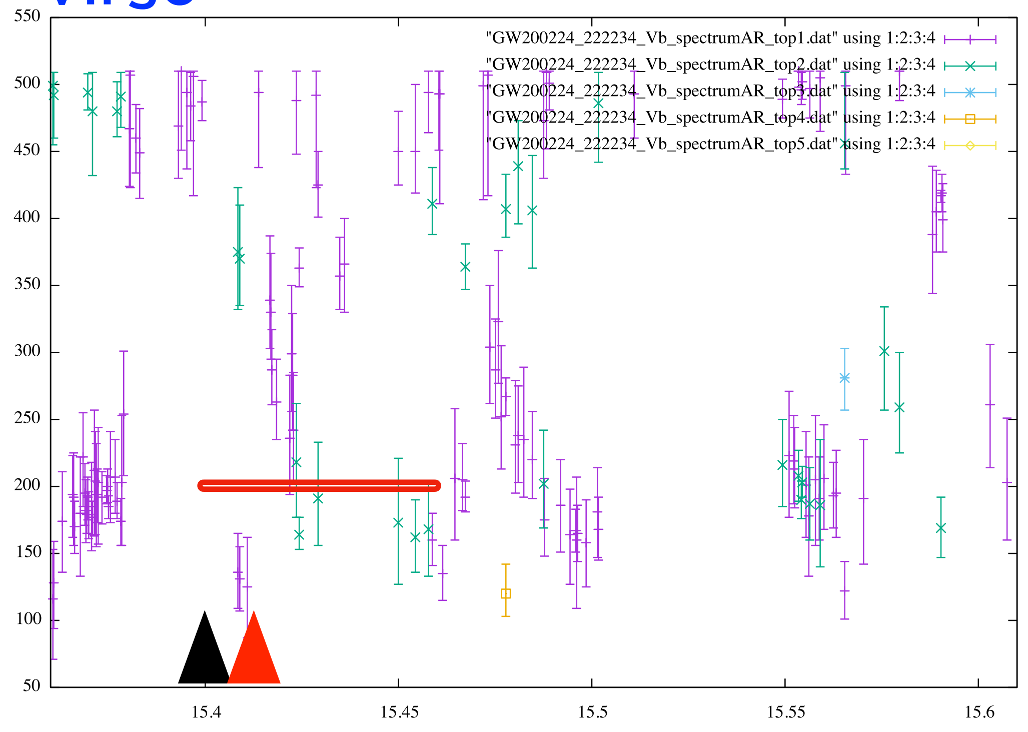

8 segments
f= 202.96 +- 6.07 Hz
t= 15.4060 --15.5452

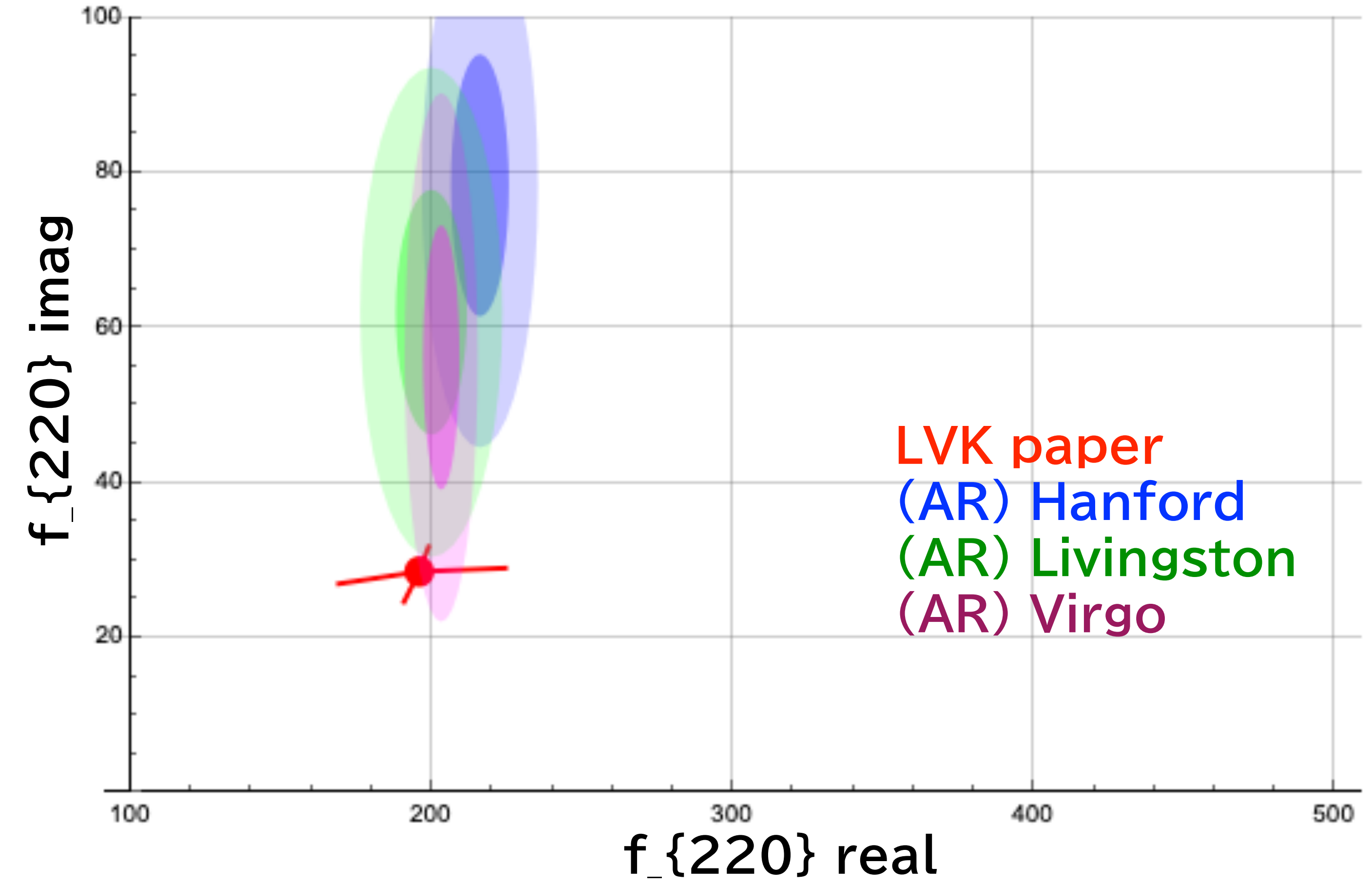

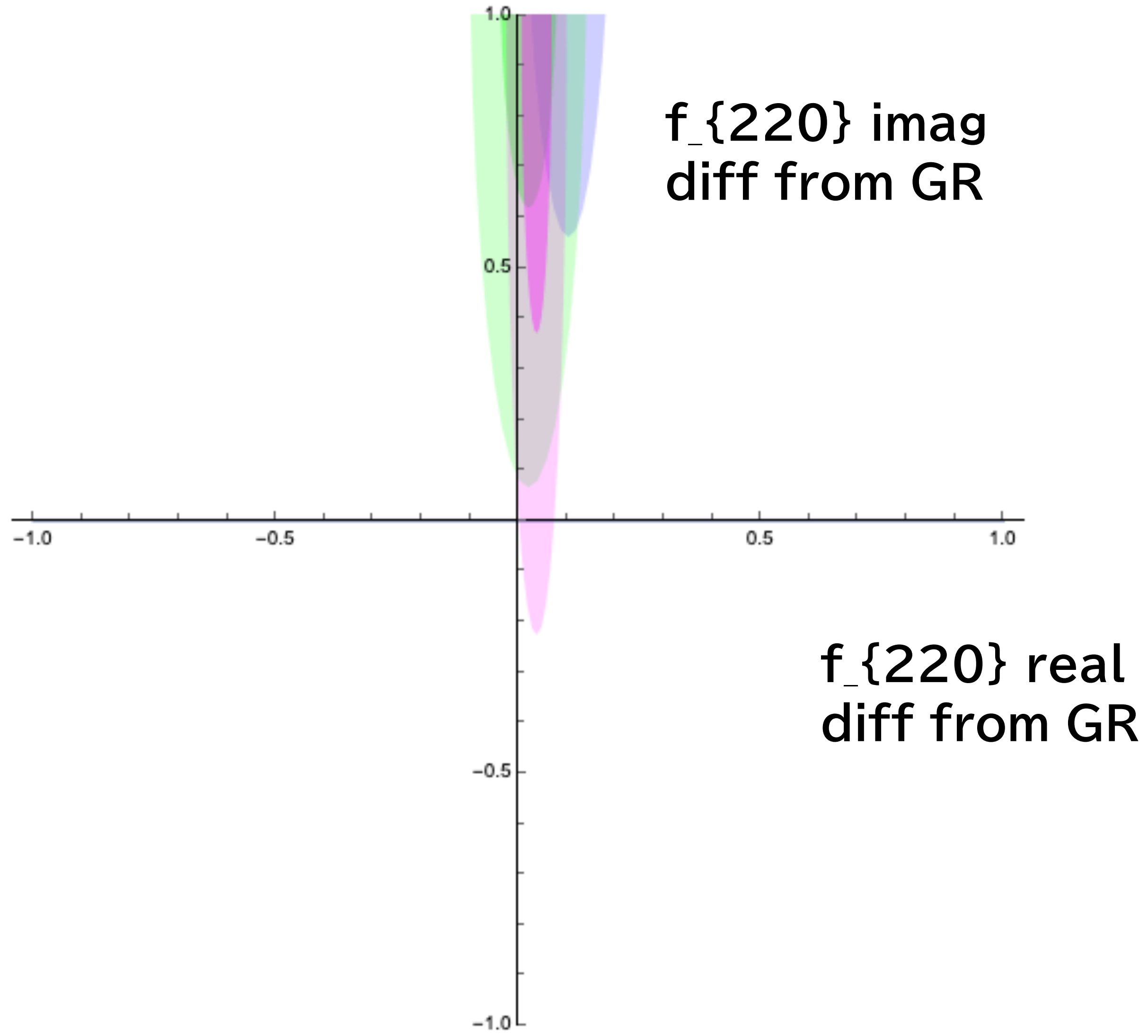

GW200224
delay time (msec) from t0
(+ delay, - advanced)

LHO = - 2.70101
LLO = 6.94325
Virgo= 9.23521
KAGRA= -18.5399

t_merger = 15.402 s
t_mergerH = 15.399
t_mergerL = 15.409
t_mergerV = 15.411

GW200311_115853

Network SNR=17.8

1 segment = 64 points
= 1/64 sec = 15.625 ms

LV paper ▸ $(M, a, z) = (59.^{+4.8}_{-3.9}, 0.69^{+0.07}_{-0.08}, 0.23^{+0.05}_{-0.07})$

f_{QNM} @Earth ▸

$f_{220} = 236.3 + i\ 36.41$ Hz, $f_{221} = 231.3 + i\ 110.5$ Hz, $f_{222} = 221.5 + i\ 186.9$ Hz
$f_{210} = 331.0 + i\ 59.62$ Hz, $f_{211} = 196.3 + i\ 111.4$ Hz, $f_{200} = 219.8 + i\ 46.87$ Hz
$f_{330} = 374.7 + i\ 37.35$ Hz, $f_{331} = 371.6 + i\ 114.8$ Hz, $f_{332} = 366.1 + i\ 206.5$ Hz
$f_{320} = 337.3 + i\ 37.65$ Hz, $f_{310} = 305.3 + i\ 50.42$ Hz, $f_{300} = 278.5 + i\ 39.2$ Hz

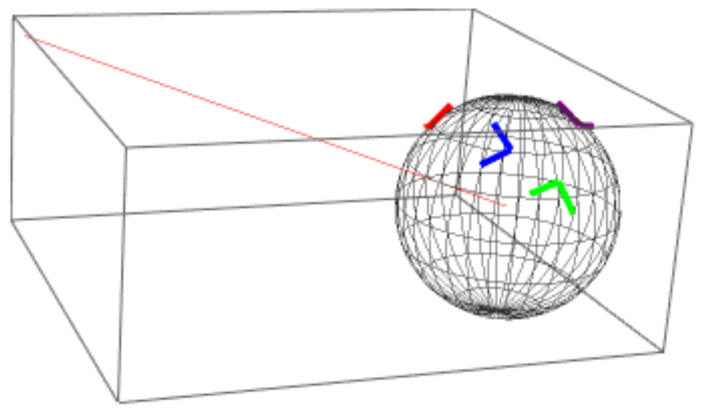

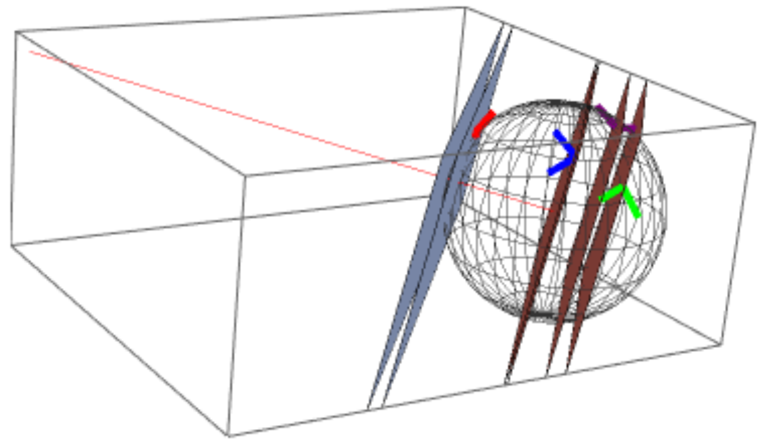

Hanford

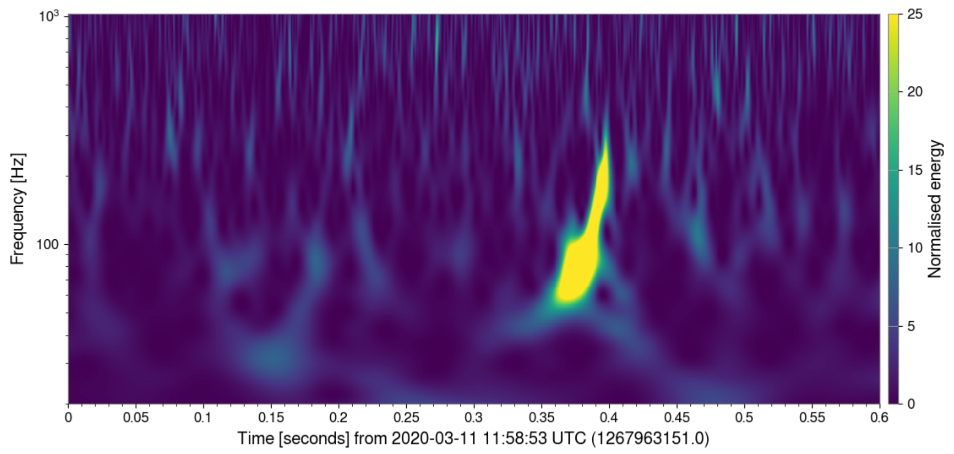

Hanford

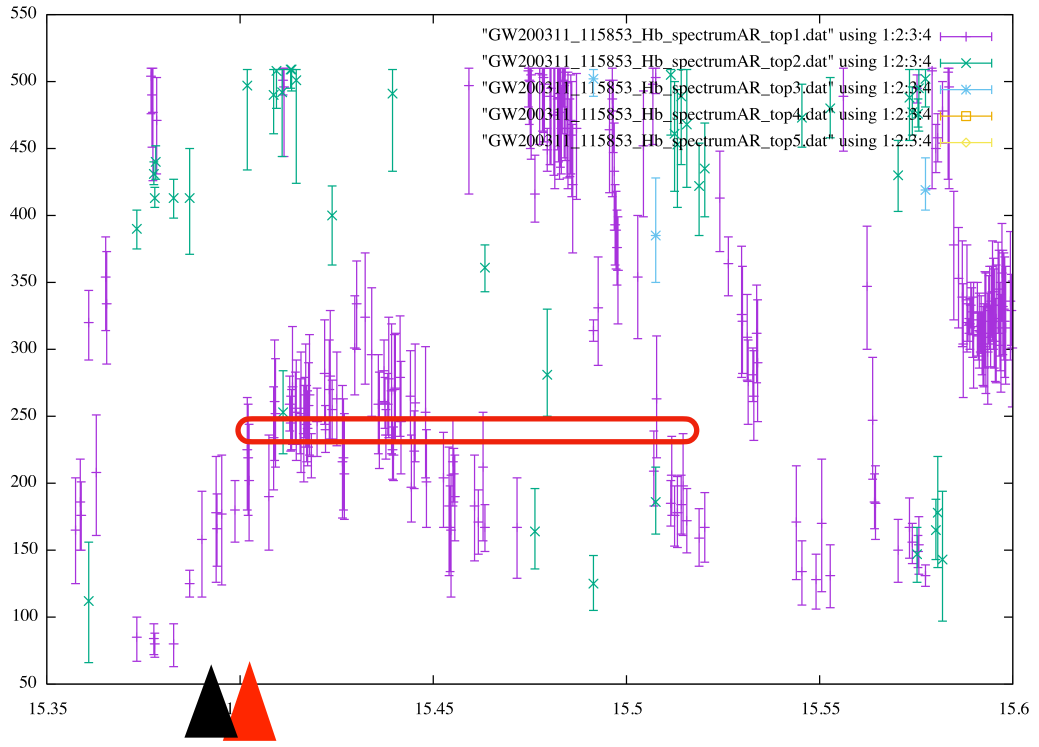

22 segments
f= 234.01 +- 6.81 Hz
t= 15.4019 --15.5437

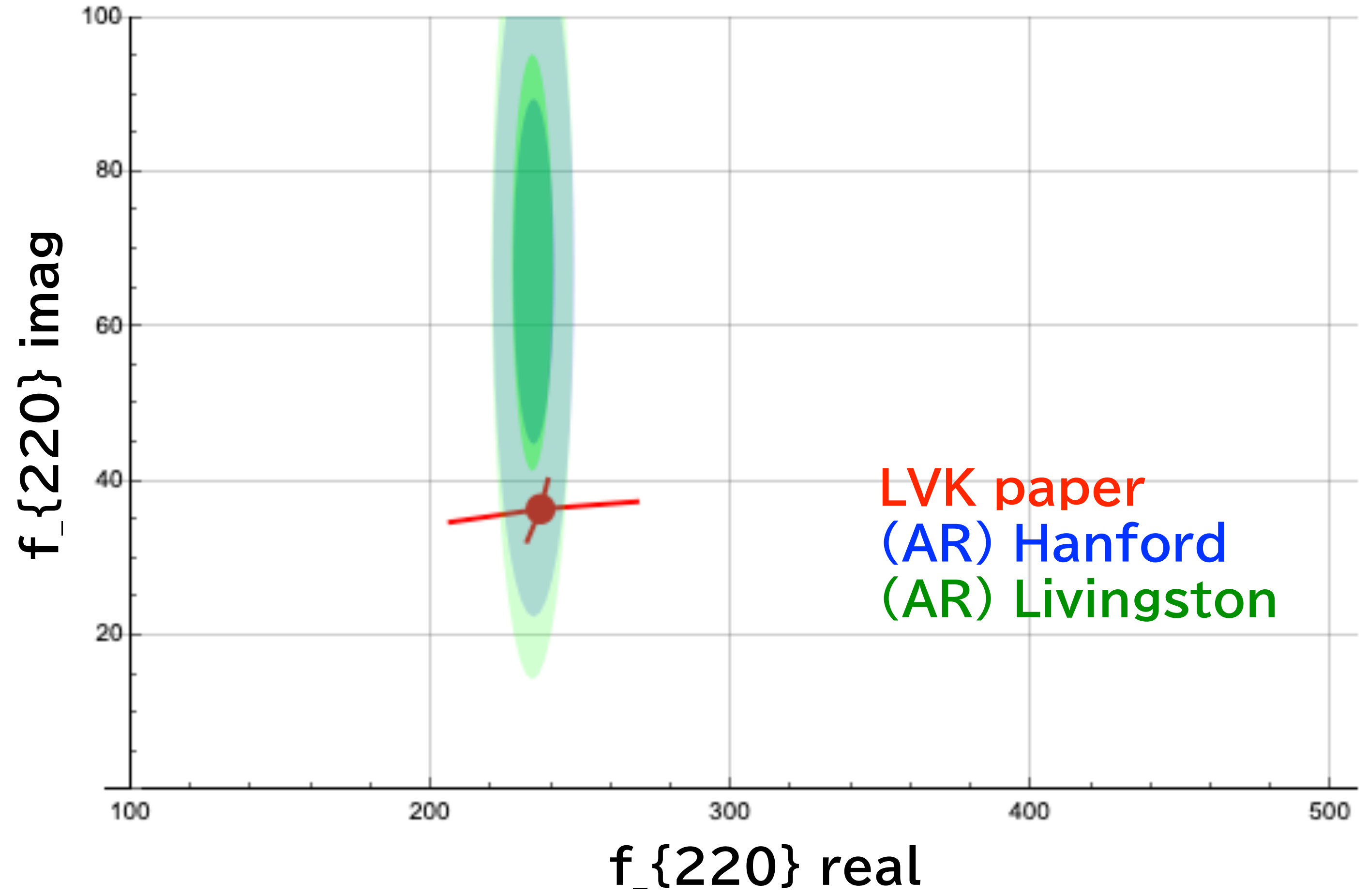

Livingston

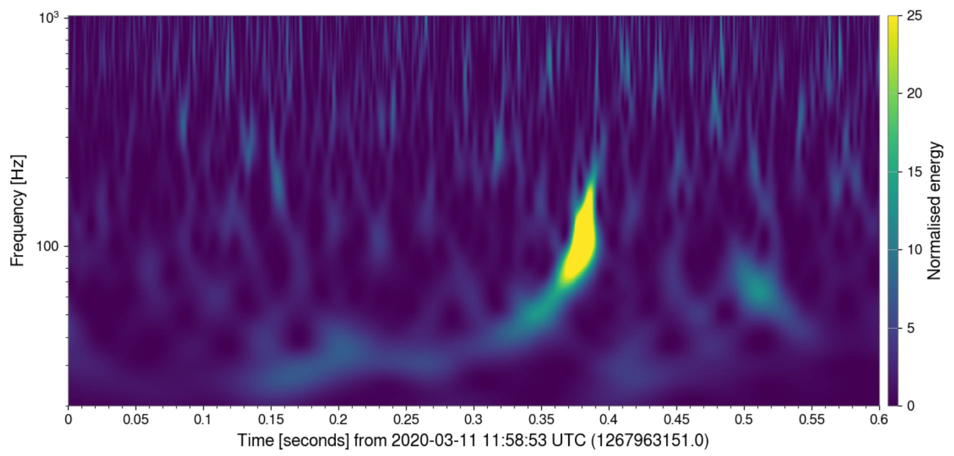

Livingston

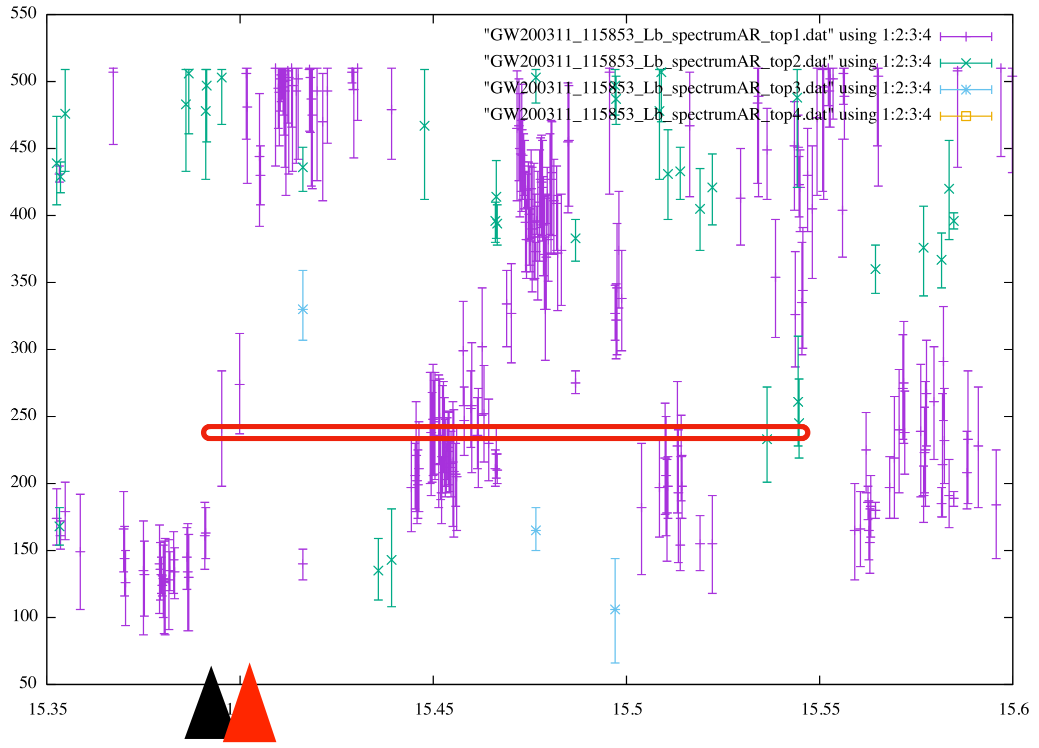

28 segments
f= 233.61 +- 6.82 Hz
t= 15.3982 -- 15.5449

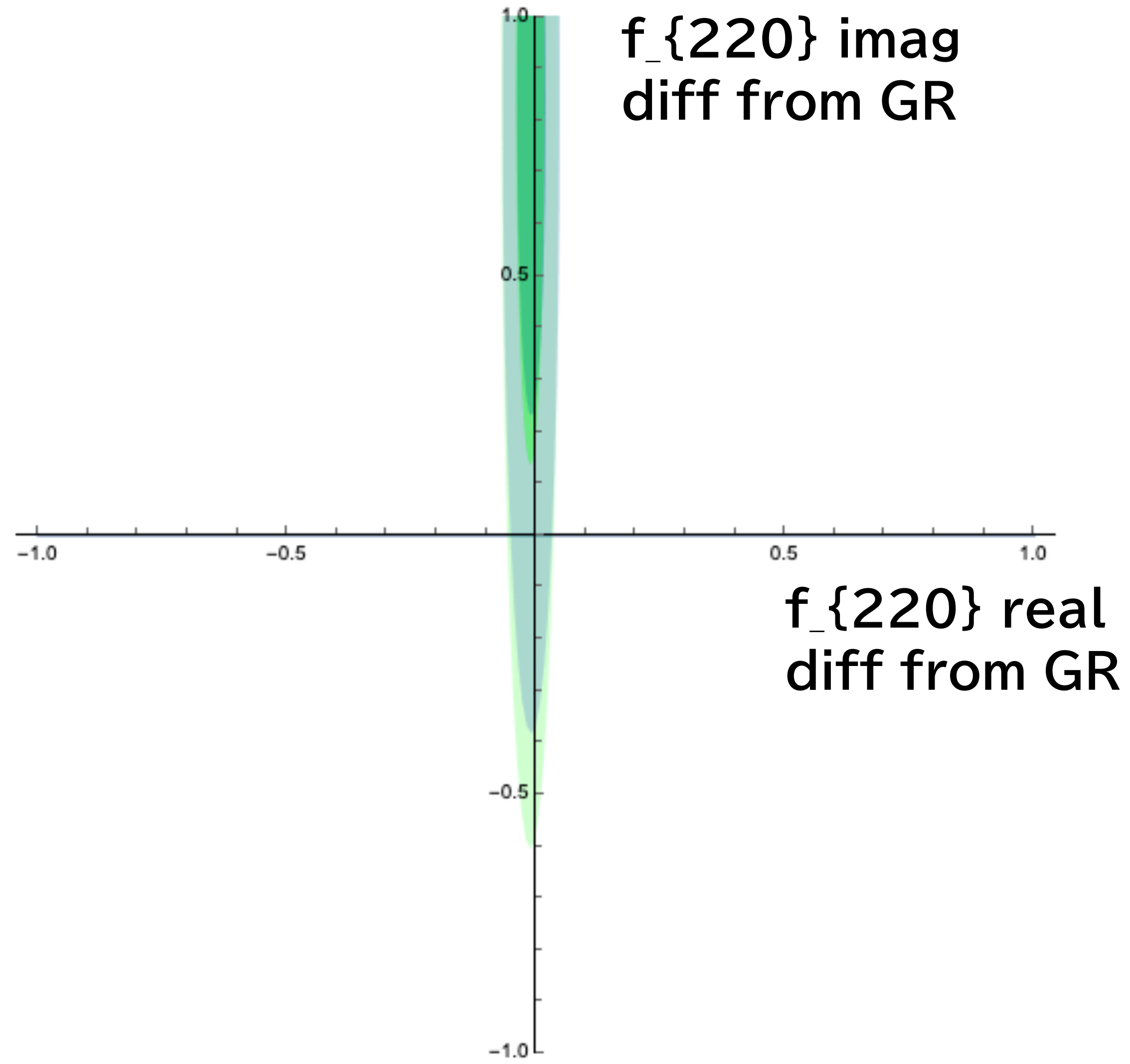

GW200311
delay time (msec) from t0
(+ delay, - advanced)

LHO = 0.48509
LLO = 10.1988
Virgo= 6.83823
KAGRA= -19.049

t_merger = 15.398 s
t_mergerH = 15.404
t_mergerL = 15.408
t_mergerV = 15.405

Virgo

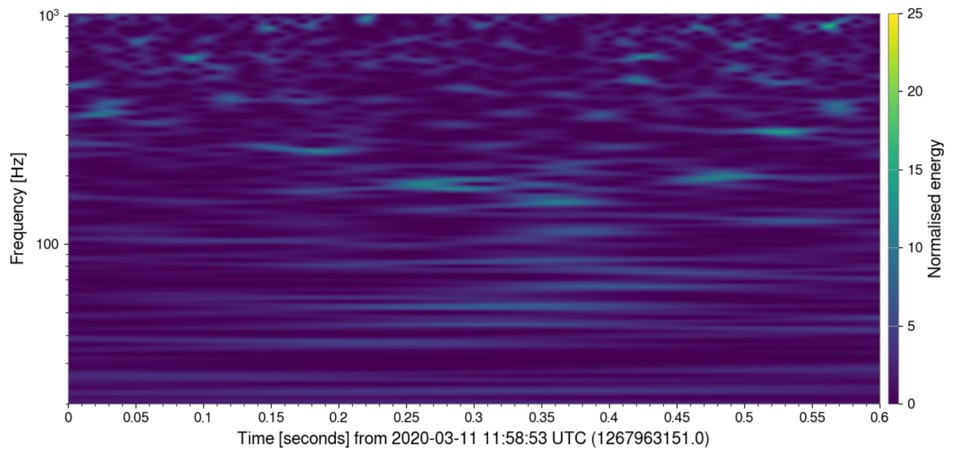

Summary & Outlook

AR method

$$
\begin{aligned}
x_n &= a_1 x_{n-1} + a_2 x_{n-2} + \cdots + a_M x_{n-M} + \varepsilon \\
&= \sum_{j=1}^{M} a_j x_{n-j} + \varepsilon
\end{aligned}
$$

AR method works for noisy real data of short length (64 pts~15ms).
We can extract frequencies and damping rates from the data itself.
No template, no theories. Can pick up several modes simultaneously.
Analysis for each detector, & can extract the merger time explicitely.

LV O1/O2/O3a & LVK O3b

For events of S/N >= 15 (total S/N), AR picks up ringdown modes.
(We used the same parameters [merger time + 200 ms],
Band Filterings [20-600Hz] for all analysis)

Can AR extract ring-down modes? **Yes**
Consistent between 3 IFs(Hanford, Livingston, Virgo) ? **Yes**
Consistent with the LVK catalog **Almost Yes**

➡ **Not perfect for f_imag (damping rate), estimating larger.**

When the ring-down starts? **3ms-5ms after merger**
Overtones? Higher modes? **Not Yet**
Consistent with GR? **Consistent, so far.**

➡ **Consistency checks with other methods & parameter trials.**
➡ **Waiting good signals (large S/N)**

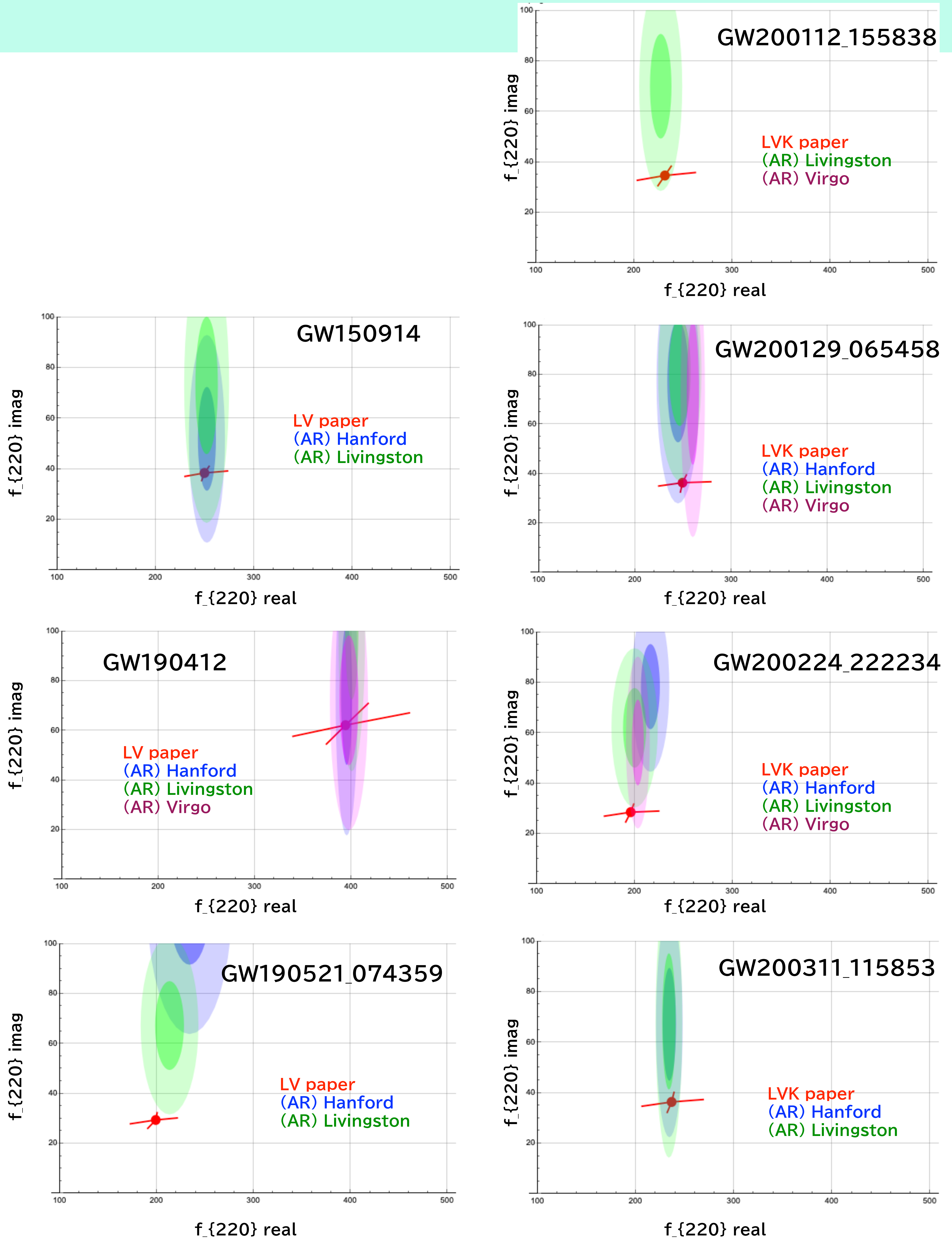

acknowledgments

This work was partially supported by

- JSPS KAKENHI Grant No. JP17H06358 (and also JP17H06357), A01: Testing gravity theories using gravitational waves, as a part of the innovative research area,
  "Gravitational wave physics and astronomy: Genesis".
- JSPS KAKENHI Grants No. 19H01901, "New directions in gravitational-wave data analysis: both in computing algorithms and hardwares including its outreach activities"
- JSPS KAKENHI Grants No. JP18K03630, "Non-linear dynamics in the modified gravity theories and the test of super-string theory".